PB81-175820

NSF/RA-800427

CIVIL ENGINEERING STUDIES

STRUCTURAL RESEARCH SERIES NO. 485

DYNAMIC RESPONSE OF TUNED SECONDARY SYSTEMS

by

G. C. RUZICKA

and

A. R. ROBINSON

A Technical Report of
Research Supported by the
NATIONAL SCIENCE FOUNDATION
under Grant Nos. ENV 75-08456,
ENV 77-07190 and PFR 80-02582

DEPARTMENT OF CIVIL ENGINEERING
UNIVERSITY OF ILLINOIS
AT URBANA-CHAMPAIGN
URBANA, ILLINOIS

NOVEMBER 1980

INFORMATION RESOURCES
NATIONAL SCIENCE FOUNDATION

REPRODUCED BY
NATIONAL TECHNICAL
INFORMATION SERVICE
U.S. DEPARTMENT OF COMMERCE
SPRINGFIELD, VA 22161

DYNAMIC RESPONSE OF TUNED SECONDARY SYSTEMS

by

GENE CONRAD RUZICKA

and

ARTHUR R. ROBINSON

A Report on a Research Project Sponsored by the

NATIONAL SCIENCE FOUNDATION

Research Grant Nos. ENV 75-08456, ENV 77-07190 and PFR 80-02582

UNIVERSITY OF ILLINOIS

Urbana, Illinois

November 1980

Any opinions, findings, conclusions or recommendations expressed in this publication are those of the author(s) and do not necessarily reflect the views of the National Science Foundation.

DYNAMIC RESPONSE OF TUNED SECONDARY SYSTEMS

Gene Conrad Ruzicka, Ph.D.
Department of Civil Engineering
University of Illinois at Urbana-Champaign, 1981

Light, flexible, "secondary" systems such as piping, penthouses and antenna towers are often attached to major structures. The purpose of this study is to investigate the dynamic response of secondary systems that are tuned to a natural frequency of the primary system.

Consideration is first given to simple structural models composed of a single-degree-of-freedom secondary system attached to a single-degree-of-freedom primary system. Formulas for the response of the secondary system are obtained for various damping configurations. The effects of a slight detuning of the secondary system are also examined.

The response expressions are then used to develop estimates for the maximum response of the secondary system. The accuracy of these estimates is assessed in a numerical study in which the exact and approximate responses are compared.

Lastly, an expression is obtained for the response of a multi-degree-of-freedom tuned secondary system attached to a multi-degree-of-freedom primary system.

ACKNOWLEDGMENT

The authors would like to thank William J. Hall, Professor of Civil Engineering, for his suggestions and interest. The record of the Mexico City earthquake used in this study was obtained with the assistance of Douglas A. Foutch, Assistant Professor of Civil Engineering.

The numerical results were obtained on the IBM 360/75, IBM 4341, and CYBER 175 computer systems of the Computer Services Office of the University of Illinois.

This study was supported by the National Science Foundation under Grants ENV 75-08456, ENV 77-07190, and PFR 80-02582. The opinions and findings expressed in this report, however, are those of the author and do not necessarily reflect the views of the National Science Foundation.

TABLE OF CONTENTS

LIST OF TABLES

LIST OF FIGURES

Figure Page

Figure Page

CHAPTER 1. INTRODUCTION

1.1 General Remarks

The components of complex structures can often be thought of as belonging either to a relatively heavy, stiff "primary" system or to a relatively light, flexible "secondary" system. In most applications, the primary system comprises the structural frame plus the larger masses, while typical secondary systems are piping, penthouses and ventilation systems. The subject of this study is the response of the secondary system when the structure is subjected to specified ground motion. This problem has long been of interest to earthquake engineers because secondary systems often perform tasks that are especially crucial during earthquakes, as in the case of building sprinkler systems and coolant circulation systems of nuclear power plants.

Special emphasis is given in the study to secondary systems that are tuned to a natural frequency of the primary system. Tuning is of great concern to the designer since it is this frequency configuration that brings about an extremely large, if not the largest, secondary system response. Ideally, the best course of action would be to design the structure so that tuning is avoided. However, because of the uncertainties and inaccuracies that are inherent in any modeling of a structure, certain frequencies of the primary and secondary systems may be closer than analytical or experimental data would indicate. As a result, it is generally advisable to assume exact tuning for primary and secondary system frequencies that appear to be in close proximity.

The accurate dynamic analysis of a tuned secondary system is essential in view of the large response that can result. Unfortunately, it is precisely when such a system is present that the conventional methods of structural dynamics break down. If a secondary system is present but is widely detuned, it is usually permissible to neglect interaction between the primary and secondary systems and utilize the well-known floor spectrum method of analysis. When the secondary system is tuned, however, its response is often large enough to affect the primary system and render the floor-spectrum method invalid. The presence of a tuned secondary system also precludes the use of modal

analysis methods. This is because structures that contain such systems have two eigenmodes with frequencies that are very close to the frequency of tuning. While these modes often contribute significantly to the response, the close spacing of the frequencies makes it difficult to compute the modal data or infer the joint response of the modes.

1.2 Object and Scope of Study

The principal object of this study is the development of procedures for computing and estimating the dynamic response of tuned secondary systems. The study is focused mainly on the most difficult analytical problem that arises from the presence of these systems; namely, evaluating the response contributed by the two closely-spaced eigenmodes mentioned earlier. The study isolates and examines this problem by considering in detail the response of the simple tuned system shown in Fig. 1. Later, more complicated tuned and detuned systems are also considered.

In Chapter 2, response formulas are derived for the response of the small mass of the simple tuned system shown in Fig. 1. The derivation employs an asymptotic procedure that uses the assumed smallness of the mass and stiffness of the secondary system to simplify the exact solutions of the equations of motion. The motions described by the response formulas are then studied qualitatively and some interesting response phenomena are deduced.

In Chapter 3, the results of Chapter 2 are used to develop estimates for the maximum response of the secondary system. First, parallel time and frequency domain analyses are used to derive a closed-form solution for the maximum response to ground motions of short duration. The parallel analyses are then extended to include a special class of long duration ground motions. Finally, the analytical results are used in conjunction with heuristic arguments to deduce a series of response estimates for long ground motions in general.

Chapter 4 discusses a numerical study that was carried out to assess the accuracy of the response estimates developed in Chapter 3. The numerical study computed, by exact and approximate methods, the response of a number of secondary systems to three widely differing

ground motions. In Chapter 4, the numerical studies are first described and the results are then evaluated in light of the analyses in Chapters 2 and 3.

In Chapter 5, a formula is derived for the general case of the response of a multi-degree-of-freedom (i.e., M-DOF) tuned secondary system that is attached at several points to an M-DOF primary system.

The results and conclusions of this study are summarized in Chapter 6.

1.3 Survey of Previous Work

The problem of analyzing the dynamic response of secondary systems has received considerable attention in recent years from investigators in earthquake engineering and related fields. The following brief survey gives additional background material for the problem and illustrates some of the methods that have been used to treat it.

The need for special methods to compute the response of secondary systems is widely recognized. The mass, damping, and stiffness influence coefficients of the secondary system are, respectively, smaller than those associated with the primary system, and, as a consequence, considerable round-off error may result when conventional methods are used to solve the equations of motion.

One way to avoid this difficulty is to assume that the secondary system does not perturb the motion of the primary system. The equations of motion of the total structure then decouple into two smaller sets of equations that allow one to solve for the responses of the primary and secondary systems in succession. Plots of maximum decoupled response of the secondary system versus frequency are widely used by designers and are generally referred to as "floor spectra."

While the computation of floor spectra is straightforward, it requires the cumbersome intermediate step of computing and storing the time histories of the points of attachment of the secondary system. Various schemes have been proposed that avoid this step and otherwise simplify the floor spectrum method. Kassawara [11] sought to develop an analogue to the modal method. To this end, a series of summation formulas were presented for use in conjunction with so-called "iterated response spectra" that were obtained

heuristically from conventional response spectra. A similar procedure was also developed by Biggs and Roesset [1]. Singh [27] and Singh [28] utilized random vibration techniques to develop methods for constructing floor spectra.

Although the floor spectrum method has been widely used, its validity has been questioned by some on the grounds that interaction between the primary and secondary systems can be significant. As was mentioned earlier, this is likely to occur when the secondary system is tuned. Interaction is also important in the so-called "vibration absorber" phenomenon [29]. Caughey [4] has studied this question analytically and has rigorously derived some sufficient conditions for applying a method quite similar to the floor spectrum approach.

A number of analytical schemes have been devised to account for dynamic interaction between component systems. Penzien and Chopra [20] considered a structure composed of an N-degree-of-freedom primary system and a single-degree-of-freedom secondary system. The structure was treated as a series of N two-degree-of-freedom systems with one-degree-of-freedom representing a mode of the primary system and the other representing the response of the secondary system induced by that mode. The maximum responses of the two-degree-of-freedom systems were then combined using the familiar root-sum-square summation formula. A simpler procedure proposed by Newmark [16] and improved by Nakhata et al. [15] uses a conservative modal summation rule in conjunction with simple approximations for the eigenvectors and frequencies of the total structure. In a recently completed work, Villaverde and Newmark [30] improved the method in Ref. [15] and also expanded it to cover structures with nonclassical damping and secondary systems with two points of attachment.

The present work marks the end of long study, the preliminary results of which were reported earlier by Ruzicka and Robinson [21]. While this study was in progress, a parallel, independent study along similar lines was conducted by Sackman and Kelly ([12], [13], [14], [22], [23], [24], [25]) at the University of California, Berkeley, and at Weidlinger Associates, Menlo Park, California. Both studies focus on the response contributed by the two closely-spaced modes of a structure containing

a tuned secondary system and use the following two-step procedure: 1. A simple formula for the response is derived by exploiting the tuning condition and the smallness of the mass and stiffness of the secondary system. 2. An estimate of the maximum response is obtained using the results of step 1. Both studies obtain the same results for step 1 but by different methods: the present study uses modal analysis and Fourier transforms while the Sackman-Kelly study uses Laplace transforms. It is in step 2 that the two studies truly differ. A brief discussion of these differences may be found at the end of Chapter 3.

1.4 Notation

The notation used in this study is listed and defined here. All terms are also defined where they first appear in the text.

a_1, a_2, A_1, A_2	miscellaneous constants
$a(t)$	ground acceleration
$A(\Omega)$	Fourier transform of $a(t)$
$A_1(\Omega)$, $A_2(\Omega)$	substitute functions for $A(\Omega)$ along positive and negative frequency axes
$\{B_1\}$, $\{B_2\}$	vectors defined in Eqs. (198a,b)
$[C]$	damping matrix of total structure
C_p, C_s	damping constants of single-degree-of-freedom primary system and single-degree-of-freedom secondary system
d	detuning parameter
$[e]$, $[e^*]$	matrices defined in Eqs. (157), (158a,b)
$E_s(t)$, $E_s^*(t)$, $E_s^{**}(t)$	envelopes of $u_s(t)$, $u_s^*(t)$ and $u_s^{**}(t)$
$[E]$	matrix defined in Eqs. (157), (158c)
f_b	fraction of energy integral concentrated in bandpass of secondary system transfer function
F_c, F_c'	Fourier cosine transform and its derivative at $\Omega=\omega$
F_s, F_s'	Fourier sine transform and its derivative at $\Omega=\omega$

F_1, F_2	constants defined in Eqs. (142), (143)
$\mathcal{F}(\cdot)$	Fourier transform operator
g, G_k	coefficients in the characteristic equation of a structure with a tuned secondary system
$h_s(t)$, $h_s^*(t)$, $h_s^{**}(t)$	exact, first order, and second order approximations to impulse response function for tuned secondary system
$h_s'(t)$	lower order component of $h_s^{**}(t)$
${}^{DC}h_s(t)$, ${}^{DC}h_s^{**}(t)$	exact and approximate impulse response functions for decoupled, tuned secondary system
$h_s^{\ell}(t)$, $h_s^1(t)$, $h_s^2(t)$	auxiliary impulse response functions defined in Eqs. (115a-c)
$H_s(\Omega)$, $H_s^*(\Omega)$, $H_s^{**}(\Omega)$	Fourier transforms of $h_s(t)$, $h_s^*(t)$, and $h_s^{**}(t)$
$H_s'(\Omega)$	Fourier transform of $H_s'(\Omega)$
${}^{DC}H_s(\Omega)$, ${}^{DC}H_s^{**}(\Omega)$	Fourier transforms of ${}^{DC}h_s(t)$, and ${}^{DC}h_s^{**}(t)$
$H_s^{\ell}(\Omega)$, $H_1(\Omega)$, $H_2(\Omega)$	Fourier transforms of $h_s^{\ell}(t)$, $h_1(t)$, and $h_2(t)$
I	impulse intensity
I^{eff}, ${}^{FS}I^{eff}$	effective impulse intensity
I_{av}^{eff}	effective impulse intensity obtained from simple averaging process
$[K]$	stiffness matrix of total structure
K_p, K_s	spring stiffnesses of single-degree-of-freedom primary and secondary systems
$[K_{pp}]$, $[K_{ss}]$	stiffness matrices of primary and secondary systems acting alone
$[{}^*K_{pp}]$	terms contributed to stiffness matrix of primary system by attached secondary system
$[K_{pp}']$	$[K_{pp}] + [K_{pp}^*]$ (see Eq. (146a))
$[\bar{K}_{pp}]$, $[{}^*\bar{K}_{pp}]$	$[K_{pp}]$ and $[{}^*K_{pp}]$ expressed in terms of modal coordinates of primary system
$[\bar{K}_{ss}]$	$[K_{ss}]$ expressed in terms of modal coordinates of secondary system

$[K_{ps}]$	stiffness matrix of primary system forces that result from secondary system motions
$[\overline{K}_{ps}]$	$[K_{ps}]$ transformed according to Eq. (151)
$\overline{K}_{pp}$, $\overline{K}^{i}_{ss}$	generalized stiffnesses of i^{th} modes of primary and secondary systems
$[M]$	mass matrix of total structure
M_p, M_s	masses of single-degree-of-freedom primary and secondary systems
$[M_{pp}]$, $[M_{ss}]$	mass matrices of primary and secondary systems acting alone
$[{}^*M_{pp}]$	terms contributed to mass matrix of primary system by attached secondary system
$[M'_{pp}]$	$[M_{pp}] + [{}^*M_{pp}]$ (see Eq. (146b))
$\overline{M}^{i}_{pp}$, $\overline{M}^{i}_{ss}$	generalized masses of i^{th} modes of primary and secondary systems
n	number of degrees-of-freedom in total structure
P	number of degrees-of-freedom in primary system
P_i	participation factor of i^{th} mode of total structure
P_1, P_2	participation factors of closely-spaced modes of total structure
P^{i}_{p}, P^{i}_{s}	participation factors of i^{th} modes of primary and secondary systems
r_i	i^{th} root of denominator of secondary system transfer function
S	number of degrees-of-freedom of secondary system
$S_V(\omega, \xi)$	pseudo-velocity spectrum of ground acceleration at frequency ω and damping ratio ξ
t	time
t_d	duration of ground motion
t^{e}_{d}	effective duration of ground motion

T	tuned period
T_B	beat period
$u_p(t)$, $\{u_p(t)\}$	response of single- and multi-degree-of-freedom primary systems relative to ground
$u_s(t)$, $\{u_s(t)\}$	response of single- and multi-degree-of-freedom secondary systems relative to ground
$u_s^*(t)$, $\{u_s^*(t)\}$	first-order approximations for response of secondary system contributed by two closely-spaced modes
$u_s^{**}(t)$, $\{u_s^{**}(t)\}$	second-order approximations for response of secondary system contributed by two closely-spaced modes
$u_s'(t)$, $\{u_s'(t)\}$	lower-order components of $u_s^{**}(t)$ and $\{u_s^{**}(t)\}$
$^{DC}u_p(t)$, $^{DC}u_s(t)$	decoupled responses of single-degree-of-freedom primary and secondary systems
$u_s^d(t)$	response of secondary system contributed by detuned modes
$u_1(t)$, $u_2(t)$	functions defined in Eqs. (50a,b)
u_s^{max}	maximum response of secondary system
$^{FS}u_s$	floor spectrum response of secondary system
$U_p(\Omega)$, $U_s(\Omega)$, $U_s^{**}(\Omega)$	Fourier transforms of $u_p(t)$, $u_s(t)$, and $u_s^{**}(t)$
$x_1(t)$, $x_2(t)$	responses of two closely-spaced modes in structure with nonproportional damping
$Y(t)$	ground displacement
$Z_1(t)$, $Z_2(t)$	functions defined in Eqs. (206a,b) and (207a,b)
$\{\alpha_p(t)\}$, $\{\alpha_s(t)\}$	responses of primary and secondary system modes in total structure
$\{\alpha_p\}$, $\{\alpha_s\}$	coordinates of primary and secondary system modes in eigenvector of total structure
$\{^1\alpha_p\}$, $\{^2\alpha_p\}$	coordinates of primary system modes in eigenvectors of the two closely-spaced modes of the total structure

$\{^1\alpha_s\}$, $\{^2\alpha_s\}$ coordinates of secondary system modes in the eigenvectors of the two closely-spaced modes of the total structure

β constant defined in Eq. (159c)

γ_p constant relating damping and stiffness matrices of primary system

γ_s constant relating damping and stiffness matrices of secondary system

γ constant relating damping and stiffness matrices of total structure when $\gamma_s = \gamma_p$

$\delta\omega$ beat circular frequency in structure with nonproportional damping (see Eqs. (86) and (206c))

δ_b half-bandwidth of transfer function

$\Delta\omega$ beat circular frequency in structure with proportional or no damping (see Eqs. (11b) and (198c))

$\Delta\omega^{\#}$ beat circular frequency of structure with slightly detuned secondary system (see Eq. (101c))

ε mass ratio (see Eqs. (3) and (159b))

ε_i constants defined in Eq. (159a)

$\varepsilon^{\#}$ effective mass ratio of structure with slightly detuned secondary system

θ constant defined in Eq. (120)

ξ_p, ξ_s damping ratios of single-degree-of-freedom primary and secondary systems

ξ_p^i ξ_s^i damping ratio of i^{th} modes of primary and secondary systems

ξ damping ratio of primary and secondary systems if $\xi_p = \xi_s$ or $\xi_p^1 = \xi_s^1$

ξ_a, ξ_d constants defined in Eqs. (75c,d) and (204a,b)

ξ_d' constant defined in Eqs. (95) and (207c)

ξ_p', ξ_s' constants defined in Eqs. (92a,b)

ξ^e envelope damping ratio

$\sigma(t)$	function defined in Eq. (32b)
τ	time
$\{\Phi^i\}$	eigenvector for i^{th} mode of total structure
$\{\phi^1\}$, $\{\phi^2\}$	eigenvectors for 2 closely-spaced modes of total structure
$\{\phi_p^i\}$, $\{\phi_s^i\}$	eigenvectors for i^{th} modes of primary and secondary systems
$[\phi_p]$, $[\phi_s]$	modal matrices of primary and secondary systems
ω	tuned circular frequency
ω_p^i, ω_s^i	circular frequencies of i^{th} modes of primary and secondary systems
ω_p, ω_s	constants defined in Eqs. (77b,c)
$[1/\omega_p^2]$, $[1/\omega_s^2]$	diagonal matrices whose i^{th} terms are $1/(\omega_p^i)^2$ and $1/(\omega_s^i)^2$
Ω	frequency domain parameter
Ω_i	circular frequency of i^{th} mode of total structure
Ω_1, Ω_2	circular frequencies of two closely-spaced modes of total structure

CHAPTER 2. RESPONSE OF SIMPLE TWO-DEGREE-OF-FREEDOM TUNED SYSTEMS

2.1 Introduction

This chapter presents a detailed analysis of the response of the simple tuned two-degree-of-freedom (2-DOF) system depicted schematically in Fig. 1. The goal is to obtain a general analytical and qualitative grasp of the response of tuned secondary systems.

There are two main reasons for examining the simple tuned system in detail. First, the simple system may be an adequate dynamic model if the primary and secondary system are tuned at their fundamental frequencies and the secondary system is attached at only one point. This is the case, for instance, if the secondary system is a slender antenna tower that is attached to a high rise building having the same fundamental frequency. Another reason for studying the simple system is that the results of the study are directly applicable to the analysis of more complicated tuned systems having the same critical feature; namely, the presence of two eigenmodes with closely spaced frequencies. It will be shown later that the contribution of the two closely spaced modes to the response of a tuned secondary system is, in general, mathematically equivalent to the response of the secondary mass of a system of the type shown in Fig. 1.

The chapter starts by analyzing an undamped tuned system in free and forced vibration. A simple formula is derived for the response of the secondary system. The formula is examined qualitatively to gain insights that will prove useful in obtaining response estimates. The analysis is then repeated for damped systems. Fourier analysis is used to extend the results to systems for which modal analysis is inconvenient. Finally, there is a discussion of the effects of a slight detuning of the primary and secondary systems.

2.2 Response of Undamped Tuned Systems

This section analyzes the response of the simple 2-DOF system of Figure 1 when no damping is present. Refined approximate solutions are derived for the cases of free and forced excitations. The motions described by the approximate solutions are then examined qualitatively.

2.2.1 Analysis of Equations of Motion

The equations of motion of the undamped tuned system of Figure 1 can be written in matrix form as:

$$\begin{bmatrix} M_p & 0 \\ 0 & M_s \end{bmatrix} \begin{Bmatrix} \ddot{u}_p(t) \\ \ddot{u}_s(t) \end{Bmatrix} + \begin{bmatrix} K_p + K_s & -K_s \\ -K_s & K_s \end{bmatrix} \begin{Bmatrix} u_p(t) \\ u_s(t) \end{Bmatrix} = -\begin{Bmatrix} M_p \\ M_s \end{Bmatrix} a(t) \qquad (1a)$$

in which:

M_p, K_p are the primary system mass and spring stiffness

M_s, K_s are the secondary system mass and spring stiffness

$\begin{Bmatrix} u_p(t) \\ u_s(t) \end{Bmatrix}$ is the response vector $\begin{Bmatrix} \text{primary displacement} \\ \text{secondary displacement} \end{Bmatrix}$ relative to the ground

$a(t)$ is the ground acceleration

t is time

Equation (1a) can also be written symbolically as:

$$[M]\{\ddot{u}\} + [K]\{u\} = -[M]\{1\}\, a(t) \qquad (1b)$$

where [M] and [K] are the mass and stiffness matrices of the total system, {u} is the response vector and {1} is a vector of ones.

It is assumed that the secondary system is tuned to the primary system of some frequency ω. This means the mass and stiffness terms are related by:

$$\frac{K_p}{M_p} = \frac{K_s}{M_s} = \omega^2 \qquad (2)$$

The "size" of the secondary system relative to the primary system is characterized by the mass ratio which is denoted:

$$\varepsilon = \frac{M_s}{M_p} = \frac{K_s}{K_p} << 1 \tag{3}$$

Equation (1a) can be rewritten in terms of ω and ε as:

$$\begin{bmatrix} 1 & 0 \\ 0 & \varepsilon \end{bmatrix} \begin{Bmatrix} \ddot{u}_p(t) \\ \ddot{u}_s(t) \end{Bmatrix} + \omega^2 \begin{bmatrix} 1+\varepsilon & -\varepsilon \\ -\varepsilon & \varepsilon \end{bmatrix} \begin{Bmatrix} u_p(t) \\ u_s(t) \end{Bmatrix} = - \begin{Bmatrix} 1 \\ 1 \end{Bmatrix} a(t) \tag{4}$$

Equation (4) can be solved for $\{u\}$ in closed form using the modal method (see [6]). We first consider the case $a(t) = 0$. The system is then in free vibration and the response is given by the formula:

$$\{u\} = \sum_{j=1}^{2} \{\phi^j\} A_j \sin(\Omega_j t + a_j) \tag{5}$$

In Eq. (5), the a_j are phase angles. The eigenvalues Ω_j^2 are the roots of the characteristic equation:

$$\begin{vmatrix} \omega^2(1+\varepsilon) - \Omega^2 & -\omega^2\varepsilon \\ -\omega^2\varepsilon & \varepsilon(\omega^2 - \Omega^2) \end{vmatrix} = 0 \tag{6}$$

The eigenvector $\{\Phi^j\}$ is obtained by substituting Ω_j into the simultaneous equations:

$$\begin{bmatrix} \omega^2(1+\varepsilon) - \Omega_j^2 & -\omega^2\varepsilon \\ -\omega^2\varepsilon & \varepsilon(\omega^2 - \Omega_j^2) \end{bmatrix} \begin{Bmatrix} \phi_p^j \\ \phi_s^j \end{Bmatrix} = 0 \tag{7}$$

Upon expanding the determinant in Eq. (6), the characteristic equation becomes:

$$\Omega^4 + \Omega^2\omega^2(2+\varepsilon) + \omega^4 = 0 \tag{8}$$

The roots of Eq. (8) are:

$$\Omega_1^2 = 1 + \frac{\varepsilon}{2} - \sqrt{\varepsilon}\sqrt{1 + \frac{\varepsilon}{4}} \tag{9a}$$

$$\Omega_2^2 = 1 + \frac{\varepsilon}{2} + \sqrt{\varepsilon}\sqrt{1 + \frac{\varepsilon}{4}} \tag{9b}$$

The expressions for the Ω_j can be approximately simplified by expanding the radical in powers of ε and then keeping only the two largest terms. For Ω_1 this process yields:

$$\begin{aligned}\Omega_1^2 &= \omega^2\left(1 + \frac{1}{2} - \sqrt{\varepsilon}\left(1 + \frac{\varepsilon}{8} - \frac{\varepsilon^2}{128} + \ldots\right)\right) \\ &\simeq \omega^2\left(1 + \frac{\varepsilon}{2} - \sqrt{\varepsilon} - \frac{\varepsilon}{8}^{3/2}\right) \\ &\simeq \omega^2(1 - \sqrt{\varepsilon}) \end{aligned} \tag{10}$$

Using Eq. (10), we can approximate Ω_1 as:

$$\begin{aligned}\Omega_1 &\simeq \omega(1 - \sqrt{\varepsilon})^{1/2} \\ &\simeq \omega\left(1 - \frac{\sqrt{\varepsilon}}{2}\right) \qquad (11a) \\ &\simeq \omega - \Delta\omega \qquad (11b)\end{aligned}$$

The parameter $\Delta\omega$ defined in Eq. (11b) will be used frequently in the sequel.

To evaluate the eigenvector $\{\phi^1\}$, we set $\phi_1^1 = 1$ and substitute Eq. (9a) into the second of Eq. (7). This yields:

$$\begin{aligned}\phi_2^1 &= \frac{1}{\sqrt{\varepsilon}}\left(1 + \frac{\varepsilon}{4}\right)^{1/2} + \frac{1}{2} \\ &\simeq \frac{1}{\sqrt{\varepsilon}} + \frac{1}{2}\end{aligned}$$

We conclude:

$$\{\phi^1\} = \begin{Bmatrix} \phi_p^1 \\ \phi_s^1 \end{Bmatrix} \simeq \begin{Bmatrix} 1 \\ \frac{1}{\sqrt{\varepsilon}} + \frac{1}{2} \end{Bmatrix} \tag{12}$$

The evaluation of ω_2 and $\{\phi^2\}$ closely parallels the evaluation of Ω_1 and $\{\phi^1\}$. It can be shown that:

$$\Omega_2 \simeq \omega(1 + \frac{\sqrt{\varepsilon}}{2}) \tag{13}$$

$$\{\phi^2\} = \begin{Bmatrix} \phi_p^2 \\ \phi_s^2 \end{Bmatrix} \simeq \begin{Bmatrix} 1 \\ -(\frac{1}{\sqrt{\varepsilon}} - \frac{1}{2}) \end{Bmatrix} \tag{14}$$

Substituting Eqs. (11)-(14) into Eq. (5) gives the following approximation for free vibration response:

$$\begin{Bmatrix} u_p(t) \\ u_s(t) \end{Bmatrix} = \begin{Bmatrix} 1 \\ \frac{1}{\sqrt{\varepsilon}}+\frac{1}{2} \end{Bmatrix} A_1 \sin [(\omega-\Delta\omega)t + a_1] + \begin{Bmatrix} 1 \\ -\frac{1}{\sqrt{\varepsilon}}+\frac{1}{2} \end{Bmatrix} A_2 \sin [(\omega+\Delta\omega)t + a_2] \tag{15}$$

The motion described by Eq. (15) will be examined qualitatively in the next subsection.

Our attention now turns to the case of forced excitation. When the system is excited by some ground acceleration a(t), the response is given by the formula:

$$\{u\} = -\sum_{j=1}^{2} \{\phi^j\} \frac{P_j}{\Omega_j} \int_0^t a(\tau) \sin \Omega_j(t-\tau)\, d\tau \tag{16}$$

The P_j are the modal participation factors and are given by:

$$P_j = \frac{\{\phi^j\}^T[M]\{1\}}{\{\phi^j\}^T[M]\{\phi^j\}} \tag{17}$$

An approximation for P_1 can be obtained by inserting Eq. (12) into Eq. (17). We then have:

$$P_1 \simeq \frac{M + \varepsilon M/2 + \sqrt{\varepsilon}M}{2M + \varepsilon M/4 + \sqrt{\varepsilon}M}$$

$$\simeq \frac{1 + \sqrt{\varepsilon}}{2 + \sqrt{\varepsilon}} \simeq \frac{1}{2}\left[1 + \frac{\sqrt{\varepsilon}}{2}\right] \tag{18a}$$

Similarly, it can be shown that:

$$P_2 \simeq \frac{1}{2}\left[1 - \frac{\sqrt{\varepsilon}}{2}\right] \tag{18b}$$

We will now use the approximations for P_j, Ω_j and $\{\phi^j\}$ to form approximations for the coefficients which precede the integrals in Eq. (16). For the first coefficient:

$$\{\phi^1\}\frac{P_1}{\Omega_1} \simeq \frac{1}{\omega}\begin{Bmatrix} \frac{1}{2}(1 + \sqrt{\varepsilon}) \\ \\ \frac{1}{2}(\frac{1}{\sqrt{\varepsilon}} + \frac{3}{2}) \end{Bmatrix} \tag{19}$$

Similarly, for the second coefficient:

$$\{\phi^2\}\frac{P_2}{\Omega_2} \simeq \frac{1}{\omega}\begin{Bmatrix} \frac{1}{2}(1 + \sqrt{\varepsilon}) \\ \\ -\frac{1}{2}(\frac{1}{\sqrt{\varepsilon}} - \frac{3}{2}) \end{Bmatrix} \tag{20}$$

Combining Eqs. (11), (13), (16), (19) and (20), we have:

$$u_p(t) \simeq -\frac{1}{\omega}\int_0^t a(\tau)\sin\omega(t-\tau)\cos\Delta\omega(t-\tau)d\tau + \frac{\sqrt{\varepsilon}}{\omega}\int_0^t a(\tau)\sin\Delta\omega(t-\tau)\cos\omega(t-\tau)\,d\tau \tag{21}$$

$$u_s(t) \simeq \frac{1}{\sqrt{\varepsilon}}\int_0^t a(\tau)\sin\omega(t-\tau)\cos\Delta\omega(t-\tau)d\tau - \frac{3}{2\omega}\int_0^t a(\tau)\sin\omega(t-\tau)\cos\Delta\omega(t-\tau)\,d\tau \tag{22}$$

We define:

$$u_s'(t) = -\frac{3}{2\omega}\int_0^t a(\tau)\sin\omega(t-\tau)\cos\Delta\omega(t-\tau)\,d\tau \tag{23a}$$

$$u_s^*(t) = \frac{1}{\omega\sqrt{\varepsilon}}\int_0^t a(\tau)\sin\Delta\omega(t-\tau)\cos\omega(t-\tau)\,d\tau \tag{23b}$$

$$u_s^{**}(t) = u_s'(t) + u_s^{*}(t) \tag{23c}$$

It is apparent from the derivation of Eq. (22) that $u_s^{**}(t)$ becomes $u_s(t)$ exactly for vanishingly small ε.

2.2.2 Qualitative Analysis of Response

Equations (15) and (22) will now be examined to obtain qualitative information about secondary system response.

Consideration is given first to the case of free vibrations. Equation (15) shows that $u_s(t)$ is the sum of two sinusoidal oscillations with close frequencies. This gives rise to the classical "beat phenomenon" in which the amplitude of the combined oscillation rises and falls as the component oscillations drift in an out of phase. To see this, we set $A_1 = A_2 = A$ and $a_1 = a_2 = 0$ in Eq. (15). This yields:

$$u_s(t) \simeq \left(\frac{1}{\sqrt{\varepsilon}} + \frac{1}{2}\right) A \sin (\omega+\Delta\omega)\, t - \left(\frac{1}{\sqrt{\varepsilon}} - \frac{1}{2}\right) A \sin (\omega-\Delta\omega)\, t$$

$$\simeq \frac{2A}{\sqrt{\varepsilon}} [\sin \Delta\omega t] \cos \omega t \tag{24}$$

The motion described by Eq. (24) is the solid curve drawn in Fig. 2. The bracketed term in Eq. (22) and its negative are the dashed curves in Fig. 2. It is seen that the dashed curves oscillate relatively slowly and closely match the peaks and troughs of the troughs of the solid curve. We define an envelope, denoted E(t), as a non-negative, slowly oscillating function that closely matches the extreme of an oscillatory motion. From Fig. (2), it can be seen that the envelope of Eq. (24) is given by:

$$E(t) = \left| \frac{2A}{\sqrt{\varepsilon}} \sin \Delta\omega t \right| \tag{25}$$

The rate of oscillation of the envelope (or "beating") is governed by $\Delta\omega = \frac{\omega\sqrt{\varepsilon}}{2} << \omega$. For this reason, $\Delta\omega$ will be referred to as the "beat frequency." The duration of the beats is characterized by the "beat period" which is denoted:

$$T_B = \frac{2\pi}{\Delta\omega} \tag{26}$$

From Eqs. (24)-(26) and Fig. 2, it can be seen that T_B is the duration of two beat lobes.

Our attention now turns to the description of secondary system response under ground excitation. The integrals in Eq. (22b) contain the terms cos $\Delta\omega(t-\tau)$ and sin $\Delta\omega(t-\tau)$. However, $\Delta\omega<<\omega$ and if ω and ε are sufficiently small, $\Delta\omega t<<1$ for a fairly long time. When $\Delta\omega t<<1$, Eq. (22) can be replaced by:

$$\begin{aligned} u_s(t) \simeq u_s^{**}(t) \simeq \frac{1}{2}\int_0^t a(\tau)(t-\tau)\cos\omega(t-\tau)\,d\tau \\ - \frac{3}{2\omega}\int_0^t a(\tau)\sin\omega(t-\tau)\,d\tau = u_s^{DC}(t);\ \Delta\omega t<<1 \end{aligned} \tag{27}$$

Straightforward calculation shows that $u_s^{DC}(t)$, defined in Eq. (27), satisfies the differential equation:

$$\ddot{u}_s^{DC}(t) + \omega^2 u_S^{DC}(t) = -a(t) - \omega\int_0^t a(t)\sin\omega(t-\tau)\,d\tau \tag{28}$$

Equation (28), however, is the equation of motion for $u_s(t)$ that results from the assumption (generally incorrect) that the secondary system does not perturb the motion of the primary system. An analysis based on this assumption is said to be a "decoupled analysis." The methodology of a decoupled analysis is depicted schematically in Fig. 3.

We see that when $\Delta\omega t<<1$, the secondary system response can be calculated using a decoupled analysis. In light of Eq. (26), this means that a decoupled analysis is valid when the elapsed time after the start of the ground motion is much less than the beat period. This result seems reasonable on physical grounds. In the early stages of the motion, the secondary spring distortion is small and the secondary spring force too small to perturb the primary system significantly. Therefore, a decoupled analysis is valid (see Fig. 3) and the secondary system is subject to a base motion input with significant frequency content close to its own natural frequency. This input makes the amplitude of the

secondary response grow rapidly until the secondary response spring force is large enough to perturb the primary system. The smaller the secondary spring stiffness (or the longer the beat period), the more time required for the second system force to reach an amplitude large enough to affect the primary system.

When $\Delta\omega t$ is not small, $u_s^{DC}(t)$ is no longer a valid approximation and $u_s(t)$ must be approximated by $u_s^{**}(t)$ as given by Eq. (23). To examine $u_s^{**}(t)$ qualitatively, we first rewrite it in the following form:

$$u_s^{**}(t) = u_1(t) \sin \omega t + u_2(t) \cos \omega t \tag{29}$$

where:

$$u_1(t) = \frac{1}{\omega\sqrt{\varepsilon}} \int_0^t a(\tau) \sin \omega\tau \sin \Delta\omega(t-\tau)\, d\tau - \frac{3}{2\omega} \int_0^t a(\tau) \cos \omega\tau \cos \Delta\omega(t-\tau)\, d\tau \tag{30a}$$

$$u_2(t) = \frac{1}{\omega\sqrt{\varepsilon}} \int_0^t a(\tau) \cos \omega\tau \sin \Delta\omega(t-\tau)\, d\tau + \frac{3}{2\omega} \int_0^t a(\tau) \sin \omega\tau \sin \Delta\omega(t-\tau)\, d\tau \tag{30b}$$

The behavior of $u_1(t)$ and $u_2(t)$ will now be examined. The first of the two terms in $u_1(t)$ is proportional to the displacement of a linear SDF (i.e., single-degree-of-freedom) system of circular frequency $\Delta\omega$ that is excited by a "ground acceleration" $a(\tau) \sin \omega\tau$. It is well known that when a linear SDF system is excited by a wide-banded function, it oscillates at a rate close to its natural frequency. Consequently, the first term in $u_1(t)$ oscillates about as rapidly as $\sin \Delta\omega t$. The second term in $u_1(t)$ is proportional to the velocity of a linear SDF system of circular frequency $\Delta\omega$ that is excited by a "ground acceleration" $a(\tau) \cos \omega\tau$ and this term also oscillates about as rapidly as $\sin \Delta\omega t$. We therefore conclude that $u_1(t)$ oscillates about as rapidly as $\sin \Delta\omega t$. It can be shown in a similar manner that $u_2(t)$ also oscillates about as rapidly as $\sin \Delta\omega t$. Since $\Delta\omega << \omega$, $u_1(t)$ and $u_2(t)$ remain essentially constant for several cycles of $\sin \omega t$ and $\cos \omega t$. We can therefore treat $u_1(t) \sin \omega t$ and $u_2(t) \cos \omega t$ as though they are rotating vectors 90 degrees out of phase and combine them accordingly. We then have:

$$u_s^{**}(t) = E^{**}(t) \cos [\omega t - \sigma(t)] \tag{31}$$

where:

$$E^{**}(t) = \{[u,(t)]^2 + [u_2(t)]^2\}^{1/2} \tag{32a}$$

$$\sigma(t) = \tan^{-1}\left[\frac{u_1(t)}{u_2(t)}\right] \tag{32b}$$

It is readily seen that $E^{**}(t)$ is the envelope of $u^{**}(t)$.

We conclude that the forced vibration as well as the free vibration of a tuned secondary system is characterized by the presence of beats and a smooth envelope function that oscillates at the beat frequency.

The analysis of $u_s^{**}(t)$ has so far included the contributions of both $u_s'(t)$ and $u_s^*(t)$. However, examination of Eqs. (23a, b) might lead one to conclude that $|u_s'(t)| << |u_s^*(t)|$ since the integrals appear to be similar in magnitude but $\frac{1}{\sqrt{\varepsilon}} >> \frac{3}{2}$. If $u_s'(t)$ can be neglected, $u_s(t) \simeq u_s^*(t)$ and we have:

$$E^{**}(t) \simeq E^{*}(t) = \tag{33}$$

$$= \frac{1}{\omega\sqrt{\varepsilon}}\left[\left(\int_0^t a(\tau)\sin\omega\tau\sin\Delta\omega(t-\tau)\,d\tau\right)^2 + \left(\int_0^t a(\tau)\cos\omega\tau\sin\Delta\omega(t-\tau)\,d\tau\right)^2\right]^{1/2}$$

To illustrate the results of this section, the time histories of two tuned secondary systems have been computed using the exact (i.e., Eq. (16)) and approximate formulas. The ground acceleration used was the earthquake accelerogram for El Centro 1940-NS (see Fig. 10). The parameters of the first system are $\varepsilon = .0025$ and $\omega = 2\pi$RPS. The approximate time history, $u_s^{**}(t)$, for this system is the solid curve shown in Fig. 4a. It is virtually identical to the exact time history, $u_s(t)$, which is shown in Fig. 4b. Two sets of dashed curves are shown in Fig. 4a. The curves comprised of the shorter dashes are plots of $E^*(t)$ and $-E^*(t)$. It can be seen that $E^*(t)$ satisfies the criteria specified earlier for an envelope; i.e., it is relatively smooth and closely matches the response extrema. The curves in Fig. 4a that are comprised of the longer dashes are plots $E^{**}(t)$ and $-E^{**}(t)$. We conclude that for this system and ground motion, little accuracy is lost

by using $u_s^*(t)$ or $u_s^{**}(t)$ instead of $u_s(t)$.

The second tuned secondary system considered is characterized by the parameters $\varepsilon = .01$ and $\omega = 2\pi$RPS. The approximate and exact time history data for this system are shown in Figs. 4c and 4d, respectively. It can be seen that most of the remarks made in regard to the previous example apply here equally as well. The most significant difference is that $E^*(t)$ is somewhat less satisfactory here than in the previous example.

2.3 Response of Tuned Systems with Proportional Damping

This section examines the equations of motion of a damped tuned system in which the damping matrix is proportional to the stiffness matrix. Before proceeding with the analysis, we present here a brief discussion of damping in general and the significance of the damping formulation considered in this section.

Damping refers to energy dissipation caused by the internal friction that is always present to some degree in structures. A common method of taking damping into account is to insert into the equations of motion the term $[C]\{\dot{u}\}$ where $[C]$ is a symmetric matrix of damping coefficients. The matrix $[C]$ is usually constructed so that it can be diagonalized by the same transformation that uncouples the equations of motion of the undamped system. This type of damping matrix is often called "classical damping".

Numerous damping formulations are possible, even within the constraints imposed by classical damping. Damping parameters are usually a function of the type of system, the materials used, the mode of construction and the maximum stress level (see [27]). Separate damping models may prove to be necessary for widely differing primary and secondary systems. This can lead to analytical difficulties because classical damping in the separate primary and secondary systems does not ensure that classical damping exists in the total system.

A commonly used classical damping formulation involves setting the damping matrix proportional to the stiffness matrix. Physically, this can be interpreted as inserting in parallel with each spring a dashpot with damping proportional to the spring stiffness. Consider now the 2-DOF damped tuned system shown in Fig. 1. Assuming stiffness proportional damping in the separate primary and secondary systems, we have:

$$C_p = \gamma_p K_p \tag{34a}$$

$$C_s = \gamma_s K_s \tag{34b}$$

It can be shown using a theorem of Caughey and O'Kelly [5] that the system of Fig. 1 is classically damped if and only if $\gamma_p = \gamma_s$. We shall then say that the system is "proportionally damped" since the damping matrix of the total system is proportional to the stiffness matrix.

In this section, we examine the system of Fig. 1 assuming proportional damping. First, the exact response formula is simplified analytically and the resulting response expression is studied qualitatively. The analytical results are then transformed into the frequency domain, principally for future reference. The case of non-proportional damping (i.e., $\gamma_p \neq \gamma_s$) will be treated in the next section.

2.3.1 Analysis of Equations of Motion

In light of our assumptions about damping, we can write:

$$\gamma_p = \gamma_s = \gamma \tag{35}$$

The damping in the separate primary and secondary systems can also be characterized by their respective damping ratios, ξ_p and ξ_s, where:

$$\xi_p = \frac{C_p}{2M_p\omega} << 1 \tag{36a}$$

$$\xi_s = \frac{C_s}{2M_s\omega} << 1 \tag{36b}$$

It is easily shown that:

$$\xi_s = \xi_p = \frac{\gamma\omega}{2} = \xi \tag{37}$$

The equations of motion may be written symbolically as:

$$[M]\{\ddot{u}\} + [C]\{\dot{u}\} + [K]\{u\} = - [M]\{1\}a(t) \tag{38}$$

where the damping matrix, [C], is:

$$[C] = \gamma \begin{bmatrix} K_p + K_s & -K_s \\ -K_s & K_s \end{bmatrix} \tag{39}$$

Equation (38) can be solved using the modal method. The secondary system response is given by:

$$u_s(t) = \frac{-P_1 \Phi_2^1}{\Omega_1 \sqrt{1 - \xi_1^2}} \int_o^t a(\tau) e^{-\xi_1 \Omega_1 (t-\tau)} \sin \Omega_1 \sqrt{1-\xi_1^2}(t-\tau)\, d\tau$$

$$\frac{-P_2 \Phi_2^2}{\Omega_2 \sqrt{1 - \xi_2^2}} \int_o^t a(\tau) e^{-\xi_2 \Omega_2 (t-\tau)} \sin \Omega_2 \sqrt{1-\xi_2^2}(t-\tau)\, d\tau \tag{40}$$

where the ξ_i are the modal damping ratios and are given by:

$$\xi_i = \frac{\gamma \Omega_i}{2} \tag{41}$$

Inserting Eqs. (7a,b) into Eq. (41) yields:

$$\xi_1 \simeq \frac{\gamma\omega}{2} \left(1 - \frac{\sqrt{\varepsilon}}{2}\right) \simeq \xi \tag{42a}$$

$$\xi_2 \simeq \frac{\gamma\omega}{2} \left(1 + \frac{\sqrt{\varepsilon}}{2}\right) \simeq \xi \tag{42b}$$

Using Eqs. (42a,b) and Eqs. (20a,b) in Eq. (40) and neglecting terms ξ_i^2, we have:

$$u_s(t) = \frac{1}{\omega\sqrt{\varepsilon}} \int_0^t a(\tau) e^{-\xi\omega(t-\tau)} \sin \Delta\omega(t-\tau) \cos \omega(t-\tau)\, d\tau$$
$$- \frac{3}{2\omega} \int_0^t a(\tau) e^{-\xi\omega(t-\tau)} \cos \Delta\omega(t-\tau) \sin \omega(t-\tau)\, d\tau \tag{43a}$$

$$= u_s^*(t) + u_s^{**}(t) = u_s(t) \tag{43b}$$

The approximate response expression of Eq. (43a) complements the undamped approximation of Eq. (22); hence, the same notation is used in Eq. (41b) and Eq. (23c).

The integrals appearing in Eq. (43a) are generally of the same order of magnitude and since $\varepsilon << 1$, it is usually true that $|u_s'(t)| << |u_s^*(t)|$. However, it will be seen in Chapter 4 that exceptions can occur. Conditions under which the contribution of $u_s'(t)$ is significant are discussed in Chapter 3.

A "ground motion" that plays an important role in the sequel is the unit impulse function, $\delta(t)$ (i.e., the Dirac Delta function). The response of the secondary system to the unit impulse function is denoted $h_s(t)$. Substituting $\delta(t)$ for a(t) in Eq. (43a) yields the approximate impulse response function:

$$h_s^{**}(t) = \frac{1}{\omega\sqrt{\varepsilon}} e^{-\xi\omega t} \sin\Delta\omega t \cos\omega t - \frac{3}{2\omega} e^{-\xi\omega t} \cos\Delta\omega t \sin\omega t \tag{44a}$$

$$= h_s^*(t) + h_s'(t) \tag{44b}$$

$$\simeq h_s(t) \tag{44c}$$

2.3.2 Qualitative Analysis of Response

The results obtained in Sec. 2.3.2 for undamped systems apply, with some minor modifications, to damped systems.

When $\Delta\omega t << 1$, the decoupled response is a good approximation for damped as well as undamped systems. To see this, we first obtain $u_s^{DC}(t)$ for the damped tuned system. With the aid of Fig. 3 it is seen that the equation of motion for $u_s^{DC}(t)$ is given by:

$$u_s^{DC} + 2\xi\omega u_s^{DC} + \omega^2 u_s^{DC} = 2\xi\omega u_p^{DC} + \omega^2 u_p^{DC} - a(t) \tag{45}$$

where u_p^{DC} is given by:

$$u_p^{DC} = \frac{-1}{\omega\sqrt{1-\xi^2}} \int_o^t a(\tau)\, e^{-\xi\omega(t-\tau)} \sin\omega\sqrt{1-\xi^2}(t-\tau)\, d\tau \tag{46}$$

Substituting Eq. (46) into Eq. (45) and solving for $u_s^{DC}(t)$ yields:

$$u_s^{DC}(t) \simeq \frac{\omega^2 - 2\xi^2\omega^2}{2\omega^2(1-\xi^2)} \int_o^t a(\tau)\, e^{-\xi\omega(t-\tau)}\, (t-\tau)\, \cos\omega\sqrt{1-\xi^2}(t-\tau)\, d\tau +$$

$$+ \frac{-3\omega^2 + 4\xi^2\omega^2}{2(\omega\sqrt{1-\xi^2})^3} \int_o^t a(\tau)\, e^{-\xi\omega(t-\tau)}\, \sin\omega\sqrt{1-\xi^2}(t-\tau)\, d\tau + \qquad (47)$$

$$- \frac{\xi\omega}{\omega\sqrt{1-\xi^2}} \int_o^t a(\tau)\, e^{-\xi\omega(t-\tau)}\, (t-\tau)\, \sin\omega\sqrt{1-\xi^2}(t-\tau)\, d\tau$$

The last term on the right-hand side of Eq. (47) is generally much smaller than the first term since the integrals are of generally the same order of magnitude and $\xi \ll 1$. Consequently:

$$u_s^{DC}(t) \simeq \frac{1}{2} \int_o^t a(\tau)\, e^{-\xi\omega(t-\tau)}\, (t-\tau)\, \cos\omega(t-\tau)\, d\tau -$$

$$- \frac{3}{2\omega} \int_o^t a(\tau)\, e^{-\xi\omega(t-\tau)}\, \sin\omega(t-\tau)\, d\tau \qquad (48)$$

It is easily seen from Eqs. (43a) and (48) that:

$$u_s(t) \simeq u_s^{DC}(t);\ \Delta\omega t \ll 1 \qquad (49)$$

The beat and envelope phenomena that characterize the response of undamped systems are also present in the response of damped systems. It is easily shown that the envelope of $u_s^{**}(t)$ is given once again by Eq. (31) where $u_1(t)$ and $u_2(t)$ are modified as follows to include the effects of damping:

$$u_1(t) \simeq \frac{1}{\omega\sqrt{\varepsilon}} \int_o^t a(\tau)\, e^{-\xi\omega(t-\tau)}\, \sin\omega\tau\, \sin\Delta\omega(t-\tau)\, d\tau -$$

$$- \frac{3}{2\omega} \int_o^t a(\tau)\, e^{-\xi\omega(t-\tau)}\, \cos\omega\tau\, \cos\Delta\omega(t-\tau)\, d\tau \qquad (50a)$$

$$u_2(t) \simeq \frac{1}{\omega\sqrt{\varepsilon}} \int_o^t a(\tau)\ e^{-\xi\omega(t-\tau)}\ \cos\omega\tau \sin\Delta\omega(t-\tau)\ d\tau +$$

$$+ \frac{3}{2\omega} \int_o^t a(\tau)\ e^{-\xi\omega(t-\tau)}\ \sin\omega\tau \cos\Delta\omega(t-\tau)\ d\tau \qquad (50b)$$

If, as seems likely, $|u_s'(t)| << |u_s^*(t)|$, then $u_s^{**}(t) \simeq u_s^*(t)$ and the envelope simplifies to:

$$E^{**}(t) \simeq \frac{1}{\omega\sqrt{\varepsilon}} \left[\left(\int_o^t a(\tau)\ e^{-\xi\omega(t-\tau)}\ \sin\omega\tau\ \sin\Delta\omega(t-\tau)\ d\tau\right)^2 + \right. \qquad (51)$$

$$\left. + \left(\int_o^t a(\tau)\ e^{-\xi\omega(t-\tau)}\ \cos\omega\tau\ \sin\Delta\omega(t-\tau)\ d\tau\right)^2\right]^{1/2} = E^*(t)$$

The integrals in Eqs. (50a,b) can be interpreted as linear combinations of the relative displacement and velocity of a damped SDF system subject to "ground accelerations" a(t) sin ωt and a(t) cos ωt. The damping ratio for this SDF system can be regarded as the "envelope damping ratio" because it governs the rate of decay of the beats of a freely oscillating damped tuned system. To obtain an expression for the envelope damping ratio, we rewrite the first integral in Eq. (51) in terms of SDF response as follows:

$$\int_o^t a(\tau)\ e^{-\xi\omega(t-\tau)}\ \sin\omega\tau\ \sin\Delta\omega(t-\tau)\ d\tau$$

$$= \int_o^t G(\tau)\ e^{-\xi^e\omega^e(t-\tau)}\ \sin\omega^e\sqrt{1-(\xi^e)^2}(t-\tau)\ d\tau \qquad (52)$$

where:

$$\xi^e = \frac{1}{\sqrt{1+\left(\frac{\Delta\omega}{\xi\omega}\right)^2}} = \frac{\xi}{\sqrt{\xi^2+\frac{\varepsilon^2}{4}}} \qquad (53a)$$

$$\omega^e = \sqrt{(\Delta\omega)^2 + (\xi\omega)^2} \qquad (53b)$$

$$G(\tau) = a(\tau)\ \sin\ \omega\tau \qquad (53c)$$

In light of the above discussion, the envelope damping ratio ξ^e is given by Eq. (53a) for a proportionally damped tuned system.

From Eq. (53a), it can be concluded that $\xi^e >> \xi$ since $\xi, \varepsilon << 1$. In other words, the envelope is damped much more heavily than the separate primary and secondary systems. It can also be concluded from Eq. (53a) that when $(\Delta\omega/\xi\omega) << 1$, $\xi^e \simeq 1$ and the envelope is critically damped. By analogy with critically damped SDF systems, this implies that the envelope does not oscillate, or that beats are absent from the response. The absence of beats, however, implies that there is no dynamic interaction between the primary and secondary systems. Consequently, one is led to conclude that when $(\Delta\omega/\xi\omega) << 1$, the primary and secondary systems are decoupled. This result, which has just been derived heuristically, was first derived rigorously by Caughey [4] using integral equation theory. A rigorous derivation using Eqs. (43a) and (47) can also be constructed as follows:

Subtracting Eq. (43a) from Eq. (47) and taking absolute values, we have:

$$|u_s^{DC}(t)-u_s(t)| \leq \frac{1}{2}\int_o^t \left|a(\tau)\ e^{-\xi\omega(t-\tau)}\left[(t-\tau) - \frac{\sin\Delta\omega(t-\tau)}{\Delta\omega}\right]\cos\omega(t-\tau)\right| d\tau +$$

$$+ \frac{3}{2\omega}\int_o^t \left|a(\tau)\ e^{-\xi\omega(t-\tau)}[1 - \cos\Delta\omega(t-\tau)]\sin\omega(t-\tau)\right| d\tau \qquad (54)$$

We assume that a(t) is bounded and therefore:

$$|a(t)| \leq a_{max} \qquad (55a)$$

where a_{max} is some number greater than 0. We also need the well-known results:

$$1 - \cos\Delta\omega(t-\tau) \geq 0 \qquad (55b)$$

$$(t-\tau) - \frac{\sin\Delta\omega(t-\tau)}{\Delta\omega} \geq 0 \qquad (55c)$$

Using Eqs. (55a-c) in Eq. (54), we have:

$$|u_s^{DC}(t) - u_s(t)| \leq \frac{1}{2} a_{max} \int_o^t e^{-\xi\omega(t-\tau)} \left[(t-\tau) - \frac{\sin\Delta\omega(t-\tau)}{\Delta\omega}\right] d\tau +$$

$$+ \frac{3}{2\omega} a_{max} \int_o^t e^{-\xi\omega(t-\tau)} \left[1 - \cos\Delta\omega(t-\tau)\right] d\tau$$

$$\leq \frac{1}{2} a_{max} \int_o^\infty e^{-\xi\omega\tau} \left[\tau - \frac{\sin\Delta\omega\tau}{\Delta\omega}\right] d\tau$$

$$+ \frac{3}{2\omega} a_{max} \int_o^\infty e^{-\xi\omega\tau} \left[1 - \cos\Delta\omega\tau\right] d\tau$$

$$= \frac{1}{2} a_{max} \cdot \frac{(\Delta\omega/\xi\omega)}{(\xi\omega)^2(1 + (\Delta\omega/\xi\omega)^2} + \frac{3}{2\omega} a_{max} \frac{(\Delta\omega/\xi\omega)^2}{\xi\omega(1 + (\Delta\omega/\xi\omega)^2)} \tag{56}$$

The result follows immediately from Eq. (56).

To illustrate the response of proportionally damped systems, the time histories of two secondary systems have been computed and plotted. The ground motion and system parameters are the same as those used in the illustrations of undamped response (see Figs. 4a-d) except for damping of $\xi = .01$ (i.e., one percent of critical) in the separate primary and secondary systems. The approximate time histories are plotted in Figs. 5a and 5c and the exact time histories are plotted in Figs. 5b and 5d. From these figures, it can be seen that the functions $u_s^{**}(t)$, $u_s^{*}(t)$ and their envelopes furnish satisfactory response data for damped as well as undamped systems.

2.3.3 Frequency Domain Analysis of Response

A frequency domain representation of the analytical results for proportionally damped systems is presented here. It will prove useful in analyzing nonproportionally damped systems and in obtaining response estimates.

The frequency domain representation is accomplished via the Fourier transform. Some basic definitions and theorems about Fourier transforms are presented here as background. For a detailed and lucid exposition on Fourier transforms, see [19].

The Fourier transform of a vector $\{x(t)\}$ is given by:

$$\{X(\Omega)\} = \int_{-\infty}^{\infty} \{x(t)\}\, e^{-i\Omega t}\, dt \tag{57}$$

where $i = \sqrt{-1}$, Ω is the frequency domain parameter, and $\{X(\Omega)\}$ is the transformed vector. We adopt the following notational convention for vectors: lower case refers to time domain representation and upper case to frequency domain representation. Equation (57) can be written symbolically as:

$$\{X(\Omega)\} = F(\{x(t)\}) \tag{58}$$

where $F(\cdot)$ denotes the linear Fourier transform operator.

The vector $x(t)$ can be recovered from $X(\Omega)$ using the inverse Fourier transform, which is given by:

$$\{x(t)\} = \frac{1}{2\pi} \int_{-\infty}^{\infty} \{X(\Omega)\}\, e^{i\Omega t}\, d\Omega = F^{-1}(\{X(\Omega)\}) \tag{59}$$

Since derivatives with respect to time appear in the equations of motion, it is useful to have a formula for the Fourier transform of a derivative. It is easily shown that:

$$F(\{\dot{x}(t)\}) = i\Omega F(\{x(t)\}) = i\Omega X(\Omega) \tag{60}$$

A repeated application of Eq. (58) shows further that:

$$F(\{\ddot{x}(t)\}) = i\Omega F(\{\dot{x}(t)\}) = -\Omega^2\{X(\Omega)\} \tag{61}$$

The frequency domain representation of $u(t)$ is readily obtained by straightforward application of Eqs. (57)-(61). Taking the Fourier transform of both sides of Eq. (38), we have

$$(-\Omega^2[M] + i\Omega[C] + [K])\{U(\Omega)\} = -[M]\{1\}A(\Omega) \tag{62}$$

Equation (62) is a set of simultaneous linear algebraic equations for the components of the vector:

$$\{U(\Omega)\} = \begin{Bmatrix} U_p(\Omega) \\ U_s(\Omega) \end{Bmatrix} \tag{63}$$

where $U_p(\Omega)$ and $U_s(\Omega)$ are the Fourier transforms of $u_p(t)$ and $u_s(t)$ respectively. Solving Eq. (62) for $U_s(\Omega)$ yields:

$$U_s(\Omega) = \frac{2\omega^2 + 4i\xi\omega\Omega - \Omega^2 + \varepsilon(\omega^2+2i\xi\omega\Omega)}{(\omega^2+2i\xi\omega\Omega-\Omega^2) - \varepsilon\Omega^2(2i\xi\omega\Omega+\omega^2)} \cdot A(\Omega) \tag{64}$$

$$= H_s(\Omega)\, A(\Omega) \tag{65}$$

The complex valued function $H_s(\Omega)$ defined in Eq. (65) will be referred to as the "transfer function". The role of the transfer function in the frequency domain is somewhat analogous to the role of the impulse response function in the time domain. In fact, as the notation implies, $h_s(t)$ and $H_s(\Omega)$ are related by Fourier transforms. To see this, we note that

$$F(\delta(t)) = \int_{-\infty}^{\infty} \delta(t)\, e^{-i\Omega t}\, dt = 1 \tag{66}$$

The result follows immediately from Eqs. (65) and (66) and the definition of $h_s(t)$.

Equation (65) was derived by transforming the equations of motion. An alternative derivation is now presented which makes direct use of the time domain solution. The time domain solution can be written:

$$u_s(t) = \int_0^t a(\tau)\, h_s(t-\tau)\, d\tau = \int_{-\infty}^{\infty} a(\tau)\, h_s(t-\tau)\, d\tau \tag{67}$$

The limits of integration may be shifted as shown because $a(t)$, $h(t) = 0$ when $t<0$. The Fourier transform of Eq. 67 is readily evaluated using the convolution theorem which states that for two functions $x(t)$ and $y(t)$:

$$F\left(\int_{\infty}^{\infty} x(t)y(t-\tau)\, dt\right) = X(\Omega)Y(\Omega) \tag{68}$$

Taking the Fourier transform of Eq. (67) and utilizing Eq. (68) yields:

$$F(u_s(t)) = A(\Omega)H_s(\Omega) = U_s(\Omega) \tag{69}$$

which is the same as Eq. (65).

We now wish to obtain approximations for $H_s(\Omega)$ that correspond to the approximate impulse response functions $h_s^*(t)$ and $h_s^{**}(t)$. This could be done by working directly with Eqs. (64) and (65). However, it is more convenient to take the Fourier transform of Eq. (44a). Straightforward calculation yields the following formulas:

$$H_s'(\Omega) = F(h_s'(t)) = -\frac{3}{2} \cdot \frac{(\xi\omega+i\Omega)^2 + (\omega^2-(\Delta\omega)^2)}{(\Omega-r_1)(\Omega-r_2)(\Omega\ r_3)(\Omega-r_4)} \tag{70a}$$

$$H_s^*(\Omega) = F(h_s^*(t)) = \frac{1}{2} \cdot \frac{(\xi\omega+i\Omega)^2 - (\omega^2-(\Delta\omega)^2)}{(\Omega-r_2)(\Omega-r_2)(\Omega-r_3)(\Omega-r_4)} \tag{70b}$$

$$H_s^{**}(\Omega) = H_s^*(\Omega) + H_s'(\Omega) = \frac{(\xi\omega+i\Omega)^2 - 2(\omega^2-(\Delta\omega)^2)}{(\Omega-r_1)(\Omega-r_2)(\Omega-r_3)(\Omega-r_4)} \tag{70c}$$

where:

$$r_{1,2} = i\xi\omega \pm (\omega+\Delta\omega) \tag{71a}$$

$$r_{3,4} = i\xi\omega \pm (\omega-\Delta\omega) \tag{71b}$$

The r_i in Eqs. (71a,b) can be shown to be good approximations for the roots of the denominator of $H(\Omega)$.

Using $H_s^*(\Omega)$ in place of $H_s(\Omega)$ in Eq. (65) gives an approximation for $U_s(\Omega)$ which is denoted:

$$U_s^*(\Omega) = H_s^*(\Omega)A(\Omega) \tag{72}$$

2.4 Response of Tuned Systems with Nonproportional Damping

The analysis of damped systems has so far been based on the simplifying assumption that $\gamma_s = \gamma_p$, or that the damping of the primary and secondary system are related to their stiffnesses by the same constant of propor-

tionality. This made it possible to solve the equations of motion using the modal method. If it is assumed more generally that $\gamma_s \neq \gamma_p$, the modal method is not applicable because the damping matrix cannot be diagonalized by the eigenmodes of the undamped system. While it is still possible to obtain a solution using an eigenfunction expansion (see [10]), it is easier to use frequency domain analysis.

The equations of motion are given symbolically by Eq. (38) with the stiffness and mass matrices as before. However, the damping matrix is:

$$[C] = \begin{bmatrix} \gamma_p K_p + {}_s K_s & -\varepsilon\gamma_s K_s \\ -\varepsilon\gamma_s K_s & \varepsilon\gamma_s K_s \end{bmatrix} \tag{73}$$

Taking the Fourier transform of Eq. (38) and utilizing Eqs. (71) and (34a,b) yields:

$$\begin{bmatrix} -\Omega^2+2i\xi_p\omega\Omega+\omega^2 & -\varepsilon(2i\xi_s\omega\Omega+\omega^2) \\ -\varepsilon(2i\xi_s\omega\Omega+\omega^2) & \varepsilon(\omega^2+2i\xi_s\omega\Omega+\omega^2) \end{bmatrix} \begin{Bmatrix} U_p(\Omega) \\ U_s(\Omega) \end{Bmatrix} = \begin{Bmatrix} -1 \\ -\varepsilon \end{Bmatrix} A(\Omega) \tag{74}$$

Solving Eq. (72) for $U_s(\Omega)$:

$$U_s(\Omega) = -\frac{(-\Omega^2+4i\xi_a\omega\Omega+2\omega^2) + \varepsilon(2i\xi_s\omega\Omega+\omega^2)}{(\Omega^2+2i\xi_a\omega\Omega+\omega^2)^2 + (\xi_d\omega\Omega)^2-\varepsilon\Omega^2(2i\xi_s\omega\Omega+\omega^2)} \cdot A(\Omega) \tag{75a}$$

$$= H_s(\Omega)\, A(\Omega) \tag{75b}$$

where

$$\xi_a = \frac{\xi_p + \xi_s}{2} \tag{75c}$$

$$\xi_d = \xi_p - \xi_s \tag{75d}$$

The function $H_s(\Omega)$ defined in Eqs. (75a,b) is the transfer function for nonproportionally damped systems. It reduces to the transfer function for proportionally damped systems (Eqs. (64) and (65)) when $\xi_p = \xi_s$.

We first consider the case of decoupled response, i.e., $\varepsilon = 0$. The transfer function becomes:

$$DC_{H_s}(\Omega) = \frac{-(-\Omega^2+4i\xi_a\omega\Omega+2\omega^2)}{(-\Omega^2+2i\xi_a\omega\Omega+\omega^2)^2 + (\xi_d\omega\Omega)^2} \tag{76}$$

Equation (76) can be inverted using contour integration [3] to obtain the impulse response function:

$$DC_{h_s}(t) = \frac{e^{-\xi_s\omega t}\cos\omega_s t - e^{-\xi_p\omega t}\cos\omega_p t}{(\xi_p - \xi_s)} - \frac{(2\xi_p-4\xi_s)\, e^{-\xi_p\omega t}\sin\omega_p t}{4\omega_p(\xi_p-\xi_s)} + \frac{(2\xi_s-4\xi_p)\, e^{-\xi_s\omega t}\sin\omega_s t}{4\omega_s(\xi_p-\xi_s)} \tag{77a}$$

where:

$$\omega_p = \omega\sqrt{1-\xi_p^2} \tag{77b}$$

$$\omega_s = \omega\sqrt{1-\xi_s^2} \tag{77c}$$

Neglecting terms ξ_p^2 and ξ_s^2 in Eqs. (77a-c), we obtain the approximate impulse response function:

$$DC_{h_s}^{**}(t) = \frac{1}{\xi_d\omega} e^{-\xi_a\omega t} \sinh\left(\frac{\xi_d\omega t}{2}\right)\cos\omega t - \frac{3}{2\omega} e^{-\xi_a\omega t}\cosh\left(\frac{\xi_d\omega t}{2}\right)\sin\omega t - \frac{\xi_a}{\xi_d\omega} e^{-\xi_a\omega t}\sinh\left(\frac{\xi_d\omega t}{2}\right)\sin\omega t \tag{78}$$

The Fourier transform of $DC_{h_s}^{**}(t)$ is given with sufficient accuracy by:

$$DC_{H_s}^{**}(t) = \frac{-(-\Omega^2+4i\xi_a\omega\Omega+2\omega^2)}{(\Omega-r_1)(\Omega-r_2)(\Omega-r_3)(\Omega-r_4)}$$

$$\simeq F(DC_{h_s}^{**}(t)) \simeq F(DC_{h_s}(t)) \tag{79}$$

in which:

$$r_{1,2} = i\xi_s\omega \pm \omega \tag{80a}$$

$$r_{2,3} = i\xi_p\omega \pm \omega \tag{80b}$$

We now consider the case of finite mass ratio, $\varepsilon>0$. It will be shown that the transfer function (Eqs. (75a,b)) can be simplified approximately to an expression having the general form of either Eq. (70c) or Eq. (79).

The first step is finding the roots of the denominator of $H_s(\Omega)$. We must solve the fourth order equation:

$$(-\Omega^2+2i\xi_a\omega\Omega+\omega^2)^2 = (2i\xi_s\omega\Omega+\omega^2)\varepsilon\Omega^2 - (\xi_d\omega\Omega)^2 \tag{81}$$

Equation (81) has, in general, four complex roots. The imaginary part of each root corresponds to damping and the real part of each root corresponds to the frequency of oscillation. Now, the damping should be small and the frequencies of oscillation should be close to $\pm\omega$. Accordingly, we expect at least one root to be of the form:

$$\Omega = a\omega i + \omega(1+b) \tag{82}$$

where a and b are real and $|a|$, $|b|<<1$. Substituting Eq. (82) for the first Ω on the right-hand side of Eq. (81) yields:

$$(-\Omega^2+2i\xi_a\omega\Omega+\omega^2)^2 = \omega^2\Omega^2(\varepsilon-\xi_d^2) + \omega^2\Omega^2\varepsilon\cdot 2\xi_s\omega i(ai\omega+b\omega+\omega) \tag{83}$$

If it is assumed that $\varepsilon-\xi_d^2 = 0(\varepsilon)$, the second term on the right-hand side of Eq. (83) can be neglected in light of our assumptions about the

magnitudes of ξ_s, a, and b. Equation (83) then becomes the biquadratic equation:

$$(-\Omega^2+2i\xi_a\omega\Omega+\omega^2)^2 = \Omega^2\omega^2(\varepsilon-\xi_d^2) \tag{84}$$

It is first assumed that $\varepsilon-\xi_d^2 > 0$. The case $\varepsilon-\xi_d^2 < 0$ will be treated later. The first two roots of Eq. (84) are:

$$\begin{aligned} r_{1,2} &= i\xi_a\omega \pm \delta\omega + \sqrt{\omega^2+(i\xi_a\omega+\delta\omega)^2} \\ &\simeq i\xi_a\omega \pm \delta\omega + \omega\left[1 + \frac{1}{2}\left(\frac{i\xi_a\omega+\delta\omega}{\omega}\right)^2\right] \\ &\simeq i\xi_a\omega \pm \delta\omega + \omega \end{aligned} \tag{85}$$

where:

$$\delta\omega = \frac{\omega\sqrt{\varepsilon-\xi_d^2}}{2} \tag{86}$$

A comparison of Eq. (82) with Eq. (83) shows that

$$a \simeq \xi_a \tag{87a}$$

$$b \simeq \pm \frac{\sqrt{\varepsilon-\xi_d^2}}{2} \tag{87b}$$

and the derivation of Eq. (85) is fully justified. It can be shown that the other two roots of Eq. (84) are also approximate solutions of Eq. (81); these roots are:

$$\begin{aligned} r_{3,4} &= i\xi_a\omega \pm \delta\omega - \sqrt{\omega^2 + (i\xi_a\omega\pm\delta\omega)^2} \\ &\simeq i\xi_a\omega \pm \delta\omega - \omega \end{aligned} \tag{88}$$

The r_i in Eqs. (85) and (88) can be used to construct an approximation for the denominator of $H_s(\Omega)$. Replacing the exact denominator by this approximation and rearranging terms yields:

$$H_s(\Omega) \simeq -\frac{(\xi_a\omega+i\Omega)^2 - 2\omega^2 + 2(\delta\omega)^2 + \omega^2(\frac{\varepsilon}{2} + \frac{\xi_d^2}{2} + \xi_a)^2 - 2i\omega\xi_a(1-\varepsilon)}{(\Omega-r_1)(\Omega-r_2)(\Omega-r_3)(\Omega-r_4)} \tag{89a}$$

$$\simeq -\frac{(\xi_a\omega+i\Omega)^2 - 2\omega^2 + 2(\delta\omega)^2}{(\Omega-r_1)(\Omega-r_2)(\Omega-r_3)(\Omega-r_4)} = H_s^{**}(\Omega) \tag{89b}$$

The last two terms in the numerator of Eq. (89a) are subsequently neglected because inversion shows that they contribute little to the response.

Comparing Eq. (89b) with Eq. (70c) shows that $H_s^{**}(\Omega)$ from Eq. (89b) is the transfer function of a proportionally damped tuned system with damping ratio ξ_a and mass ratio $(\varepsilon-\xi_d^2)$. Consequently when $\varepsilon-\xi_d^2 > 0$,

$$u_s^{**}(t) = -\frac{3}{2\omega}\int_0^t a(\tau)e^{-\xi_a\omega(t-\tau)} \sin\omega(t-\tau)\cos\delta\omega(t-\tau)d\tau$$

$$+\frac{2}{\delta\omega}\int_0^t a(\tau)e^{-\xi_a\omega(t-\tau)} \sin\delta\omega(t-\tau)\cos\omega(t-\tau)d\tau \tag{90}$$

We now consider the case $\varepsilon-\xi_d^2 < 0$. The roots of Eq. (84) are given by:

$$r_{1,2} \simeq \xi'\omega i \pm \omega \tag{91a}$$

$$r_{3,4} \simeq \xi_s'\omega i \pm \omega \tag{91b}$$

in which:

$$\xi_p' = \xi_a + \frac{\sqrt{\xi_d^2-\varepsilon}}{2} \tag{92a}$$

$$\xi_s' = \xi_a - \frac{\sqrt{\xi_d^2-\varepsilon}}{2} \tag{92b}$$

The r_i in Eqs. (91a,b) can be used to construct an approximation for the denominator of $H_s(\Omega)$. The transfer function is then given with sufficient accuracy by:

$$H_s(\Omega) \simeq - \frac{(-\Omega^2+4i\xi_a\omega\Omega+2\omega^2) + \varepsilon(2i\xi_s\omega\Omega+\omega^2)}{(\Omega-r_1)(\Omega-r_2)(\Omega-r_3)(\Omega-r_4)}$$

$$\simeq - \frac{(-\Omega^2+4i\xi_a\omega\Omega+2\omega^2)}{(\Omega-r_1)(\Omega-r_2)(\Omega-r_3)(\Omega-r_4)} = H_s^{**}(\Omega) \tag{93}$$

Comparing Eq. (93) with (79) shows that $H_s^{**}(\Omega)$ from Eq. (93) is the transfer function of a decoupled tuned secondary system with damping ratio ξ_s' attached to a primary system with damping ξ_p'. Consequently, when $\varepsilon-\xi_d^2 < 0$,

$$u_s^{**}(t) = \frac{1}{\xi_d'\omega}\int_0^t a(\tau)e^{-\xi_a\omega(t-\tau)} \sinh \frac{\xi_d'\omega}{2}(t-\tau)\cos\omega(t-\tau)d\tau$$

$$- \frac{3}{2\omega}\int_0^t a(\tau)e^{-\xi_a\omega(t-\tau)} \cosh \frac{\xi_d'\omega}{2}(t-\tau)\sin\omega(t-\tau)d\tau$$

$$- \frac{\xi_a}{\xi_d'\omega}\int_0^t a(\tau)e^{-\xi_a\omega(t-\tau)} \sinh \frac{\xi_d'\omega}{2}(t-\tau)\sin\omega(t-\tau)d\tau \tag{94}$$

where:

$$\xi_d' = \xi_p' - \xi_s' = \sqrt{\xi_d^2 - \varepsilon} \tag{95}$$

Since the decoupled analysis is widely used (sometimes incorrectly) by engineers in practice, the analyst may often have response data available based on Eq. (94). Consequently, it will be assumed that when

nonclassical damping is present, $\varepsilon - \xi_d^2 > 0$ since this requires a more elaborate analysis which includes dynamic interaction between effective primary and secondary systems.

2.5 Response of Slightly Detuned Systems

We have thus far considered systems in which the secondary system is precisely tuned to the primary system. In practice, an analyst or designer is more likely to encounter situations in which the primary and secondary systems have frequencies which are close together but differ slightly. In this section, the results of Section 2.3 are modified to include this possibility.

Consider the system of Figure 1. The frequencies of the primary and secondary systems are given by:

$$\frac{K_p}{M_p} = \omega^2 \tag{96a}$$

$$\frac{K_s}{M_s} = \omega^2(1+d\sqrt{\varepsilon}) \tag{96b}$$

in which the magnitude of d is such that

$$|d\sqrt{\varepsilon}| \ll 1 \tag{97}$$

It is assumed that damping is proportional to stiffness or:

$$C_p = \gamma K_p = 2\xi M_p \omega \tag{98a}$$

$$C_s = \gamma K_s = 2\xi M_p \omega\varepsilon(1+d\sqrt{\varepsilon}) \tag{98b}$$

The equations of motion are given symbolically by Eq. (38) where [M] is as before and:

$$[K] = K_p \begin{bmatrix} 1+\varepsilon(1+d\sqrt{\varepsilon}) & -\varepsilon(1+d\sqrt{\varepsilon}) \\ -(1+d\sqrt{\varepsilon}) & (1+d\sqrt{\varepsilon}) \end{bmatrix} \tag{99a}$$

$$[C] = \gamma[K] \tag{99b}$$

The equations can be solved exactly using the modal method and the solution can be simplified approximately to yield a convenient formula for the response. The calculations closely parallel those of Sections 2.2.1 and 2.3.1 but are much more tedious. The final result is:

$$u_s(t) \simeq \frac{1}{\omega\sqrt{\varepsilon}^{\#}} \int_0^t a(\tau) e^{-\xi\omega^{\#}(t-\tau)} \sin \Delta\omega^{\#}(t-\tau) \cos \omega^{\#}(t-\tau) d\tau$$

$$- \frac{3}{2\omega} \int_0^t a(\tau) e^{-\xi\omega^{\#}(t-\tau)} \cos \Delta\omega^{\#}(t-\tau) \sin \omega^{\#}(t-\tau) d\tau \qquad (100)$$

in which:

$$\varepsilon^{\#} = \left(1 + \frac{d^2}{4}\right) \varepsilon \qquad (101a)$$

$$\omega^{\#} = \left(1 + \frac{d\sqrt{\varepsilon}}{4}\right) \omega \qquad (101b)$$

$$\Delta\omega^{\#} = \frac{\omega\sqrt{\varepsilon}^{\#}}{2} \simeq \frac{\omega^{\#}\sqrt{\varepsilon}^{\#}}{2} \qquad (101c)$$

A comparison of Eq. (100) with Eq. (43a) shows that the response of a proportionally damped, slightly detuned system is similar to the response of a tuned system with mass ratio $\varepsilon^{\#}$ and tuned frequency $\omega^{\#}$. This result underscores the importance of the results in Sections 2.2 and 2.3 and further justifies the attention that has been devoted to tuned systems.

CHAPTER 3. RESPONSE ESTIMATES FOR TWO-DEGREE-OF-FREEDOM TUNED SYSTEMS

3.1 Introduction

In Chapter 2, we derived some simplified formulas for accurately computing the response of a tuned secondary system. While evaluation of these formulas is straightforward, it is often quite tedious and must usually be done on a computer. Consequently, use of these formulas is usually warranted only in the final stages of design when the final structural model has taken shape and the need for accuracy is greatest. In the early stages of design, when the structural model is only tentative, it is more useful and appropriate to estimate the maximum dynamic response using approximate but simple procedures.

In this chapter, we use the analytical results and insights of Chapter 2 to obtain simple estimates for the maximum response of a tuned secondary system. The analyses are restricted to proportionally damped systems, but as was shown in Secs. 2.4 and 2.5, the results are directly applicable to many non-proportionally damped and detuned systems. First, a rigorous, closed form solution is derived in the time domain for ground motions of short duration. Then, an alternative derivation is presented using frequency domain arguments. Finally, a combination of time domain and frequency domain arguments is used to extend the estimate heuristically to cover ground motions of long duration. The accuracy of the response estimates is assessed in Chapter 4.

3.2 Response Estimates for Ground Motions of Short Duration

3.2.1 Time Domain Analysis

We derive here a rigorous, closed form solution for the maximum response of a secondary system when the ground motion is of short duration. For the time being, "short duration" means simply a time duration, t_d, that is much less than the beat period, or $\Delta\omega t_d \ll 1$. Later, it will be seen that an additional requirement must also be satisfied in order for a gound motion to be considered short.

Before proceeding with the derivation, it proves useful to examine in detail the response of a particular system to a short duration ground motion.

Consider, as an extreme case, a tuned secondary system with $\omega = .25\pi$, $\varepsilon = .0036$ and $\xi = .01$. The period of the separate primary and secondary systems is 8 seconds and the beat period (Eq. (26)) is 267 seconds. Let this system be excited by the earthquake El Centro 1940-NS , which lasts 33 seconds and is plotted in Fig. 10.

The exact secondary system response to the earthquake is plotted in Fig. 6a. As in Figs. 3a-d, 4a-d, the solid curve is the response time history and the dashed curve is the envelope. From Fig. (6a) it can be seen that the maximum secondary system response is virtually identical to the envelope peak of the first beat lobe. This takes place at about t = 70 seconds, which is well after the earthquake ends. Indeed, most of the first beat lobe and much of the rise to its peak takes place after the earthquake ends, or when the system is in free vibration. This suggests that it might be useful to compare this response to that caused by an impulse function, for then the entire response is free vibration.

Accordingly, let us now excite the same system by the "ground motion" $a(t) = I\delta(t)$ where I is the impulse intensity. The value of I is adjusted so that the maximum response is the same as that caused by the earthquake. The resulting response is plotted in Fig. 6b. It is evident that the response caused the earthquake (Fig. 6a) is substantially the same as the response caused by the impulse. It will be seen shortly that this is generally the case when the ground motion is of short duration.

We now proceed to derive an estimate for the maximum secondary system response. It is assumed that the response is given with sufficient accuracy by $u_s^*(t)$ (Eqs. (43a,b)); this will be checked later. With negligible loss of accuracy, the envelope response will be used throughout.

The envelope of $u_s^*(t)$ is given by Eq.(51), which is reproduced here:

$$E^*(t) \simeq \frac{1}{\omega\sqrt{\varepsilon}}\Big[\Big(\int_0^t a(\tau)\, e^{-\xi\omega(t-\tau)}\, \sin\omega\tau\, \sin\Delta\omega(t-\tau)\, d\tau\Big)^2 + \Big(\int_0^t a(\tau)\, e^{-\xi\omega(t-\tau)}\, \cos\omega\tau\, \sin\Delta\omega(t-\tau)\, d\tau\Big)^2\Big]^{\frac{1}{2}} \qquad (51)$$

It is expected that the maximum response will take place after the end of the ground motion, or when $t > t_d$. For this portion of the response, we

have, after some manipulation:

$$E^*(t) \simeq \frac{e^{-\xi\omega t}}{\omega\sqrt{\varepsilon}} \Big[\Big(\sin\Delta\omega t \int_o^{t_d} a(\tau)\, e^{\xi\omega\tau} \sin\omega\tau \cos\Delta\omega\tau\, d\tau - \cos\Delta\omega t \int_o^{t_d} a(\tau)\, e^{\xi\omega\tau} \sin\omega\tau \sin\Delta\omega\tau\, d\tau\Big)^2 + \Big(\sin\Delta\omega t \int_o^{t_d} a(\tau)\, e^{\xi\omega\tau} \cos\omega\tau \cos\Delta\omega\tau\, d\tau - \cos\Delta\omega t \int_o^{t_d} a(\tau)\, e^{\xi\omega\tau} \cos\omega\tau \sin\Delta\omega\tau\, d\tau\Big)^2\Big]^{\frac{1}{2}};\ t>t_d \qquad (102)$$

Now by assumption, $\Delta\omega t_d << 1$ and we can use the approximations $\sin\Delta\omega\tau \simeq \Delta\omega\tau << 1$, $\cos\Delta\omega\tau \simeq 1$ in the integrals of Eq. (102). This leads us to expect that the coefficient of each $\cos\Delta\omega t$ will be considerably less than the coefficient of the $\sin\Delta\omega t$ enclosed within the same wet of parentheses. Consequently, it seems reasonable to neglect the terms containing $\cos\Delta\omega t$ in Eq. (102) and we have:

$$E^*(t) \simeq \frac{e^{-\xi\omega t}}{\omega\sqrt{\varepsilon}} |\sin\Delta\omega t| \, x \, x\Big[\Big(\int_o^{t_d} a(\tau)\, e^{\xi\omega\tau} \sin\omega\tau\, d\tau\Big)^2 + \Big(\int_o^{t_d} a(\tau)\, e^{\xi\omega\tau} \cos\omega\tau\, d\tau\Big)^2\Big]^{\frac{1}{2}};\ t>t_d \qquad (103)$$

It now proves necessary to introduce the requirement $\xi\omega t_d << 1$; this is the second requirement that must be satisfied if a ground motion is to be considered short. When $\xi\omega t_d << 1$, $e^{\xi\omega\tau} \simeq 1$ and we have:

$$E^*(t) \simeq \frac{e^{-\xi\omega t}}{\omega\sqrt{\varepsilon}} |\sin\Delta\omega t| \Big[\Big(\int_o^{t_d} a(\tau) \sin\omega\tau\, d\tau\Big)^2 + \Big(\int_o^{t_d} a(\tau) \cos\omega\tau\, d\tau\Big)^2\Big]^{\frac{1}{2}}$$

$$\simeq \frac{e^{-\xi\omega t}}{\omega\sqrt{\varepsilon}} |\sin\Delta\omega t| \, |A(\omega)|;\ t>t_d \qquad (104)$$

where $|A(\omega)|$ is the norm of the Fourier transform, or as it is more commonly referred to, the Fourier amplitude spectrum.

Let us now see what happens when the ground acceleration is an impulse function. Using $a(\tau) = I\delta(\tau)$ in Eq. (51) gives:

$$E^*(t) = \frac{e^{-\xi\omega t}}{\omega\sqrt{\varepsilon}} |\sin\Delta\omega t| \; |I| \tag{105}$$

Comparing Eq. (104) with Eq. (105), it is seen that the envelope response to a short ground motion is given approximately by the envelope response to an impulse of intensity $|A(\omega)|$.

The maximum secondary system response, which we denote u_s^{max}, is virtually identical to the maximum envelope response. Using Eq. (104), it is easily shown that:

$$u_s^{max} \simeq \frac{|A(\omega)|e^{-\frac{\xi\omega}{\Delta\omega}\tan^{-1}(\frac{\Delta\omega}{\xi\omega})}}{2((\Delta\omega)^2 + (\xi\omega)^2)^{\frac{1}{2}}}; \; \Delta\omega t_d << 1, \; \xi\omega t_d << 1$$

An important special case is when the mass ratio is so small that a decoupled analysis is valid for all t. The maximum response obtained from a decoupled analysis is often called the "floor spectrum" and is denoted FS_{u_s}. The floor spectrum for short duration ground motions is obtained by letting $\Delta\omega$ approach zero in Eq. (106). This yields:

$$FS_{u_s} \simeq \frac{|A(\omega)|e^{-1}}{2\xi\omega}; \; \xi\omega t_d << 1 \tag{107}$$

Equation (106) enables us to check an important assumption used in its derivation; namely, that $u_s^*(t) \simeq u_s^{**}(t)$. From Eq. (43b), it is evident that the maximum error introduced by this assumption is bounded by $\max_t |u_s'(t)|$ which can be estimated as follows:

From Eqs. (43a,b) we have:

$$u_s(t) \simeq u_s^{**}(t) = u_s'(t) + u_s^*(t) \tag{43b}$$

$$u_s'(t) = -\frac{3}{2\omega}\int_o^t a(\tau)\ e^{-\xi\omega(t-\tau)}\ \sin\omega(t-\tau)\ \cos\Delta\omega(t-\tau)\ d\tau$$

$$= -\frac{3}{4\omega}\int_o^t a(\tau)\ e^{-\xi\omega(t-\tau)}\ \sin(\omega-\Delta\omega)(t-\tau)\ d\tau -$$

$$-\frac{3}{4\omega}\int_o^t a(\tau)\ e^{-\xi\omega(t-\tau)}\ \sin(\omega+\Delta\omega)(t-\tau)\ d\tau \qquad (108)$$

From Eq. (108) it is evident that:

$$\max_t|u_s'(t)| \leq \frac{3}{4\omega}(S_V(\omega-\Delta\omega,\xi) + S_V(\omega+\Delta\omega,\xi)) \qquad (109a)$$

where $S_V(\omega,\xi)$ is the pseudo-velocity spectrum of a(t) at circular frequency ω and damping ratio ξ. The pseudo-velocity spectrum is usually fairly constant in the frequency interval $[\omega-\Delta\omega,\omega+\Delta\omega]$ for most values of ω and ε of practical interest and it can be concluded that:

$$\max_t|u_s'(t)| \leq \frac{3}{2\omega}\ S_V(\omega,\xi) \qquad (109b)$$

In view of Eqs. 106, 43b and (109b), $u_s(t) \simeq u_s^*(t)$ if:

$$\frac{3}{2\omega}S_V(\omega,\xi) << \frac{|A(\omega)|e^{-\frac{\xi\omega}{\Delta\omega}\tan^{-1}\frac{\Delta\omega}{\xi\omega}}}{2((\Delta\omega)^2 + (\xi\omega)^2)^{\frac{1}{2}}} \qquad (110)$$

It can be easily shown that:

$$\frac{e^{-\frac{\xi\omega}{\Delta\omega}\tan^{-1}\frac{\Delta\omega}{\xi\omega}}}{\sqrt{(\Delta\omega)^2+(\xi\omega)^2}} >> \frac{1}{\omega} \qquad (111)$$

and, therefore, Ineq. (110) is satisfied if:

$$S_V(\omega,\xi) = 0(|A(\omega)|) \qquad (112)$$

Inequality (112) generally holds for most ground motions of practical interest, and in fact, $S_V(\omega,0)$ is often used as a conservative, first order estimate for $|A(\omega)|$ (see [9] and [26]). However, as will be seen in

Chapter 4, there are instances when $S(\omega,\xi) >> |A(\omega)|$ to such an extent that Ineq. (110) is violated. In these instances, $u_s'(t)$ must be considered in the computation of $u_s(t)$ and Eqs. (106b) and (107) are rendered invalid.

3.2.2 Frequency Domain Analysis

In this article, the results of Sec. 3.2.1 are rederived using a frequency domain analysis. The alternative derivation sheds new light on the results and is essential for the development of response estimates for long duration earthquakes.

In Chapter 2, it was shown that a Fourier transform analysis of the equations of motion gives:

$$u_s(t) = F^{-1}(U_s(\Omega)) = \frac{1}{2\pi}\int_{-\infty}^{\infty} H_s(\Omega)A(\Omega)e^{i\Omega t}d\omega \tag{112}$$

It is assumed that $H_s(\Omega) \simeq H_s^*(\Omega)$; this is equivalent to assuming $u_s(t) \simeq u_s^*(t)$ as was done in Sec. 3.2.1. Replacing $H_s(\Omega)$ by $H_s^*(\Omega)$ in Eq. (112) yields:

$$u_s^*(t) = \frac{1}{2\pi}\int_{-\infty}^{\infty} H_s^*(\Omega)A(\Omega)e^{i\Omega t}d\Omega \tag{113}$$

Certain properties of $H_s^*(\Omega)$ enable us to evaluate the integral in Eq. (113) in closed form when the ground motion is of short duration. The analysis presented here closely follows the one used by Papoulis (Ref. [19] Chapter 7).

From Eqs. (44a,b) we have:

$$h_s^*(t) = \frac{1}{\omega\sqrt{\varepsilon}}e^{-\xi\omega t}\sin\Delta\omega t\cos\omega t \tag{114}$$

Let us define:

$$h_s^{\ell}(t) = \frac{1}{2\omega\sqrt{\varepsilon}}e^{-\xi\omega t}\sin\Delta\omega t \tag{115a}$$

$$h_s^1(t) = h_s^{\ell}(t)e^{-i\omega t} \tag{115b}$$

$$h_s^2(t) = h_s^{\ell}(t)e^{i\omega t} \tag{115c}$$

It is apparent that:

$$h_s^*(t) = h_1(t) + h_2(t) \tag{116a}$$

$$H_s^*(\Omega) = H_1(\Omega) + H_2(\Omega) \tag{116b}$$

By virtue of the shifting property of Fourier Transforms [4], $H_s^1(\Omega)$ is obtained by shifting $H_s^\ell(\Omega)$ an amount $-\omega$ along the frequency axis. Similarly, $H_s^2(\Omega)$ is obtained by shifting $H_s^\ell(\Omega)$ an amount $+\omega$ along the frequency axis.

The relationships among the various transfer functions can be visualized with the aid of Figs. 7a-c where plots of $|H_s^\ell(\Omega)|$, $|H_s^1(\Omega)|$, $|H_s^2(\Omega)|$, and $|H_s(\Omega)|$ have been drawn. The plots have been normalized with respect to max $|H_s(\Omega)|$ and scales have been omitted from the ordinate axes. The system parameters are ω=1 RPS, ε=.0256, and ξ=.04.

Figures 7a-c reveal important information about the frequency sensitivity of the transfer functions. It can be seen that $H_s^1(\Omega)$ has significant values only in the frequency band $(\omega-\delta_b, \omega+\delta_b)$ where δ_b is some number with $S_b << \omega$. Similarly, it can be seen that $H_s^2(\Omega)$ has significant values only in the frequency band $(-\omega-\delta_b, -\omega+\delta_b)$. However, $H_s^*(\Omega)$ is significant in both $(\omega+\delta_b, \omega+\delta_b)$ and $(-\omega-\delta_b, -\omega+\delta_b)$. From the bandedness of the transfer functions and Eq. (116), it can be concluded that:

$$\begin{aligned} H_s^2(\Omega) &\simeq H_s^*(\Omega), \quad \Omega \geq 0 \\ H_s^2(\Omega) &\simeq 0, \quad \Omega \leq 0 \end{aligned} \tag{117a}$$

$$\begin{aligned} H_s^1(\Omega) &\simeq H_s^*(\Omega), \quad \Omega < 0 \\ H_s^1(\Omega) &\simeq 0, \quad \Omega \geq 0 \end{aligned} \tag{117b}$$

The definition of the half-bandwidth, δ_b, is somewhat subjective. Each bandpass should include the two peaks that correspond to the characteristic frequencies of the system and some additional interval which increases with damping. In this study, satisfactory results were obtained using:

$$\delta_b = 2\xi\omega, \quad \varepsilon=0 \tag{118a}$$

$$\delta_b = \Delta\omega+\xi\omega, \quad \varepsilon>0 \tag{118b}$$

The bandedness of $H_s^*(\Omega)$ considerably simplifies the task of approximating $u_s^*(t)$, because instead of using the exact $A(\Omega)$ in Eq. (112), we can use any well-behaved functions that coincide with $A(\Omega)$ in the bandpasses. In other words, we can say:

$$u_s^*(t) \simeq \frac{1}{2\pi}\int_{-\infty}^{\infty} H_s^2(\Omega)\ A_2(\Omega)\ e^{i\Omega t}\ d\Omega + \frac{1}{2\pi}\int_{-\infty}^{\infty} H_s^1(\Omega)\ A_1(\Omega)\ e^{i\Omega t}\ d\Omega \tag{119}$$

where $A_2(\Omega)=A(\Omega)$ in the interval $(-\omega-\delta_b,\ -\omega+\delta_b)$ and $A_1(\Omega)=A(\Omega)$ in the interval $(\omega-\delta_b,\ \omega+\delta_b)$.

Equation (119) can often be used to obtain an approximation for $u_s^*(t)$ if $A(\Omega)$ behaves simply in the bandpasses. Let us assume that $A(\Omega)$ is constant in the bandpasses. We can write:

$$A(\Omega) = \begin{cases} |A(\omega)|e^{i\theta}, & \omega-\delta_b<\Omega<\omega+\delta_b \\ |A(\omega)|e^{-i\theta}, & -\omega-\delta_b<\Omega<-\omega+\delta_b \end{cases} \tag{120}$$

where θ is a constant phase angle. Suitable $A_1(\Omega)$ and $A_2(\Omega)$ are:

$$A_1(\Omega) = |A(\omega)|e^{i\theta} \tag{121}$$

$$A_2(\Omega) = |A(\omega)|e^{-i\theta} \tag{122}$$

Substituting Eqs. (121) and (122) into Eq. (119 gives:

$$\begin{aligned} u_s^*(t) &\simeq |A(\omega)|e^{-i\theta}F^{-1}(H_s^2(\Omega)) + |A(\omega)|e^{i\theta}F^{-1}(H_s^1(\Omega)) \\ &= |A(\omega)|\frac{e^{-\xi\omega t}}{\omega\sqrt{\varepsilon}}\sin\Delta\omega t\ \cos(\omega t+\theta) \end{aligned} \tag{123}$$

The envelope is:

$$E^*(t) \simeq |A(\omega)|\frac{e^{-\xi\omega t}}{\omega\sqrt{\varepsilon}}|\sin\Delta\omega t| \tag{124}$$

Equation (124) is in agreement with Eq. (104) and the response maximum is given by Eq. (106).

We have thus been able to obtain the same estimate for maximum response using time domain and frequency domain analyses. However, these derivations used different sets of assumptions regarding the ground motion. The time domain derivation used the assumptions $\Delta\omega t_d << 1$ and $\xi\omega t_d << 1$; these will henceforth be called the "time conditions." The frequency domain analysis used the assumption that the Fourier transform of the ground motion is constant in the bandpass zones; this will henceforth be known as the "bandpass condition." The relationships between the time conditions and the bandpass condition will now be examined.

We first show that the bandpass condition is satisfied if the time conditions are satisfied. To see this, consider the real part of $A(\Omega)$, which is given by:

$$R(A(\Omega)) = \int_0^{t_d} a(\tau)\ \cos\omega\tau\ d\tau \tag{125}$$

At the far end of the bandpass zone on the positive axis:

$$\begin{aligned} R(A(\omega+\Delta\omega+\xi\omega)) &= \int_0^{t_d} a(\tau)\cos(\omega+\Delta\omega+\xi\omega)\,d\tau \\ &= \int_0^{t_d} a(\tau)\cos\omega\tau\cos(\Delta\omega+\xi\omega)\tau d\tau - \int_0^{t_d} a(\tau)\sin\omega\tau\sin(\Delta\omega+\xi\omega)\tau d\tau \end{aligned} \tag{126}$$

From Eq. (126), it can be shown that when $\Delta\omega t_d$ and $\xi\omega t_d$ are sufficiently small, $R(A(\omega+\Delta\omega+\xi\omega))\simeq R(A(\omega))$. A similar result applies to the imaginary part of $A(\Omega)$. Consequently, when the time conditions are satisfied, $A(\omega+\Delta\omega+\xi\omega)\simeq A(\omega)$. The remainder of the proof is similar.

We will now show that the converse of the last result is not true. That is, the time conditions need not hold if the bandpass condition is satisfied. It proves useful to first introduce the notion of "effective time duration," t_d^e, which we define as the duration of the uninterrupted portion of the ground motion that contributes significantly to the frequency content in the vicinity of ω. We are motivated to introduce this notion by the observation that for many earthquakes, the spectral content

is determined by a relatively short segment where the acceleration amplitude is greatest. Let us imagine a ground motion whose effective duration is such that $\Delta\omega t_d^e << 1$ and $\xi\omega t_d^e << 1$ but whose true duration is such that the original time conditions are violated. It is apparent that for this ground motion, the bandpass condition is satisfied even though the time conditions are not and our result is proved.

The bandpass condition, as it has thus far been defined, requires that both the real and imaginary parts of $A(\Omega)$ be constant in the bandpasses. However, a shift of a(t) along the time axis can significantly alter these functions but does not change the maximum response of the secondary system. It will therefore be assumed in what follows that the bandpass condition is satisfied if $|A(\Omega)|$, which is unaltered by a time shift of a(t), is constant in the bandpasses.

3.3 Response Estimates for Ground Motions of Long Duration

3.3.1 Preliminary Discussion

A ground motion is said to be of long duration if its Fourier amplitude spectrum is not constant in the bandpass zones; that is, when the bandpass condition defined in Sec. 3.2.2 is violated.

Before treating the problem of estimating the response to long ground motions, we examine briefly the following examples which illustrate the differences between short and long ground motions.

Figure (10a) represents the frequency domain data relevant to the short ground motion example that was discussed in Sec. 3.2.1. The solid curve in Fig. (7a) is a portion of the Fourier amplitude spectrum of the earthquake El Centro 1940-NS. The dashed curve is part of $|H_s^*(\Omega)|$ for a tuned system with ω=.25πRPS, ε=.0036, and ξ=.01. It is apparent from Fig. 10a that the Fourier amplitude spectrum is virtually constant in the bandpass. This is to be expected since it was shown in Sec. 3.2.1 that the strict time conditions are satisfied by the ground motion and system under consideration. Let us now see what happens when the ground motion is kept the same but the system is modified by raising the tuned frequency to ω=20πRPS. The frequency domain data relevant to this case is shown in Fig. 10b. We see that the Fourier amplitude spectrum now fluctuates considerably in the bandpass, an important consequence of the long duration excitation.

We now turn to the problem at hand, i.e., estimating the maximum response to long ground motions. This proves to be much more difficult than estimating the response to short ground motions. A simple, rigorous closed form solution that is applicable to all long duration ground motions does not appear to be possible since, as will be seen, the details of Fourier spectrum in the bandpass matter very much.

Long ground motions can be classifed according to the degree of the polynomials needed to represent $A(\Omega)$ adequately in the bandpasses. From this point of view, a short ground motion can be regarded as one for which $A(\Omega)$ can be approximated by a constant in the bandpasses. Obviously, the next approximation for $A(\Omega)$ that should be considered is a linear function; this is a reasonable method of attack for the shorter end of the long duration range. In principle, it is possible to continue the process and obtain results for quadratic and higher order variations of $A(\Omega)$. In practice, the higher order analyses are tedious to perform and yield formulas that are wholly unsuited for use as simple approximations. Consequently, in what follows we shall present detailed analyses only for long ground motions where $A(\Omega)$ varies linearly in the bandpasses. Although the results from such analyses would appear to have only limited applicability, it will be seen that they do, in fact, provide useful information about the response of secondary systems to long ground motions in general.

The case where $A(\Omega)$ exhibits linear bandpass behavior is taken up in Sec. 3.3.2. An approximate response formula corresponding to such behavior is derived using time and frequency domain analyses. In Sec. 3.3.3, the results of Sec. 3.3.2 are used in conjunction with heuristic arguments to develop response estimates for long duration ground motions.

3.3.2 Analysis of Response for Linear Variation of $A(\Omega)$ in Bandpasses

Although the ground motions considered here are defined in terms of their frequency domain characteristics, it proves instructive to begin with a time domain derivation.

Take a ground motion that violates the short duration time conditions but is still short enough to ensure that the maximum response occurs after the ground motion ends. For simplicity, it is assumed that $t_d = t_d^e$. When $t > t_d$, the envelope is given by Eq. (102). The slowly varying exponential

and sinusoidal terms in the integrands of Eq. (102) have the series representations:

$$e^{\xi\omega\tau} = 1 + \xi\omega\tau + \frac{(\xi\omega\tau)^2}{2!} + \quad \ldots \tag{127a}$$

$$\sin\Delta\omega\tau = \Delta\omega\tau - \frac{(\Delta\omega\tau)^3}{3!} + \ldots \tag{127b}$$

$$\cos\Delta\omega\tau = 1 - \frac{(\Delta\omega\tau)^2}{2} + \ldots \tag{127c}$$

In Sec. 3.2.1, the time conditions enabled us to neglect all but the constant terms in the series. Obviously, the next category of ground motions we should consider are those whose durations necessitate the inclusion of the linear as well as the constant terms in the series. In general, the linear terms must be included when $\Delta\omega t_d$ and $\xi\omega t_d$ are significant but $\frac{(\Delta\omega t_d)^2}{2} << 1$ and $\frac{(\xi\omega t_d)^2}{2} << 1$. We then have for $\tau \leq t_d$:

$$e^{\xi\omega\tau} \simeq 1 + \xi\omega\tau \tag{128a}$$

$$\sin\Delta\omega\tau \simeq \Delta\omega\tau \tag{128b}$$

$$\cos\Delta\omega\tau \simeq 1 \tag{128c}$$

Substituting Eqs. (128a-c) into Eq. (102) and neglecting second-order product terms, we have:

$$E^*(t) = \frac{e^{-\xi\omega t}}{\omega\sqrt{\varepsilon}} \{\sin^2\Delta\omega t[|A(\omega)| + 2\xi\omega(F_c F_s' - F_s F_c') + (\xi\omega)^2((F_s')^2 + F_c')^2)] +$$

$$+ \sin\Delta\omega t[(\Delta\omega)(F_s F_c' - F_c F_s') - (\Delta\omega)(\xi\omega)((F_s') + (F_c')^2)] +$$

$$+ \cos^2\Delta\omega t[(\Delta\omega)^2((F_c')^2 + (F_s')^2)]\}^{1/2}; \; t>t_d \tag{129}$$

where:

$$F_s = \int_0^{t_d} a(\tau) \sin\omega\tau \, d\tau, \quad F_s' = \frac{dF_s}{d\omega} \tag{130a}$$

$$F_c = \int_0^{t_d} a(\tau)\cos\omega\tau\, d\tau, \quad F_c' = \frac{dF_c}{d\omega} \tag{130b}$$

Equation (129) can also be obtained from a corresponding approximate frequency domain analysis by using the linear bandpass approximation for $A(\Omega)$ that was alluded to earlier. The basic tool of the frequency domain analysis is Eq. (119) which is rewritten here:

$$u_s^*(t) \simeq \frac{1}{2\pi}\int_{-\infty}^{\infty} H_s^2(\Omega)A_2(\Omega)e^{i\Omega t} + \frac{1}{2\pi}\int_{-\infty}^{\infty} H_s^1(\Omega)A_1(\Omega)e^{i\Omega t}d\Omega \tag{119}$$

The functions $A_1(\Omega)$ and $A_2(\Omega)$ must, as explained earlier, coincide with $A(\Omega)$ in the bandpasses. The bandpass behavior of $A(\Omega)$ must, in turn, be that which is implied by the duration limitations if a result consistent with these limitations is to be obtained. It can be shown that if $\frac{(\Delta\omega t_d)^2}{2} << 1$ and $\frac{(\xi\omega t_d)^2}{2} << 1$, then $A(\Omega)$ varies linearly in the bandpasses. We can thus use:

$$A_2(\Omega) = F_c - iF_s + (F_c' - iF_s')(\Omega-\omega) \tag{131a}$$

$$A_1(\Omega) = F_c + iF_s + (-F_c' - iF_s')(\Omega+\omega) \tag{131b}$$

Substituting Eqs. (132a, b) into Eq. (119) and using:

$$\left(\frac{d^n\delta(t)}{dt^n}\right) = \int_{-\infty}^{\infty} \frac{d^n\delta(t)}{dt^n} e^{-i\Omega t}dt = (i\Omega)^n \tag{132}$$

we arrive at:

$$u_s^*(t) \simeq \frac{e^{-\xi\omega t}}{\omega\sqrt{\varepsilon}} \{\sin\omega t[(F_s-\xi\omega F_c') \sin\Delta\omega t + \Delta\omega F_c' \cos\Delta\omega t] +$$

$$+ \cos\omega t[F_c + \xi\omega F_s') \sin\Delta\omega t - \Delta\omega F_s' \cos\Delta\omega t]\} \tag{133}$$

Taking the envelope of u_s^* gives, once again, Eq. (129).

It should be noted that the time domain analysis gives results only for $t > t_d$ whereas the frequency domain analysis appears to give results for all $t > 0$. Since the maximum response occurs, by assumption when $t > t_d$, the

results of the two analyses can be regarded as consistent for our purposes.

We could use Eq. (129) to obtain a quantitative response estimate analogous to the short duration result (Eq. 106); however, our interest in Eq. (129) lies primarily in its qualitative implications. We note that Eq. (129) differs from its short duration counterpart (Eq. (104)) by the presence of terms containing F_c, F'_c, F_s and F'_s. The presence of these terms indicates that the response is explicitly a function of the bandpass behavior of the real and imaginary parts of $A(\Omega)$. This is in marked contrast to the case of short duration ground motions where, as was shown earlier, only the Fourier amplitude spectrum, $|A(\Omega)|$, at $\Omega=\omega$ significantly affects the response.

Equation (129) is valid only when $A(\Omega)$ varies linearly in the bandpasses. When $A(\Omega)$ exhibits more complicated behavior, an approximation analogous to Eq. (129) can be obtained using the following procedure:

1. Approximate $A(\Omega)$ in the bandpasses by as many terms of its Taylor series as necessary and substitute the resulting approximations into Eq. (121).
2. Evaluate the integrals in Eq. (121) with the aid of Eq. (132) to obtain $u^*_s(t)$.
3. Compute the envelope of $u^*_s(t)$.

While application of the above procedure is straightforward, the response formula that results from it is quite complicated if more than linear terms of the Taylor series are used. The complexity of the resulting formula renders it useless for developing fast, simple response estimates. However, without actually going through the approximation procedure, we can see that the approximate envelope must contain the coefficients of the truncated Taylor series used to approximate $A(\Omega)$ in the bandpasses. Consequently, for long ground motions in general, the response is significantly affected by the details of the behavior of the real and imaginary parts of $A(\Omega)$ in the bandpasses.

3.3.3 Development of Response Estimates

The discussion in Sec. 3.3.2 clearly revealed the difficulties of developing a general response estimate for long ground motions. To develop a rigorous estimate, we need detailed data about $A(\Omega)$ and this is not usually

available. Even if it were, the data would have to be used in conjunction with rather elaborate formulas and this defeats our purpose of proposing rational but simple estimates.

While a simple, rigorous estimate is beyond our reach, there are other possibilities. Consider once again Eq. (129). If F_s' and F_c' are not too large, the terms containing $(\Delta\omega)^2$ and $(\xi\omega)^2$ can be neglected. We then have:

$$E^*(t) \simeq \frac{e^{-\xi\omega t}}{\omega\sqrt{\varepsilon}} \{\sin^2\Delta\omega t[|A(\omega)| + 2\xi\omega(F_c F_s' - F_s F_c')] + \\ + \sin\Delta\omega t[\Delta\omega(F_s F_c' - F_c F_s')]\}^{1/2} \qquad (134)$$

If $\Delta\omega$ is not too large, the general appearance of $E^*(t)$ from Eq. (134) is a succession of beat lobes of decreasing amplitude. This is also the general appearance of $E^*(t)$ when the ground motion is short. It is recalled, however, that a short ground motion is effectively perceived by the secondary system as an impulse function. This suggests that Eq. (138) could be replaced by the envelope of the response to an impulse function; in other words we can write:

$$E^*(t) \simeq I^{eff} \frac{e^{-\xi\omega t}}{\omega\sqrt{\varepsilon}} |\sin\Delta\omega t| \qquad (135)$$

where I^{eff} is the effective impulse intensity.

In order to apply Eq. (135), we must first determine I^{eff}. Eq. (134) suggests that I^{eff} is a function of both real and imaginary parts of the Fourier transform of the ground motion ($A(\Omega)$). Unfortunately, at best only the Fourier amplitude spectrum, $|A(\Omega)|$, is known to the designer. It is possible to relate I^{eff} to $|A(\Omega)|$ alone in an approximate manner by employing the following equation, which is a consequence of Parseval's theorem [3]:

$$\int_0^\infty |u_s^*(t)|^2 dt = \frac{1}{\pi}\int_0^\infty |A(\Omega)|^2 |H_s^*(\Omega)|^2 \, d\Omega \qquad (136)$$

The left-hand side of Eq. (136) is usually referred to as the "energy integral" of the response. By assumption, $u_s^*(t)$ is effectively the

response to $a(t) = I^{eff}\,\delta(t)$ and thus for the energy integral:

$$\int_0^\infty |u_s^*(t)|^2\,dt \simeq \frac{(I^{eff})^2}{\omega^2\sqrt{\varepsilon}} \int_0^\infty (e^{-\xi\omega t}\,\sin\Delta\omega t\,\cos\omega t)^2\,dt$$

$$= \frac{(I^{eff})^2}{32(\xi\omega)^3}\,(1 + (\Delta\omega/\xi\omega)^2) \qquad (137)$$

In evaluating the right-hand side of Eq. (136), we can take advantage of the bandedness of $H_s^*(\Omega)$ and replace the infinite integral by an integral over the bandpass; thus:

$$\int_0^\infty |A(\Omega)|^2 |H_s^*(\Omega)|^2 d\Omega \simeq \frac{1}{f_b} \int_{\omega-\delta_b}^{\omega+\delta_b} |A(\Omega)|^2 |H_s^*(\Omega)|^2\,d\Omega \qquad (138)$$

where f_b is the fraction of the total area under $|H_s^*(\Omega)|^2$ that lies in the bandpass. The factor $\frac{1}{f_b}$ has been inserted into Eq. (138) to account approximately for the contribution of that portion of the integrand that lies outside the bandpass. Finally, by equating the right-hand sides of Eqs. (137) and (138), we find that:

$$(I^{eff})^2 \simeq \frac{32(\xi\omega)^2}{f_b(1 + (\Delta\omega/\xi\omega)^2)} \int_{\omega-\delta_b}^{\omega+\delta_b} |A(\Omega)|^2 |H_s^*(\Omega)|^2\,d\Omega \qquad (139)$$

Once I^{eff} has been determined, it can be used in Eq. (134) to give an approximate envelope. The maximum response of this envelope - an approximation of the true maximum response - is given by:

$$u_s^{max} \simeq \frac{I^{eff}\, e^{-\frac{\xi\omega}{\Delta\omega}\tan^{-1}\frac{\Delta\omega}{\xi\omega}}}{2\sqrt{(\Delta\omega)^2 + (\xi\omega)^2}} \qquad (140)$$

Equations (139) and (140) define a procedure for estimating the maximum response of a secondary system to a long duration ground motion. The procedure can be summarized as follows:

1. Using plots of $|H_s^*(\Omega)|$ and $|A(\Omega)|$, evaluate $\int_{\omega-\delta_b}^{\omega+\delta_b} |A(\Omega)|^2 |H_s^*(\Omega)|^2\,d\Omega$. (Plots of $H_s^*(\Omega)$ have been provided in Fig. 9 for this purpose.)
2. Determine I^{eff} from Eq. (139). (To this end, f_b has been tabulated for several values of $\frac{\Delta\omega}{\xi\omega}$ in Table 1.)

3. Determine u_s^{max} from Eq. (140).

The response estimate obtained from the above procedure will henceforth be referred to as "Approximation 1."

We recall that the development of Approximation 1 was based, in part, on the assumption that $u_s(t) \simeq u_s^*(t)$. In Sec. 3.2.1, this assumption was shown to be valid for short ground motions provided Eq. (112) is satisfied. The corresponding requirement for long ground motions is obtained by using I^{eff} in place of $|A(\Omega)|$ in Eq. (112). In other words, $u_s^*(t) \simeq u_s(t)$ and Approximation 1 are valid if:

$$S_V(\omega,\xi) = o(I^{eff}) \tag{141}$$

If Eq. (141) is violated, the contribution of $\dot{u}_s'(t)$ must be included in the calculation of $u_s(t)$. Since $u_s(t) \simeq u_s^*(t) + u_s'(t)$, it seems that $u_s(t)$ could be estimated by directly adding the estimated maximum responses of $\dot{u}_s'(t)$ and $u_s^*(t)$. Unfortunately, this procedure often results in extremely conservative estimates. An improved estimate is obtained by proceeding as follows:

Let us first assume that the floor spectrum is known. The floor spectrum, we recall, is the maximum response obtained using a decoupled analysis. Since decoupled analyses are widely used in practice, it is reasonable to assume that floor spectrum data will usually be available to the designer. The proposed approximate procedure also requires a floor spectrum estimate which incorporates $u_s'(t)$. This is obtained by using the direct summation procedure mentioned above in conjunction with Eqs. (43a, b), (109), and (140). We thus have:

$$FS_{u_s} \simeq \max_t |u_s'(t)| + \max_t |u_s^*(t)|$$

$$\simeq \frac{3}{2\omega} S_V(\omega,\xi) + \frac{FS_I^{eff}}{2\xi\omega e} = F_1 \tag{142}$$

where FS_I^{eff} is the effective impulse intensity computed from Eq. (139) when $\varepsilon=0$. When $\varepsilon>0$, the direct summation procedure gives:

$$u_s^{max} \simeq \frac{3}{2\omega} S_V(\omega,\xi) + \frac{I^{eff}\, e^{-\frac{\xi\omega}{\Delta\omega} \tan^{-1} \frac{\xi\omega}{\Delta\omega}}}{2\sqrt{(\Delta\omega)^2 + (\xi\omega)^2}} = F_2 \qquad (143)$$

The factor $\frac{F_1}{F_2}$ is a rough estimate of the ratio of the maximum response to the exact floor spectrum. Consequently:

$$u_s^{max} \simeq \frac{F_1}{F_2} FS_{u_s} \qquad (144)$$

The estimate obtained from Eq. (144) will henceforth be referred to as "Approximation 2." The applicability of Approximation 2 is unaffected by the relative magnitudes of $S_V(\omega,\xi)$ and I^{eff}.

Both Approximations 1 and 2 require that I^{eff} be computed using Eq. (139). However, if $A(\Omega)$ exhibits highly erratic behavior in the bandpass, as is sometimes the case, evaluating the integral in Eq. (139) can be extremely tedious. When $A(\Omega)$ exhibits such erratic bandpass behavior, the calculations can be simplified by using, in place of $(I^{eff})^2$ from Eq. (139), the average value of $\frac{1}{f_b}|A(\Omega)|^2$ in the bandpass. The effective impulse intensity obtained in this manner is denoted I_{av}^{eff}. The response estimate obtained by using I_{av}^{eff} in place of I^{eff} in Eq. (144) will be referred to as "Approximation 1A." Similarly, the response estimate obtained by using I_{av}^{eff} in place of I^{eff} in Eqs. (142) to (149) will be referred to as "Approximation 2A."

We shall now discuss briefly the expected accuracy of the approximate methods just developed. If $|A(\Omega)|$ is constant in the bandpass, Approximations 1 and 1A give the same results as the rigorous short ground motion solution derived earlier. As the behavior of $|A(\Omega)|$ in the bandpass becomes more erratic, the accuracy of Approximation 1 should degrade.

It was shown in Sec. 3.2.2 that the fluctuation of $A(\Omega)$ in the bandpass is, roughly speaking, related to the magnitudes of the parameters $\xi\omega t_d$ and $\Delta\omega t_d$. Thus, as a rule of thumb, we can say that the accuracy of Approximations 1 and 1a should diminish as damping, frequency, mass ratio and ground motion duration increase. A similar statement applies to Approximations 2 and 2A. However, Approximations 2 and 2A always give

the correct answer (i.e., the floor spectrum) when the mass ratio is sufficiently small. Also, Approximations 2 and 2A should give better results than Approximations 1 and 1A when Eq. (142) does not hold.

It should be noted that strictly speaking, the use of the approximations developed above is justified only when $A(\Omega)$ exhibits linear behavior in the bandpass. However, as will be seen in Chapter 4, the approximations often provide good response data even when $|A(\Omega)|$ (hence $A(\Omega)$) exhibits highly erratic bandpass behavior.

The response estimates developed here will now be compared with those obtained in the parallel study by Sackman and Kelly (see, for example, [23]pgs. 26-31). To develop their estimates, Sackman and Kelly start with a modified expression for $u_s^*(t)$ and consider short ground motions characterized by $\Delta\omega t_d << 1$. A heuristic time domain analysis then leads to a result which differs from Eq. (140) only in that $S_V(\omega,\xi)$ appears in place of I^{eff}. The contribution of $u_s'(t)$ is later factored in along with that of the detuned modes using the root-sum-square approximation.

From the discussion earlier in this chapter, it is apparent that the numerical differences between the estimates obtained here and the Sackman-Kelly estimates are roughly proportional to the difference between the pseudo-velocity and Fourier amplitude spectra in the vicinity of the tuned frequency.

CHAPTER 4. ASSESSMENT OF RESPONSE ESTIMATES FOR TUNED SECONDARY SYSTEMS

4.1 Introduction

This Chapter examines the results of the numerical studies that were conducted to assess the accuracy of the response estimates developed in Chapter 3. Before examining the results, we shall first discuss the ground motions and then the systems considered in the numerical studies.

4.1.1 Ground Motions Considered

The response estimates presented in Chapter 3 were developed on the basis of general frequency domain considerations and without regard to some deterministic or probabilistic ground motion model. Consequently, we are free to test the estimates using any ground motion whose accelerogram has a well-defined Fourier transform. To utilize this flexibility to the utmost but at the same time limit the volume of computations to a reasonable amount, it was decided to test the estimates using a small number of widely differing ground motions.

The first ground motion considered is the earthquake El Centro 1940-NS. This is a prime example of a white noise type California earthquake and has been used extensively in earthquake engineering research.

The second ground motion considered is the Mexico City earthquake of May 11, 1962. This earthquake is much longer than El Centro and its frequency content reflects filtering by the infilled valley of soft soil which underlies Mexico City.

The last ground motion considered is the Vrancea earthquake of March 4, 1977. Specifically, we have used the time history recorded at INCERC in Bucharest, Rumania, which is about 110 kilometers from the epicenter. This earthquake record is representative of a class of ground motions in which the energy is concentrated in a short, relatively simple pulse.

The three earthquakes considered in this Chapter fall into three of the four categories that Newmark and Rosenblueth have used to classify all ground motions (Ref. [18], pg. 225). Consequently, the results presented in this Chapter should give a good idea of the accuracy of the response estimates for most ground motions likely to be encountered.

4.1.2 System Parameters Considered

The classically damped, tuned, secondary systems dealt with here are completely characterized by the parameters T, ξ and ε where $T = \frac{2\pi}{\omega}$ is the natural period of the primary and secondary systems. The values assigned to each of these parameters in the numerical studies will now be discussed in turn.

The fundamental period, is, in general, the most important structural characteristic that influences the dynamic behavior of a structure. A rule of thumb [18] states that the fundamental period of a structure in seconds is about one-tenth the number of stories; consequently, it is expected that the fundamental periods of interest will range from .1 to 10 sec. The range 2 sec to 5 sec corresponds to high-rise commercial structures and towers; the range .5 sec to 2 sec corresponds to mid-rise residential and commercial structures; and the range .1 sec to .5 sec corresponds to low-rise and very stiff structures, such as nuclear power plants. In this study the following nine periods were used in conjunction with all three ground motions: 10 sec, 8 sec, 5 sec, 3 sec, 1 sec, .8 sec, .5 sec, .3 sec and .1 sec.

The most difficult structural characteristic to evaluate is damping. Newmark and Hall [17] have recommended damping ratios ranging from .005 for lightly stressed piping to .2 for heavily stressed bolted steel structures. At the higher end of the damping range mentioned above, the floor spectrum, which is generally known, can be expected to be applicable in view of the results of Sec. 2.3.2. Consequently, the emphasis of the numerical studies has been placed on relatively low damping ratios. For all ground motions and periods considered, the damping ratio ξ was assigned the values .01, .03 and .05. It will be seen later that when $\xi = .05$, the responses do not differ very much from the floor spectrum, suggesting that it was reasonable not to have considered higher values of damping.

In selecting values of the mass ratio ε, we have been guided mainly by analytical considerations. A major purpose of this study is the development of analytical methods that circumvent the difficulties caused by the smallness of ε. Hence, an upper bound for ε should be some number above which these difficulties are not encountered when conventional response methods are used. In addition, ε should be bounded so as to satisfy the limitation $\sqrt{\varepsilon} << 1$ which was specified earlier. In this study, it was found that both of the

above requirements were fulfilled by setting $\varepsilon \leq .09$. In setting a lower bound for ε, we recall that the floor spectrum is valid when ε is small enough to satisfy $\frac{\Delta\omega}{\xi\omega} << 1$. Since we are primarily interested in cases where there is significant interaction between the primary and secondary systems, a suitable lower bound for ε is some value at the upper end of the floor spectrum range. This bound criterion was satisfied by setting $\varepsilon \geq .000036$ when $\xi = .01$ and $\varepsilon \geq .0009$ when $\xi = .03$ and $\xi = .05$. The actual values of ε used in this study fall within the bounds specified above and are listed in Table 2.

4.1.3 Discussion

In the numerical studies, each system within the ranges of parameters described above was subjected to each of the three ground motions. For each system, the exact maximum response was computed along with the maximum responses predicted by Approximations 1 and 2 (see Sec. 3.3.3). In addition, the responses predicted by Approximations 1A and 2A were computed for systems with periods of .3 sec and .1 sec. In the following sections, the response data for each of the three ground motions are discussed in turn.

4.2 Discussion of Response Data for El Centro 1940-NS Earthquake Record

The time history data for the ground motion are shown in Fig. 10, and the frequency domain data for the ground motion are shown in Fig. 11. Figure 12 gives detailed representations of the frequency domain data in the vicinity of T = 10 sec (ω = .628 RPS), T = 1 sec (ω = 6.28 RPS) and T = .1 sec (ω = 62.8 RPS). The purposes of Fig. 12 are to illustrate the complexity of behavior of the Fourier amplitude spectrum and to show the relative magnitudes of the Fourier and pseudo-velocity spectra.

The response results are shown in Figs. 13-18. We shall consider first the results for T = 10 sec, which are shown in Fig. 13. It can be seen that for $\xi = .01$, there is excellent agreement between the exact responses and Approximations 1 and 2. However, when $\xi = .03$ and $\xi = .05$, the accuracy of the response estimates deteriorates significantly. To see why this happens, consider Fig. 12a, which shows the spectral behavior of the ground motion in the vicinity of T=10 sec. It can be seen that near T=10 sec, the Fourier amplitude spectrum forms a deep valley; consequently the wide bandpasses of the more highly damped systems encompass significant spectral fluctuations.

It is recalled from Sec. 3.3 that if the Fourier amplitude spectrum fluctuates considerably in the bandpass, the conditions for an exact, closed form solution are violated and the response estimates are, at best, approximate solutions. The accuracy of the response estimates is also adversely affected by the fact that the Fourier amplitude spectrum is often significantly less than the pseudo-velocity spectrum in the vicinity of T = 10 sec (Fig. 12a). When such a disparity exists, the contribution of $u_s'(t)$ (Eqs. (43a, b)), which is neglected by Approximation 1, may be significant. For example, Eq. (109) predicts that for $\xi = .05$, $\max_t|u_s'(t)|\approx.43$ meters, which is more than half the maximum response. It can be seen from Fig. 13 that when $\xi = .05$, Approximation 1 gives generally poor results. However, Approximation 2, which includes the contribution of $u_s'(t)$, gives good results only when $\varepsilon < .01$.

The response data for T = 8 sec is also shown in Fig. 13. It can be seen that both response estimates give generally excellent results with just a slight decay in accuracy at the higher mass and damping ratios. The improved accuracy of the estimates over that observed for T = 10 sec is largely the result of the generally smooth behavior of the Fourier amplitude spectrum and the close agreement of the pseudo-velocity and Fourier spectra in the vicinity of T = 8 sec (Fig. 11).

The response data for T = 5 sec and T = 3 sec is shown in Fig. 14. It can be seen that once again, the response estimates are in good agreement with the exact responses. At worst, the estimates exceed the exact result by 30% at some of the higher damping and mass ratios.

The periods considered thus far are relatively long and are usually associated only with tall buildings and towers. The shorter periods considered next pose more severe tests for the response estimates (see Sec. 3.4) but are also more typical of actual structural periods.

The response data for T = 1 sec and T = .8 sec are shown in Fig. 15. The behavior of the Fourier amplitude spectra in the vicinity of T = 1 sec is shown in Fig. 12b. From Fig. 15, it can be seen that for T = 1 sec, the response estimates are in reasonable agreement with the exact results for $\varepsilon < .01$. For $\varepsilon > .01$, Approximation 2 is overly conservative by as much as 100% while Approximation 1 gives somewhat better agreement. Consistent with with previous results, the accuracy of the estimates generally deteriorates at higher mass and damping ratios. For T = .8 sec, the response estimates

are in reasonable agreement with the exact responses except for "spikes" at $\varepsilon = .0144$. Contrary to previous results, the accuracy of the estimates is somewhat better at the higher damping ratios.

The response data for T = .5 sec is shown in Fig. 16. Both response estimates give generally conservative results with the overall level of accuracy being comparable to that observed for T = 1 sec and T = .8 sec.

The periods considered next are relatively short and can therefore be expected to pose severe tests for the response estimates (see Sec. 3.4).

The response data for T = .3 sec is shown in Fig. 17. When $\xi = .01$, Approximations 1 and 2 give generally fair results but are sometimes over-conservative by as much as 100%. On the other hand, Approximations 1A and 2A give generally excellent results when $\xi = .01$. At the higher damping ratios, Approximation 1 gives results that are overly conservative by as much as 80% although Approximation 2 gives superb results. The accuracy of Approximations 1A and 2A is intermediate between Approximations 1 and 2 at the higher damping ratios, although Approximation 2A gives generally unconservative, and hence undesirable results. In assessing the relative merits of the four approximations for T = .3 sec, due account should be taken of the relative ease of calculating Approximations 1A and 2A.

The response data for T = .1 sec is shown in Fig. 18. The general appearance of Fig. 18 is quite similar to Fig. 17 and the remarks made regarding T = .3 sec apply equally to T = .1 sec.

To summarize the results for El Centro, it appears that Approximations 1 and 2 provide generally acceptable response estimates for periods as short as .5 sec. For shorter periods Approximation 2 provides good results while Approximations 1a and 2A provide somewhat poorer results but with less computational effort.

4.3 Discussion of Response Data for May 11, 1962 Mexico City Earthquake Record

The time history data for the ground motion are shown in Fig. 19 and the frequency domain data are shown in Figs. 20 and 21.

In discussing the results, we shall follow the procedure of the previous section and discuss the longer periods first.

The response data for T = 10 sec and T = 8 sec are shown in Fig. 22. The accuracy of the response estimates is reasonably good although somewhat

poorer than the excellent predictions for the T = 8 sec responses to El Centro (Fig. 13). The deterioration of the accuracy of the estimates at higher damping and mass ratios is consistent with earlier observations.

The response data for T = 5 sec and T = 3 sec is shown in Fig. 23. The response estimates give good predictions for T = 5 sec and for T = 3 sec when ξ = .01. However, the accuracy of the estimates is significantly decreased for T = 3 sec at the higher damping and mass ratios. Apparently, both Approximations 1 and 2 exaggerate the effects of the sharp rise in the Fourier amplitude spectrum that takes place between T = 3 sec and T = 5 sec (Fig. 20). It should be noted that the peak of the pseudo-velocity and Fourier amplitude spectra at T = 2.5 sec coincide with the fundamental period of the soil underlying Mexico City.

The response data for T = 1 sec and T = .8 sec are shown in Fig. 24. The accuracy of the response estimates is comparable with that for the corresponding El Centro results (Fig. 15) although the major inaccuracies occur for different system parameters. Generally speaking, Approximations 1 and 2 overestimate the response, as has usually been the case for the systems and ground motions considered thus far.

The response data for T = .5 sec are shown in Fig. 25. The accuracy of the estimates is generally reasonable and is comparable with that observed for the corresponding El Centro results (see Fig. 17).

The response data for T = .3 sec, which is shown in Fig. 26, indicate that Approximation 1 provides generally fair predictions for ξ = .01 but significantly poorer, albeit conservative, results for the higher damping ratios. Approximation 2, on the other hand, provides generally good predictions for all damping ratios. Overall, the accuracy of Approximations 1 and 2 is quite similar to that observed for the corresponding El Centro results (Fig. 17). Approximations 1A and 2A are generally intermediate in quality between Approximations 1 and 2 but somewhat poorer than the corresponding El Centro results.

The response data for T = .1 sec are shown in Fig. 18. It can be seen that Approximation 1 provides extremely unconservative predictions. The principal reason for this is that the Fourier amplitude spectrum in the vicinity of T = .1 sec (ω = 62.8 RPS) is considerably less than the pseudo-velocity spectrum (see Fig. 21c) and as a result, the contribution of $u_s'(t)$

forms a significant part of the response. For example, when $\xi = .01$, $\max_t |u_s'(t)|$ is about .00032 meters, which is more than half the maximum response. Another reason for the poor accuracy of Approximations 1 and 1A is that they seriously underestimate the contribution of $u_s^{**}(t)$. Calculations show that for $\xi = .01$ and $\epsilon = .000144$, $\max_t |u_s^{**}(t)|$ is about .0002 meters while Approximation 1 predicts .00005 meters and Approximation 1A predicts .00004 meters. The poor accuracy of the predictions is not surprising in view of the chaotic behavior of the Fourier amplitude spectrum in the vicinity of the tuned frequency.

In conclusion, the response estimates are generally about as accurate for the Mexico City earthquake as they are for the El Centro earthquake. The agreement of the estimates breaks down for the same reasons cited for El Centro - namely - when the Fourier amplitude spectrum fluctuates considerably and when the Fourier amplitude and pseudo-velocity spectra differ widely.

4.4 Discussion of Response Data for March 4, 1977 Vrancea Earthquake Record

The time history data for the ground motion are shown in Fig. 28 and the frequency domain data are shown in Figs. 29 and 30.

The response data for T = 10 sec and T = 8 sec are shown in Fig. 31. It is apparent that for both periods, Approximation 1 significantly underestimates the response whereas Approximation 2 gives generally good predictions. The poor accuracy of Approximation 1 is to be expected in view of the spectral behavior of the ground motion. From Figs. 29 and 30a, it can be seen that for periods greater than 5 sec, the Fourier amplitude spectrum is insignificant in comparison with the pseudo-velocity spectrum, and consequently, the contribution of $u_s'(t)$, which is neglected by Approximation 1, forms a significant part of the response.

The response data for T = 5 sec are shown in Fig. 32. The improved accuracy of Approximation 1 for T = 5 sec over that observed for the higher periods (Fig. 31) reflects the significant increase in the Fourier amplitude spectrum that takes place as the period drops below T = 5 sec (Fig. 29). The accuracy of the response estimates for T = 3 sec is quite good and is generally comparable with the corresponding El Centro results for the same period (Fig. 14).

The response data for T = 1 sec and T = .8 sec are shown in Fig. 33. The accuracy of the response estimates for T = 1 sec is good for ξ = .01 and ξ = .03 but deteriorates at the higher mass ratios when ξ = .05. Both estimates give good results for T = .8 sec when ξ = .01 but the accuracy of Approximation 1 deteriorates somewhat for ξ = .03 and even more so for ξ = .03. The poor accuracy of Approximation 1 when ξ = .05 can probably be attributed to the contribution of $u_s'(t)$ since Eq. (109) predicts that $\max_t |u_s'(t)|$ is about .1 meters, or, about half the exact maximum response.

The response data for T = .5 sec are shown in Fig. 34. The response estimates are quite good and are generally somewhat more accurate than the corresponding results for El Centro and Mexico City (Figs. 16 and 25).

The response data for T = .3 sec and T = .1 sec are shown in Figs. 35 and 36 respectively. In general, Approximation 2 furnishes the most satisfactory estimates. Approximations 1A and 2A give generally satisfactory results when T = .3 sec but usually underestimate the results, sometimes quite seriously when T = .1 sec.

In summary, only Approximation 2 appears to give consistently reliable predictions for responses to the Vrancea earthquake. Approximation 1 is generally unreliable because the Fourier amplitude spectrum is often considerably less than the pseudo-velocity spectra. Approximations 1A and 2A are somewhat less satisfactory predictions here than for the El Centro and Mexico City earthquakes.

CHAPTER 5. RESPONSE OF MULTI-DEGREE-OF-FREEDOM TUNED SECONDARY SYSTEMS

5.1 Introduction

In this chapter, expressions are derived for the response of a tuned M-DOF (i.e., multi-degree-of-freedom) secondary system that is attached to a M-DOF primary system. First, the eigenvalue problem for the undamped total system is set up and solved approximately. Later, response expressions for various forms of damping are presented.

5.2 Approximate Solution of the Eigenvalue Problem

5.2.1 Formulation of the Eigenvalue Problem

A primary system with attached secondary system is shown schematically in Fig. 37. To assemble the equations of motion, we treat the primary and secondary systems as substructures and assign the attachment point degrees of freedom to the primary system. The equations of motion may then be written in global coordinates as:

$$\begin{bmatrix} [M'_{pp}] & 0 \\ 0 & [M_{ss}] \end{bmatrix} \begin{Bmatrix} \{\ddot{U}_p(t)\} \\ \{\ddot{U}_s(t)\} \end{Bmatrix} + \begin{bmatrix} [K'_{pp}] & [K_{ps}] \\ [K_{sp}] & [K_{ss}] \end{bmatrix} \begin{Bmatrix} \{U_p(t)\} \\ \{U_s(t)\} \end{Bmatrix} = 0 \qquad (145)$$

where:

$\{U_p(t)\}, \{U_s(t)\}$ are primary and secondary system response vectors of dimensions P and S, respectively.

$[M'_{pp}], [K'_{pp}]$ are PxP mass and stiffness matrices of the primary system with the secondary system held fixed.

$[M_{ss}], [K_{ss}]$ are SxS mass and stiffness matrices of the secondary system with the attachment points held fixed.

$[K_{ps}] = [K_{sp}]^T$ is the matrix of stiffness coefficients of primary system forces that result from the motion of secondary system degrees of freedom.

In general, $[M'_{pp}]$ and $[K'_{pp}]$ can be expressed as:

$$[K'_{pp}] = [K_{pp}] + [{}^*K_{pp}] \tag{146a}$$

$$[M'_{pp}] = [M_{pp}] + [{}^*M_{pp}] \tag{146b}$$

where $[M_{pp}]$ and $[K_{pp}]$ are the mass and stiffness matrices of the primary systems alone and $[{}^*M_{pp}]$ and $[{}^*K_{pp}]$ reflect the contributions of the secondary system. For the lumped mass models considered here:

$$[{}^*M_{pp}] = 0 \tag{146c}$$

The matrices $[M_{pp}]$ and $[M_{ss}]$ are, of course, positive definite. The constraints on the primary and secondary systems are assumed sufficient to prevent rigid body motions, it follows that $[K_{pp}]$ and $[K_{ss}]$ are positive definite.

Equation (145) can be expressed in terms of the modal coordinates of the primary and secondary systems via the transformations:

$$\{u_p(t)\} = [\phi_p]\{\alpha_p(t)\} \tag{147a}$$

$$\{u_s(t)\} = [\phi_p]\{\alpha_s(t)\} \tag{147b}$$

where $[\phi_p]$ and $[\phi_s]$ are the modal matrices of the primary and secondary systems, respectively. It is convenient to normalize the eigenvectors so that their norms are of the same order of magnitude. A suitable norm for this purpose is the sum of the absolute values of the elements. Substituting Eqs. (146a-c) and (147a,b) into Eq. (145) and using modal orthogonality, we obtain:

$$\begin{bmatrix} [\bar{M}_{pp}] & 0 \\ 0 & [\bar{M}_{ss}] \end{bmatrix} \begin{Bmatrix} \{\ddot{\alpha}_p(t)\} \\ \{\ddot{\alpha}_s(t)\} \end{Bmatrix} + \begin{bmatrix} [\bar{K}_{pp}] + [{}^*\bar{K}_{pp}] & [\bar{K}_{sp}] \\ [\bar{K}_{ps}] & [\bar{K}_{ss}] \end{bmatrix} \begin{Bmatrix} \{\alpha_p(t)\} \\ \{\alpha_s(t)\} \end{Bmatrix} = 0 \tag{148}$$

where:

$$[\bar{M}_{pp}] = [\phi_p]^T [M_{pp}][\phi_p] \tag{149a}$$

$$[\bar{K}_{pp}] = [\Phi_p]^T[K_{pp}][\Phi_p] \tag{149b}$$

$$[*\bar{K}_{pp}] = [\phi_p]^T[*K_{pp}][\phi_p] \tag{149c}$$

$$[\bar{M}_{ss}] = [\phi_s]^T[M_{ss}][\phi_s] \tag{150a}$$

$$[\bar{K}_{ss}] = [\phi_s]^T[K_{ss}][\phi_s] \tag{150b}$$

$$[\bar{K}_{ps}] = [\phi_p]^T[K_{ps}][\phi_s] = [\bar{K}_{sp}]^T \tag{151}$$

The elements of the diagonal matrices $[\bar{M}_{pp}]$ and $\bar{K}_{pp}]$ are the generalized masses and stiffnesses of the primary system. The i^{th} terms of $[\bar{M}_{pp}]$ and $[\bar{K}_{pp}]$ are related by:

$$(\omega_p^i)^2 = \frac{\bar{K}_{pp}^i}{\bar{M}_{pp}^i} \tag{152a}$$

where ω_p^i is the i^{th} natural frequency of the primary system. Similarly, the j^{th} terms of the diagonal matrices $[\bar{M}_{ss}]$ and $[\bar{K}_{ss}]$ are related by:

$$(\omega_s^j)^2 = \frac{\bar{K}_{ss}^i}{\bar{M}_{ss}^j} \tag{152b}$$

where ω_s^i is the j^{th} natural frequency of the secondary system. It is assumed that the first mode of the primary system is tuned to the first mode of the secondary system at the frequency ω. Consequently:

$$\omega_s^1 = \omega_p^1 = \omega \tag{153}$$

By definition, the secondary system is much lighter and much more flexible than the primary system. We can therefore say that:

$$||\bar{M}_{ss}|| << ||\bar{M}_{pp}|| \tag{154a}$$

$$||*\bar{K}_{pp}||, \ ||\bar{K}_{ps}|| << ||\bar{K}_{pp}|| \tag{154b}$$

where $||\cdot||$ denotes the norm referred to earlier.

We now introduce into Eq. (148):

$$\{\alpha_p(t)\} = \{\alpha_p\} \sin\Omega t \tag{155a}$$

$$\{\alpha_s(t)\} = \{\alpha_s\} \sin\Omega t \tag{155b}$$

where $\{\alpha_p\}$ and $\{\alpha_s\}$ are vectors of modal coordinates of the primary and secondary system. We thus obtain the eigenvalue problem:

$$\begin{bmatrix} [\bar{K}_{pp}]+[{}^*\bar{K}_{pp}]-\Omega^2[M_{pp}] & [\bar{K}_{ps}] \\ [\bar{K}_{sp}] & [\bar{K}_{ss}]-\Omega^2[\bar{M}_{ss}] \end{bmatrix} \begin{Bmatrix} \{\alpha_p\} \\ \{\alpha_s\} \end{Bmatrix} = 0 \tag{156}$$

Dividing each row of Eq. (156) by the term $\bar{K}^i_{pp}$ or $\bar{K}^i_{ss}$ that lies on the principal diagonal, we have:

$$\begin{bmatrix} [I]+[e^*]-\Omega^2[1/\omega_p^2] & [e] \\ [E] & [I]-\Omega^2[1/\omega_s^2] \end{bmatrix} \begin{Bmatrix} \{\alpha_p\} \\ \{\alpha_s\} \end{Bmatrix} = 0 \tag{157}$$

where:

$$e^*_{ij} = \frac{{}^*\bar{K}^{ij}_{pp}}{\bar{K}^i_{pp}} \tag{158a}$$

$$e_{ij} = \frac{\bar{K}^{ij}_{ps}}{\bar{K}^i_{pp}} \tag{158b}$$

$$E_{ij} = \frac{\bar{K}^{ii}_{sp}}{\bar{K}^i_{ss}} \tag{158c}$$

and $[1/(\omega_p)^2]$ and $[1/(\omega_s)^2]$ are diagonal matrices where i^{th} elements are $(1/\omega_p^i)^2$ and $(1/\omega_s^i)^2$, respectively.

To simplify the appearance of forthcoming equations, we define:

$$\varepsilon_i = e^*_{ii} \tag{159a}$$

$$\varepsilon = \frac{M_s^1}{M_p^1} \tag{159b}$$

$$\beta = E_{11} \tag{159c}$$

By combining Eqs. (153), (158b,c) and (159b,c), we obtain:

$$e_{11} = \beta\varepsilon \tag{159d}$$

We shall now make some order-of-magnitude estimates for the terms that have just been defined. These estimates will prove useful in solving the eigenvalue problem.

In view of Eq. (154a), it is expected that $\varepsilon<<1$. Equation (158b) suggests that the E_{ij} (hence β) are O(1) since both the numerator and denominator are generalized stiffnesses of the secondary system. It therefore follows that e_{11} is $O(\varepsilon)$. The other e_{ij} and the e^*_{ij} are, like e_{11}, ratios relating generalized stiffnesses of the secondary system to generalized stiffnesses of the primary system. It is therefore assumed that e^*_{ij}, $e_{ij} = O(\varepsilon)$.

5.2.2 Approximate Solution of Characteristic Equation

The first step in solving Eq. (157) is obtaining the roots of the characteristic equation:

$$\begin{vmatrix} [I]+[e^*]-\Omega^2[1/\omega_p^2] & [e] \\ [E] & [I]-\Omega^2[1/\omega_s^2] \end{vmatrix} = 0 \tag{160}$$

In general, the roots of Eq. (160) cannot be evaluated exactly. An approximate analytical solution is therefore derived.

The determinant in Eq. (160) can be expanded using the formula (see [8]):

$$|a_{ij}| = \sum_{(j)} (-1)^j a_{1j_1} a_{2j_2} \cdots a_{nj_n} \tag{161}$$

where n = P+S and the summation varies over all the n! permutations of the order of the second subscripts. The exponent is +1 or -1 if the permutation is of even order or odd order, respectively.

In view of the structure of the characteristic determinant, each of the factors appearing in the summation of Eq. (161) can be put in the form:

$$(-1)^j a_{j_1} a_{2_{j_2}} \cdots a_{n_{j_n}} = g\varepsilon^s$$

where the exponent s is the number of terms e_{ij} and e^*_{k1} $(k \neq \ell)$ appearing in the factor and g contains no ε. The characteristic equation can thus be put in the form:

$$\sum_{k=0}^{P} G_k \varepsilon^k = 0 \tag{162}$$

where T_k is independent of ε.

In general, it is impractical to carry out the entire expansion appearing in Eq. (162). However, since $\varepsilon \ll 1$, the characteristic equation can be simplified approximately by neglecting all but the lowest order terms in ε. A similar method has been used to analyze the vibrations of a mechanical system with nonclassical damping (see [7], pp. 231-235). We consider first the "zeroth order" approximation to the characteristic equation, which is given by:

$$G_o = 0$$

It is easily shown that T_o is the product of the terms on the principle diagonal of the characteristic determinant. Consequently, the

characteristic equation is approximately:

$$G_o = \prod_{i=1}^{P} [1+\varepsilon_i-(\Omega/\omega_p^i)^2] \prod_{j=1}^{S} [1-(\Omega/\omega_s^j] = 0 \tag{163}$$

The solutions of Eq. (163) are:

$$\Omega^2 \simeq (\omega_p^i)^2(1+\varepsilon_i), \quad i=1,\ldots,P \tag{164a}$$

$$\Omega^2 \simeq (\omega_s^j)^2, \quad j=1,\ldots,S \tag{164b}$$

Equation (163), unfortunately, does not contain terms from [e] or [E]. These matrices account for dynamic interaction between the primary and secondary system, which should be important at least for the two eigenmodes with frequencies near ω. To account for interaction approximately and to check Eqs. (164a,b), we examine:

$$G_o + G_1\varepsilon = 0 \tag{165}$$

which is the next approximation for the characteristic equation. $T_1\varepsilon$ contains all factors in the determinant having terms of $O(\varepsilon)$ and is given by:

$$T_1\varepsilon = -\sum_{i=1}^{P} \prod_{\substack{k=1 \\ k\neq i}}^{P} [1+\varepsilon_k-(\Omega/\omega_p^k)^2] \sum_{j=1}^{S} e_{ij}E_{ji} \prod_{\substack{\ell=1 \\ \ell\neq j}}^{S} [1-(\Omega/\omega_s^\ell)^2] \tag{166}$$

Equation (165) will now be solved approximately. Equations (164a,b) suggest that Eq. (165) has roots close to the eigenvalues of the separate primary and secondary systems. We consider first the eigenvalues close to $(\omega_p^m)^2$, $m\neq 1$. Equation (165) can be written:

$$[1+\varepsilon_m-(\Omega/\omega_p^m)^2]\{\prod_{\substack{i=1 \\ i\neq m}}^{P} [1+\varepsilon_i-(\Omega/\omega_p^i)^2] \prod_{j=1}^{S} [1-(\Omega/\omega_s^i)^2] -$$

$$-\sum_{\substack{i=1 \\ i\neq m}}^{P} \prod_{\substack{k=1 \\ k\neq i,m}}^{P} [1+\varepsilon_k-(\Omega/\omega_p^k)^2] \sum_{j=1}^{S} e_{ij}E_{ij} \prod_{\substack{\ell=1 \\ \ell\neq j}}^{S} [1-(\Omega/\omega_s^\ell)^2]\} =$$

$$= \prod_{\substack{k=1\\k\neq m}}^{P} [1+\varepsilon_k-(\Omega/\omega_p^k)^2] \sum_{j=1}^{S} e_{mj}E_{jm} \prod_{\substack{\ell=1\\\ell\neq j}}^{S} [1-(\Omega/\omega_s^\ell)^2] \tag{167}$$

The second term in the braces in Eq. (167) has e_{ij} in each of its factors and is therefore much smaller, in general, than the preceding term. Consequently:

$$[1+\varepsilon_m-(\Omega/\omega_p^m)^2]\{\prod_{\substack{i=1\\i\neq m}}^{P} [1+\varepsilon_i-(\Omega/\omega_p^i)^2] \prod_{j=1}^{S} [1-(\Omega/\omega_s^j)^2\} \simeq$$

$$\simeq \prod_{\substack{k=1\\k\neq m}}^{P} [1+\varepsilon_k-(\Omega/\omega_p^k)^2] \sum_{j=1}^{S} e_{mj}E_{jm} \prod_{\substack{\ell=1\\\ell\neq j}}^{S} [1-(\Omega/\omega_s^\ell)^2] \tag{168}$$

and therefore:

$$\Omega^2 \simeq (\omega_p^m)^2(1 + \varepsilon_m - \sum_{j=1}^{S} \frac{(\omega_s^j)^2 e_{mj}E_{jm}}{(\omega_s^j)^2-(\omega_p^m)^2}), \quad m\neq 1 \tag{169}$$

$$= (\omega_p^m)^2(1 + O(\varepsilon))$$

It can be shown in a similar manner that the eigenvalues close to $(\omega_s^m)^2$, $m\neq 1$, are given by:

$$\Omega^2 = (\omega_s^m)^2(1 - \sum_{j=1}^{P} \frac{(\omega_p^j)^2 e_{jm}E_{mj}}{(\omega_p^j)^2-(\omega_s^m)^2} + O(\varepsilon)), \quad m=2,\ldots,S \tag{170}$$

All that remains is to find the two eigenvalues close to $(\omega_p^1)^2 = (\omega_s^1)^2 = \omega$. To do this, we write

$$[1+\varepsilon_1-(\Omega/\omega)^2][1-(\Omega/\omega)^2] \prod_{i=2}^{P} [1+\varepsilon_i-(\Omega/\omega_p^i)^2] \prod_{j=2}^{S} [1-(\Omega/\omega_s^j)^2] -$$

$$- \sum_{i=2}^{P} \prod_{\substack{k=2\\k\neq i}}^{P} [1+\varepsilon_k=(\Omega/\omega_p^k)^2] \sum_{j=2}^{S} e_{ij}E_{ji} \prod_{\substack{\ell=2\\\ell\neq j}}^{S} [1-(\Omega/\omega_s^\ell)^2]\} \simeq$$

$$\simeq \prod_{k=2}^{P} [1+\varepsilon_k-(\Omega/\omega_p^k)^2]\beta^2\varepsilon \prod_{\ell=2}^{S} [1-(\Omega/\omega_s^\ell)^2]$$

$$+ \prod_{k=2}^{P} [1+\varepsilon_k-(\Omega/\omega_p^k)^2] \sum_{j=2}^{S} e_{1j}E_{j1} \prod_{\substack{\ell=1 \\ \ell\neq j}} [1-\Omega/\omega_s^\ell)^2] +$$

$$+ \sum_{i=2}^{P} \prod_{\substack{k=1 \\ k\neq i}}^{P} [1+\varepsilon_k-(\Omega/\omega_p^k)^2]e_{i1}E_{1i} \prod_{\ell=2}^{S} [1-(\Omega/\omega_s^\ell)^2] \qquad (171)$$

The second term enclosed in the brackets on the left-hand side of Eq. (171) is $O(\varepsilon)$ and is therefore much smaller than the preceding term. On the right-hand side, all the terms are $O(\varepsilon)$. However, each of the factors in the last two terms contains $[1+\varepsilon_1-(\Omega/\omega)^2]$ or $[1-(\Omega/\omega)^2]$ and is therefore relatively insignificant near $\Omega=\omega$. We can thus write:

$$[1+\varepsilon_1-(\Omega/\omega)^2][1-(\Omega/\omega)^2] \simeq \beta^2 \varepsilon \qquad (172)$$

The roots of Eq. (172) are:

$$(\Omega_1)^2 \simeq \omega^2(1 + \frac{\varepsilon_1}{2} - |\beta|\sqrt{\varepsilon}) \qquad (173a)$$

$$(\Omega_2)^2 \simeq \omega^2(1 + \frac{\varepsilon_1}{2} + |\beta|\sqrt{\varepsilon}) \qquad (173b)$$

5.2.3 Evaluation of Eigenvectors and Participation Factors

In what follows, α_p^i denotes the contribution of the i^{th} mode of the primary system to a mode of the total structure. Similarly, α_s^j denotes the contribution of the j^{th} mode of the secondary system to a mode of the total structure.

We first obtain the eigenvectors corresponding to eigenvalues of the structure near $(\omega_p^i)^2$, i=2,...,P. Consider the j^{th} row of the second set of Eq. (156):

$$\sum_{k=1}^{P} E_{jk}\alpha_p^k + [1-(\Omega/\omega_s^j)^2] \alpha_s^j = 0 \qquad (174)$$

Since the eigenvalue Ω^2 is very close to $(\omega_p^i)^2$, it seems reasonable to assume that α_p^i is much greater than the other modal coordinates of the

primary system, this will be checked later. Equation (175) then simplifies to:

$$E_{ji}\alpha_p^i + [1-(\Omega/\omega_s^j)^2]\ \alpha_s^j \simeq 0 \tag{175}$$

Using Eq. (169) in Eq. (178) and setting $\alpha_p^i = 1$, we have:

$$\alpha_s^j \simeq -\frac{E_{ji}}{1-(\omega_p^i/\omega_s^j)^2} + O(\varepsilon),\ j=1,\ldots,S \tag{176}$$

By substituting Eq. (179a) into the k^{th} row of the first set of Eq. (159), it can be shown that:

$$\alpha_p^k = O(\varepsilon),\ k\neq 1,\ i \tag{177}$$

and the derivation is fully justified.

The next step is computing the modal participation factor. If the equations of motion in global coordinates are given symbolically by Eq. (38), then the participation factor for an eigenmode of the total system is given by:

$$P_i = \frac{\{\alpha_p\}^T[\phi_p]^T[M_{pp}]\{1\} + \{\alpha_s\}^T[\phi_s][M_{ss}]\{1\}}{\{\alpha_p\}^T[\phi_p]^T[M_{pp}][\phi_p]\{\alpha_p\} + \{\alpha_s\}^T[\phi_s]^T[M_{ss}][\phi_s]\{\alpha_s\}} \tag{178}$$

Combining Eqs. (176-178), we have

$$P \simeq P_p^i \qquad ,\ i\neq 1 \tag{179}$$

where P_p^i is the participation factor of mode i of the primary system.

An analysis quite similar to the one just presented shows that the modal data corresponding to eigenvalues near $(\omega_s^i)^2$, j=2,...,S are:

$$\alpha_p^k \simeq -\frac{e_{ki}}{1-(\omega_s^i/\omega_p^k)^2}\ ,\ k=1,\ldots,P \tag{180}$$

$$\alpha_s^j \simeq 1 \tag{181}$$

$$\alpha_s^\ell = O(\varepsilon), \quad \ell \neq j \tag{182}$$

By substituting Eqs. (180-182) into Eq. (178), we obtain:

$$P = P_s^j - \sum_{k=1}^{P} \frac{e_{kj}}{M_s^j[1-(\omega_s^j/\omega_p^k)^2]} P_p^k M_p^k + O(\varepsilon) \tag{183}$$

where P_s^j is the participation factor of the j^{th} mode of the secondary system.

We now obtain the modal data corresponding to the eigenvalues $(\Omega_1)^2$ and $(\Omega_2)^2$ of the total structure (i.e., the two closely spaced modes). Consider the first rows of the first and second sets of Eq. (157):

$$[1+\varepsilon_1-(\Omega/\omega)^2]\ {}^\ell\alpha_p^1 + \sum_{k=2}^{P} e_{1k}^* \alpha_p^k + \beta\varepsilon\, {}^\ell\alpha_s^1 + \sum_{k=2}^{S} e_{1k}\, {}^1\alpha_s^k = 0 \tag{184a}$$

$$\beta\, {}^\ell\alpha_p^1 + \sum_{k=2}^{P} E_{jk}\, {}^\ell\alpha_p^k + [1-(\Omega/\omega)^2]\ {}^\ell\alpha_s^1 = 0 \tag{184b}$$

where ℓ is 1 or 2 depending on the mode being considered. Since the eigenvalues are close to $(\omega_p^1)^2 = (\omega_s^1)^2$, we expect that the largest contributions to the eigenvectors will come from ${}^\ell\alpha_p^1$ and ${}^\ell\alpha_s^1$; this will be checked later. Equations (185a,b) then simplify to:

$$[1+\varepsilon_1-(\Omega/\omega)^2]\ \alpha_p^1 + \beta\varepsilon\alpha_s^1 \simeq 0 \tag{185a}$$

$$\beta\alpha_p^1 + [1-(\Omega/\omega)^2]\ \alpha_s^1 \simeq 0 \tag{185b}$$

Setting $\Omega^2 = (\Omega_1)^2$ and solving, we have:

$${}^1\alpha_p^1 \simeq 1 \tag{186a}$$

$${}^1\alpha_s^1 \simeq -\frac{\varepsilon_1}{2\beta\varepsilon} - \frac{|\beta|}{\beta\sqrt{\varepsilon}} \tag{186b}$$

Similarly, for $\Omega^2 = (\Omega_2)^2$, we have:

$$ {}^{2}\alpha_p^1 \simeq 1 \tag{187a} $$

$$ {}^{2}\alpha_s^1 \simeq -\frac{\varepsilon_1}{2\beta\varepsilon} + \frac{|\beta|}{\beta\sqrt{\varepsilon}} \tag{187b} $$

Approximations are now derived for the contributions of the detuned modes of the primary and secondary systems to the two closely-spaced modes of the total system. These small contributions give rise to the so-called "non-dominant tuning pole response terms" that were first obtained by Sackman and Kelly [23].

We first consider the contributions of the primary system modes. These are obtained by considering the i^{th} row of the first set of Eq. (157):

$$ \sum_{\substack{k=1 \\ k\neq i}}^{P} e_{ik}^{*}\, {}^{\ell}\alpha_p^k + [1+e_{ik}^{*}-(\Omega/\omega_p^i)^2]\, {}^{\ell}\alpha_p^i + \sum_{k=1}^{S} e_{ik}\, {}^{\ell}\alpha_s^k = 0 \tag{188} $$

In view of our assumptions about the magnitudes of the ${}^{\ell}\alpha_p^k$ and the ${}^{\ell}\alpha_s^k$, the summations in Eq. (189) will be dominated by the terms containing ${}^{\ell}\alpha_p^1$. Consequently, setting $\Omega=\Omega_1$ in Eq. (189), we have:

$$ {}^{1}\alpha_p^i \simeq -\frac{e_{i1}|\beta|}{\beta\sqrt{\varepsilon}[1-(\omega/\omega_p^i)^2]} + O(\varepsilon),\ i=2,\ldots,P \tag{189a} $$

$$ \simeq O(\sqrt{\varepsilon}) $$

Similarly:

$$ {}^{2}\alpha_p^i \simeq \frac{e_{i1}|\beta|}{\beta\sqrt{\varepsilon}[1-(\omega/\omega_p^i)^2]} + O(\varepsilon),\ i=2,\ldots,P \tag{189b} $$

$$ \simeq -\,{}^{1}\alpha_p^i $$

The contributions of the detuned secondary system modes are obtained by considering the second set of Eq. (156). The j^{th} row of this set is:

$$\sum_{k=1}^{P} E_{jk}\ {}^{\ell}\alpha_p^k + [1-(\Omega/\omega_s^j)^2]\ {}^{\ell}\alpha_s^j = 0 \qquad (190)$$

For the two closely-spaced modes, the summation in Eq. (191) is dominated by $E^{j1}\ {}^{\ell}\alpha_s^1$ and consequently:

$${}^{1}\alpha_s^j \simeq {}^{2}\alpha_s^j \simeq -\frac{E_{j1}}{[1-(\omega/\omega_s^j)^2]} + O(\sqrt{\varepsilon}),\ j=2,\ldots,S \qquad (191)$$

It is easily shown that the results in Eqs. (190a,b) and Eq. (192) are small enough to have negligible impact on our estimates for the ${}^{\ell}\alpha_p^1$ and the ${}^{\ell}\alpha_s^1$ (see Eqs. (187a,b) and (188a,b)) and consequently, our derivation is fully justified.

The participation factors for the modes corresponding to eigenvalues $(\Omega_1)^2$ and $(\Omega_2)^2$ are denoted P_1 and P_2. By substituting our results for the ${}^{\ell}\alpha_p^i$ and the ${}^{\ell}\alpha_s^j$ into Eq. (179), we obtain:

$$P_1 \simeq \frac{1}{2}[P_p^1(1 - \frac{\varepsilon_1}{2|B|\sqrt{\varepsilon}}) + \sum_{i=2}^{P} {}^{1}\alpha_p^i P_p^i \frac{M_p^i}{M_p^2} - \sqrt{\varepsilon}\ P_s^1 \frac{|\beta|}{\beta}] + O(\varepsilon) \qquad (192a)$$

$$P_2 \simeq \frac{1}{2}[P_p^1(1 + \frac{\varepsilon_1}{2|B|\sqrt{\varepsilon}}) - \sum_{i=2}^{P} {}^{1}\alpha_p^i P_p^i \frac{M_p^i}{M_p^2} + \sqrt{\varepsilon}\ P_s^2 \frac{|\beta|}{\beta}] + O(\varepsilon) \qquad (192b)$$

5.3 Evaluation of Secondary System Response

5.3.1 Response of Systems with Proportional Damping

The response of the total structure to a ground motion is given by Eq. (38) where the stiffness and mass matrices are as shown in Eq. (148). If the damping in the primary and secondary systems is proportional to stiffness, the damping matrix is given by:

$$[C] = \begin{bmatrix} \gamma_p[K_{pp}] + \gamma_s[K_{ps}^*] & \gamma_s[K_{ps}] \\ \gamma_s[K_{sp}] & \gamma_s[K_{ss}] \end{bmatrix} \qquad (193)$$

where γ_p and γ_s are constants. We consider here the case $\gamma_p = \gamma_s = \gamma$.

The total structure is the proportionally damped in the sense of Sec. 2.3 and the response is given by:

$$\{u(t)\} = -\sum_{i=1}^{P+S} \frac{P_i\{\phi^i\}}{\Omega_i} \int_o^t a(\tau)\, e^{-\xi_i\Omega_i(t-\tau)} \sin\Omega_i(t-\tau)\, d\tau \qquad (194)$$

where:

$$\xi_i = \frac{\gamma\Omega_i}{2} \qquad (195)$$

It proves convenient to consider separately the response contributed by the two closely-spaced modes (i=1,2) and the response contributed by the detuned modes (i=3,...,p+s).

By combining the appropriate results from Secs. 5.2.2 and 5.2.3, it can be shown that the response of the secondary system contributed by the two closely-spaced modes is given approximately by:

$$\{u_s^{**}(t)\} = \{u_s^{*}(t)\} + \{u_s'(t)\} \qquad (196)$$

where:

$$\{u_s^{*}(t)\} = \{B_1\}\frac{-1}{\omega|\beta|\sqrt{\varepsilon}} \int_o^t a(\tau)\, e^{-\xi\omega(t-\tau)} \sin\Delta\omega(t-\tau)\, \cos\omega(t-\tau)\, d\tau \qquad (197a)$$

$$\{u_s'(t)\} = \{B_2\}\frac{1}{\omega} \int_o^t a(\tau)\, e^{-\xi\omega(t-\tau)} \sin\omega(t-\tau)\, \cos\Delta\omega(t-\tau)\, d\tau \qquad (197b)$$

and:

$$\{B_1\} = \{\phi_s^1\}\, P_p^1\, \frac{|\beta|^2}{\beta} \qquad (198a)$$

$$\{B_2\} = \{\phi_s^1\}\left[-P_s^1 + P_p^1\, \frac{|\beta|^2}{2\beta} + \sum_{i=1}^{P} \frac{e_{i1} P_p^i M_p^i}{\varepsilon[1-(\omega/\omega_p^i)^2]\, M_p^1}\right] + \sum_{j=2}^{S} \frac{E_{j1}\{\phi_s^j\}P_p^1}{[1-(\omega/\omega_s^j)^2]} \qquad (198b)$$

$$\Delta\omega = |\beta|\omega\, \frac{\sqrt{\varepsilon}}{2} \qquad (198c)$$

A comparison of Eqs. (197a,b) with Eqs. (43a,b) shows that $\{u_s^{**}(t)\}$, $\{u_s^{*}(t)\}$, and $\{u_s'(t)\}$ are analogous, respectively, to $u_s^{**}(t)$, $u_s^{*}(t)$, and $u_s'(t)$. Also, it is seen that if $||\{u_s'(t)\}|| << ||\{u_s^{*}(t)\}||$, then $\{u_s^{**}(t)\}$ is proportional to the response of a simple tuned secondary system (see Fig. 1) with a "mass ratio" of $|\beta|^2\varepsilon$.

The response of the secondary system contributed by the detuned modes is denoted by $\{u_s^d(t)\}$. By combining the appropriate results from Secs. 5.2.2 and 5.2.3, we obtain:

$$\{u_s^d(t)\} = -\sum_{j=1}^{S}\left(P_s^j - \sum_{k=1}^{P}\frac{e_{kj}P_p^k M_p^k}{[1-(\omega_s^j/\omega_p^k)^2]M_s^j}\right)\{\phi_s^j\}\frac{1}{\omega_s^j}\int_o^t a(\tau)\, e^{-\xi_s^j\omega_s^j(t-\tau)}\sin\omega_s^j(t-\tau)\, d\tau +$$

$$+\sum_{i=2}^{P}\sum_{k=1}^{S}\frac{E_{ik}P_p^i\{\phi_s^k\}}{[1-(\omega_p^i/\omega_s^k)^2]}\frac{1}{\omega_p^i}\int_o^t a(\tau)\, e^{-\xi_p^i\omega_p(t-\tau)}\sin\omega_p^i(t-\tau)\, d\tau \qquad (199a)$$

where:

$$\xi_p^i = \frac{\gamma\omega_p^i}{2} \qquad (199b)$$

$$\xi_s^i = \frac{\gamma\omega_s^i}{2} \qquad (199c)$$

It is easily demonstrated that a decoupled analysis furnishes the same result for $\{u_s^d(t)\}$ as Eq. (199a). This shows that interaction between the primary and secondary systems can be neglected when considering the response of the detuned modes of the total structure.

The total response of the secondary system, denoted by $\{u_s(t)\}$, is obtained by summing the response of the closely-spaced and detuned modes; thus:

$$\{u_s(t)\} \simeq \{u_s^{**}(t)\} + \{u_s^d(t)\} \qquad (200)$$

5.3.2 Response of Systems with Nonproportional Damping

If $\gamma_p \neq \gamma_s$, the damping matrix of the total structure is not proportional to the stiffness matrix and, in general, the damping is nonclassical.

If, however, the damping coefficients are sufficiently small, as is assumed here, the undamped eigenmodes approximately uncouple provided their corresponding frequencies are widely spaced. Consequently, Eq. (199a) for the response of the detuned modes holds but with:

$$\xi_p^i = \frac{\gamma_p \omega_p^i}{2} \tag{201a}$$

$$\xi_s^j = \frac{\gamma_s \omega_s^j}{2} \tag{201b}$$

The two closely-spaced modes are, in general, coupled when the damping is nonproportional. To isolate these modes, we use the transformations:

$$\{u_p(t)\} = [\phi_p][\{^1\alpha_p\}\{^2\alpha_p\}]\begin{Bmatrix} x_1 \\ x_2 \end{Bmatrix} \tag{202a}$$

$$\{u_p(t)\} = [\phi_s][\{^1\alpha_p\}\{^2\alpha_p\}]\begin{Bmatrix} x_1 \\ x_2 \end{Bmatrix} \tag{202b}$$

where x_1 and x_2 are modal coordinates. Substituting Eqs. (202a,b) into Eq. (38) and using modal orthogonality, we obtain:

$$\ddot{x}_1 + 2\xi_a\omega\dot{x}_1 + \xi_d\omega\dot{x}_2 + (\Omega_1)^2 x_1 = -P_1 a(t) \tag{203a}$$

$$\ddot{x}_2 + \xi_d\omega\dot{x}_1 + 2\xi_a\omega\dot{x}_2 + (\Omega_2)^2 x_2 = -P_2 a(t) \tag{203b}$$

where:

$$\xi_a = \frac{\xi_p^1 + \xi_s^1}{2} \tag{204a}$$

$$\xi_d = \xi_p^1 - \xi_s^1 \tag{204b}$$

Equations (202a,b) can be solved using Fourier transforms. After substituting the solutions into Eq. (203b), we have:

$$\{u_s^{**}(t)\} = \{B_1\}Z_1(t) + \{B_2\}Z_2(t) \tag{205}$$

where:

$$Z_1(t) = -\frac{1}{2\delta\omega}\int_o^t a(\tau)\, e^{-\xi_a\omega(t-\tau)} \sin\delta\omega(t-\tau)\, \cos\omega(t-\tau)\, d\tau \tag{206a}$$

$$Z_2(t) = \frac{1}{\omega}\int_o^t a(\tau)\, e^{-\xi_a\omega(t-\tau)} \sin\omega(t-\tau)\, \cos\delta\omega(t-\tau)\, d\tau \tag{206b}$$

$$\delta\omega = \omega\,\frac{\sqrt{\beta^2\varepsilon-\xi_d^2}}{2} \tag{206c}$$

if $(\beta^2\varepsilon-\xi_d^2)>0$; and:

$$Z_1(t) = -\frac{1}{\xi_d^1\omega}\int_o^t a(\tau)\, e^{-\xi_a\omega(t-\tau)} \sinh\frac{\xi_d'\omega}{2}(t-\tau)\, \cos\omega(t-\tau)\, d\tau \tag{207a}$$

$$Z_2(t) = \frac{1}{\omega}\int_o^t a(\tau)\, e^{-\xi_a\omega(t-\tau)} \cosh\frac{\xi_d'\omega}{2}(t-\tau)\, \sin\omega(t-\tau)\, d\tau \tag{207b}$$

$$\xi_d' = \sqrt{\xi_d^2 - \beta^2\varepsilon} \tag{207c}$$

if $(\beta^2\varepsilon-\xi_d^2)<0$.

CHAPTER 6. CONCLUSIONS

6.1 Summary and Conclusions

The most crucial and difficult problem involved in computing the dynamic response of a tuned secondary system is evaluating the response contributed by two closely-spaced eigenmodes. Formulas for this response have been derived with the aid of an asymptotic procedure. The systems considered were undamped, classically damped, non-classically damped as well as slightly detuned. For most of the systems, the response was shown to be characterized by the presence of "beats" and an envelope function that closely matches the response maxima.

Estimates of the maximum secondary system response contributed by the two closely-spaced modes were developed from the response formulas. The estimates indicated that the maximum response depends primarily on the Fourier amplitude spectrum of the ground motion. Responses predicted by the exact approximate method were compared in a numerical study. Three distinct types of behavior were observed depending on the behavior of the Foutier amplitude and pseudo-velocity spectra in the vicinity of the tuned frequency:

Case 1: The Fourier amplitude spectrum exhibits moderate or little fluctuation and is comparable in magnitude to the pseudo-velocity spectrum. In this case, Approximations 1 and 2 of Chapter 3 furnish good to excellent results and, in fact, Approximation 1 may sometimes be regarded as an "exact" closed form solution for engineering purposes.

Case 2: The Fourier amplitude spectrum exhibits extreme fluctuation and is comparable in magnitude to the pseudo-velocity spectrum. In this case, Approximation 2 furnishes acceptable results while Approximation 3 usually furnishes poorer, but conservative, results.

Case 3: The Fourier amplitude spectrum is much smaller than the pseudo-velocity spectrum. In this case, a term that is negligible in Cases 1 and 2 contributes significantly to

the response and only Approximation 2 furnishes satisfactory estimates.

Consideration was next given to MDOF systems. The asymptotic procedure used earlier was employed to derive a formula for the response of an MDOF tuned secondary system attached to an MDOF primary system. The response contributed by the detuned modes was seen to be similar to the analogous decoupled analysis result. Likewise, the response contributed by the closely-spaced modes was seen to be similar in form to the response of the simple system dealt with in Chapter 2.

6.2 Suggestions for Future Research

This study has clearly shown that knowledge of the Fourier amplitude spectrum is essential if the response of a tuned secondary system is to be estimated accurately. Since Fourier spectra are not as widely available as response spectra, some attention should be given to the development of approximate procedures for generating Fourier spectra from response spectra. The concept of a "design Fourier spectrum" analogous to a design response spectrum could be developed for use in building codes.

Effort should also be devoted to remedying what is felt is the principal weakness of this study; namely, the failure to accurately estimate the response to ground motions that fall into Case 2 above. A stochastic approach will probably be needed to do this.

REFERENCES

1. Biggs, J. M., and Roesset, J. M., "Seismic Analysis of Equipment Mounted on a Massive Structure, Seismic Design for Nuclear Power Plants," Seismic Design for Nuclear Power Plants, R. J. Hansen, ed., Cambridge, Mass., 1970.

2. Bisplinghoff, R. L., Ashley, H., and Halfman, R. L., Aeroelasticity, Addison-Wesley Publishing Co., Inc., Reading, Mass., 1955.

3. Carrier, G. F., Krook, M., and Pearson, C., Complex Variables: Theory and Technique, McGraw-Hill Book Co., Inc., New York, N.Y., 1971.

4. Caughey, T. K., "Design of Subsystems in Large Structures," Technical Memorandum 33-484, Jet Propulsion Laboratory, Pasadena, Calif., June, 1971.

5. Caughey, T. K., and O'Kelly, M. E. J., "Classical Normal Modes in Damped Linear Dynamic Systems," Journal of Applied Mechanics, Vol. 32, No. 3, 1965, pp. 583-588.

6. Clough, R. W., and Penzien, J., Dynamics of Structures, McGraw-Hill Book Co., Inc., New York, N.Y., 1975.

7. Gantmacher, F., Lectures in Analytical Mechanics, MIR Publishers, Moscow, USSR, 1970.

8. Hohn, F. E., Elementary Matrix Algebra, 3rd ed., The Macmillan Company, New York, N.Y., 1973.

9. Hudson, D. E., "Some Problems in the Application of Spectrum Techniques to Strong Motion Earthquake Analysis," Bulletin of the Seismological Society of America, Vol. 52, No. 2, 1962, pp. 417-430.

10. Hurty, W. C., and Rubinstein, M. F., Dynamics of Structures, Prentice-Hall, Inc., New York, N.Y., 1964.

11. Kassawara, R. P., "Earthquake Response of Light Multiple-Degree-of-Freedom Systems by Spectrum Techniques," thesis presented to the University of Illinois at Urbana, Ill., in 1970, in partial fulfillment of the requirements for the degree of Doctor of Philosophy.

12. Kelly, J. M., and Sackman, J. L., "Equipment-Structure Interaction at High Frequencies," Report No. DNA 4298T, Weidlinger Associates, Menlo Park, Calif., 1977.

13. Kelly, J. M., and Sackman, J. L., "Response Spectra Design Methods for Tuned Equipment-Structure Systems," Journal of Sound and Vibration, Vol. 59, No. 2, 1978, pp. 171-179.

14. Kelly, J. M., and Sackman, J. L., "Shock Spectra Design Methods for Equipment in Impulsively Loaded Structures," Report No. DNA 5267F, Weidlinger Associates, Menlo Park, Calif., November, 1979.

15. Nakhata, T., Newmark, N. M., and Hall, W. J., "Approximate Dynamic Response of Light Secondary Systems, Structural Research Series No. 396, Civil Engineering Studies, University of Illinois, Urbana, Ill., 1973.

16. Newmark, N. M., "Earthquake Response Analysis of Reactor Structures," Nuclear Engineering and Design, Vol. 20, No. 2, 1972, pp. 303-322.

17. Newmark, N. M., and Hall, W. J., "Seismic Design Criteria for Nuclear Reactor Facilities," Proceedings of the Fourth World Conference on Earthquake Engineering, Vol. 2, Paper B-4, pp. 37-50, Santiago, Chile, 1969.

18. Newmark, N. M., and Rosenblueth, E., Fundamentals of Earthquake Engineering, Prentice-Hall, Inc., Englewood Cliffs, N.J., 1971.

19. Papoulis, A., The Fourier Integral and its Applications, 1st ed., McGraw-Hill, New York, N.Y., 1962.

20. Penzien, J., and Chopra, A. K., "Earthquake Response of Appendage on a Multi-Story Building," Proceedings of the Third World Conference on Earthquake Engineering, New Zealand, 1965.

21. Ruzicka, G. C., and Robinson, A. R., "Dynamics of Tuned Secondary Systems," Proceedings of the Second ASCE Engineering Mechanics Division Specialty Conference, North Carolina State University, Raleigh, N.C., 1977.

22. Sackman, J. L., and Kelly, J. M., "Transient Analysis of Equipment-Structure Interaction at High Frequencies," Report No. DNA 4675F, Weidlinger Associates, Menlo Park, Calif., May, 1978.

23. Sackman, J. L., and Kelly, J. M., "Rational Design Methods for Light Equipment in Structures Subjected to Ground Motion," Report No. UCB/EERC-78/19, Earthquake Engineering Research Center, University of California, Berkeley, Calif., September, 1978.

24. Sackman, J. L., and Kelly, J. M., "Equipment Response Spectra for Nuclear Power Plant Systems," Transactions of the Fifth International Conference on Structural Mechanics in Reactor Technology, Paper K9/1, West Berlin, 1979.

25. Sackman, J. L., and Kelly, J. M., "Seismic Analysis of Internal Equipment and Components in Structures," Engineering Structures, Vol. 1, No. 1, July, 1979, pp. 179-190.

26. Scanlan, R. H., and Sachs, K., "Earthquake Time Histories and Response Spectra," Journal of the Engineering Mechanics Division, ASCE, Vol. 100, No. EM4, Proc. Paper 10703, August, 1974, pp. 635-655.

27. Singh, A. K., "A Stochastic Model for Predicting Maximum Response of Light Secondary Systems," thesis presented to the University of Illinois at Urbana, Ill., in 1972, in partial fulfillment of the requirements for the degree of Doctor of Philosophy.

28. Singh, M. P., "Generation of Seismic Floor Spectra," Journal of the Engineering Mechanics Division, ASCE, Vol. 101, No. EM5, Proc. Paper 11651, October, 1975, pp. 593-607.

29. Thomson, W. T., Theory of Vibrations with Applications, Prentice-Hall, Inc., Englewood Cliffs, N.J., 1972.

30. Villaverde, R., and Newmark, N. M., "Seismic Response of Light Attachments to Buildings," Structural Research Series No. 469, University of Illinois, Urbana, Ill., February, 1980.

Table 1. Values of f_b Appearing in Equation (139)

$\frac{\Delta\omega}{\varepsilon\omega}$	f_b
0.0	.960
0.1	.847
0.2	.933
0.3	.879
0.4	.888
0.5	.895
0.6	.899
0.7	.902
0.8	.903
0.9	.904
1.0	.904
2.0	.892
3.0	.876
4.0	.863
5.0	.852
6.0	.844
7.0	.836
8.0	.830
9.0	.825
10.0	.821

Table 2. Parameters of Tuned Systems Considered in Numerical Studies

Tuned Periods

T (sec)
0.1
0.3
0.5
0.8
1.0
3.0
5.0
8.0
10.0

$\xi = .01$		$\xi = .03$		$\xi = .05$	
ε	$\frac{\Delta\omega}{\xi\omega}$	ε	$\frac{\Delta\omega}{\xi\omega}$	ε	$\frac{\Delta\omega}{\xi\omega}$
.000036	0.3	.00090	0.5	.0009	0.3
.000144	0.6	.001296	0.6	.0016	0.4
.000324	0.9	.001764	0.7	.0025	0.5
.000576	1.2	.002304	0.8	.0036	0.6
.000900	1.5	.003600	1.0	.0049	0.7
.001296	1.8	.014400	2.0	.0064	0.8
.001764	2.1	.032400	3.0	.0081	0.9
.002304	2.4	.057600	4.0	.0100	1.0
.003600	3.0	.090000	5.0	.0225	1.5
.014400	6.0			.0400	2.0
.032400	9.0			.0625	2.5
.057600	12.0			.0900	3.0
.090000	15.0				

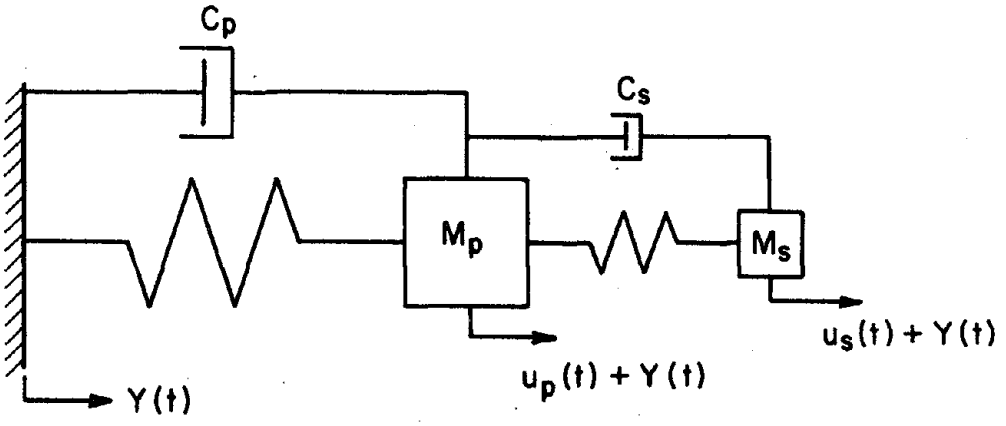

$$\omega^2 = \frac{K_p}{M_p} = \frac{K_s}{M_s} \qquad \epsilon = \frac{K_s}{K_p} = \frac{M_s}{M_p} << 1$$

$$a(t) = \ddot{Y}(t)$$

Figure 1. Simple Two-Degree-of-Freedom Tuned System

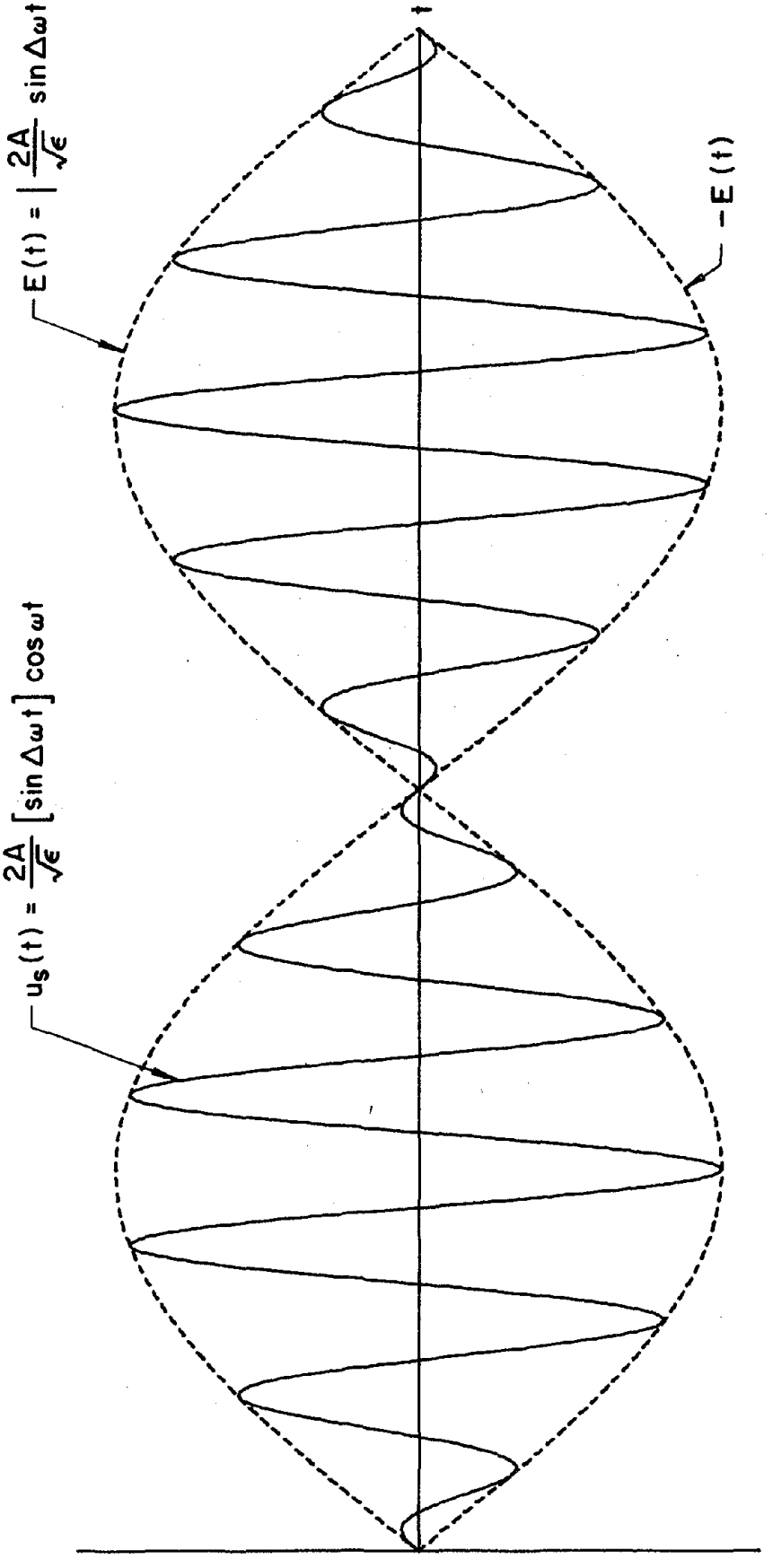

Figure 2. Response of Undamped Tuned Secondary System in Free Vibration

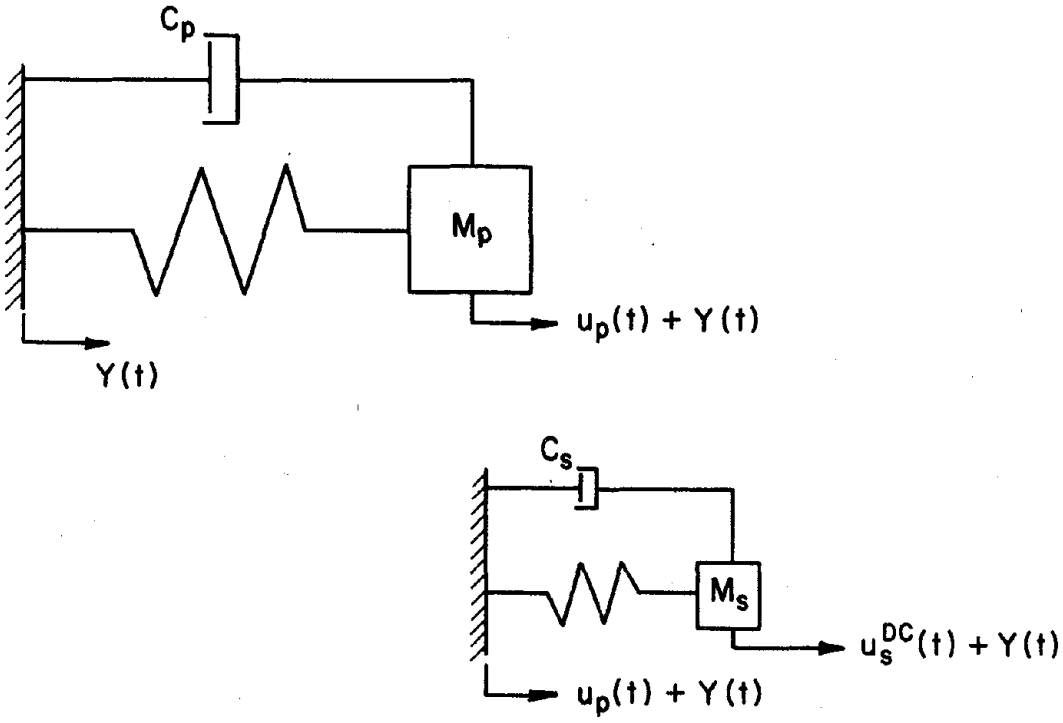

$u_s^{DC}(t)$ = Decoupled Response

Figure 3. Schematic Illustration of Decoupled Analysis Method

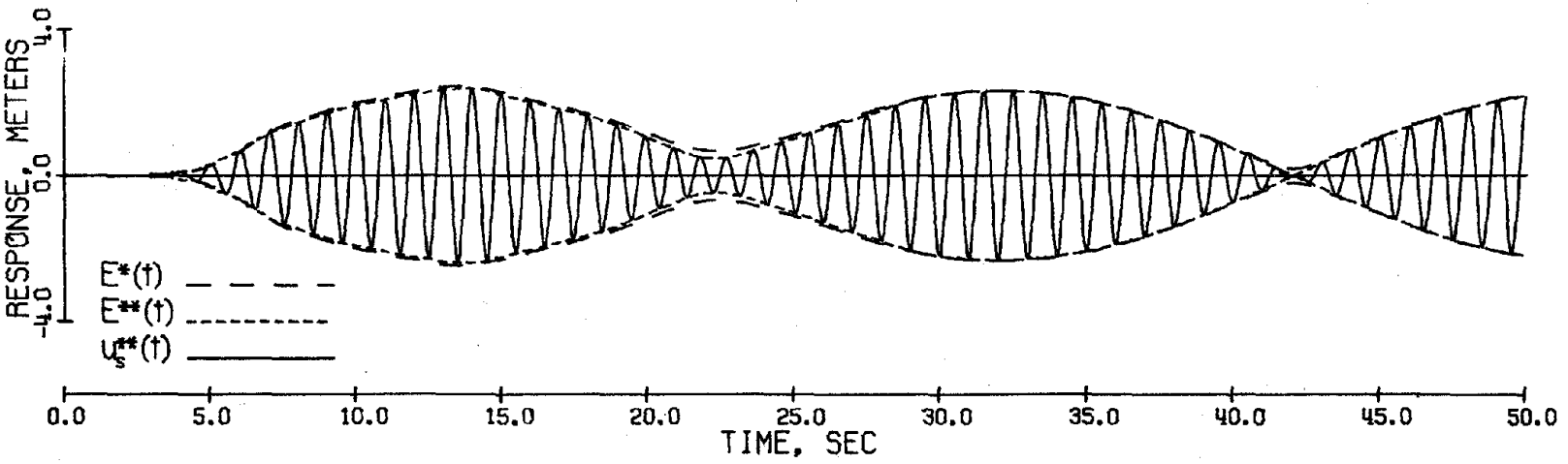

Figure 4a. Approximate Response of Undamped Tuned Secondary System to El Centro Earthquake, $\omega = 2\pi$RPS, T = 1 sec, $\varepsilon = .0025$

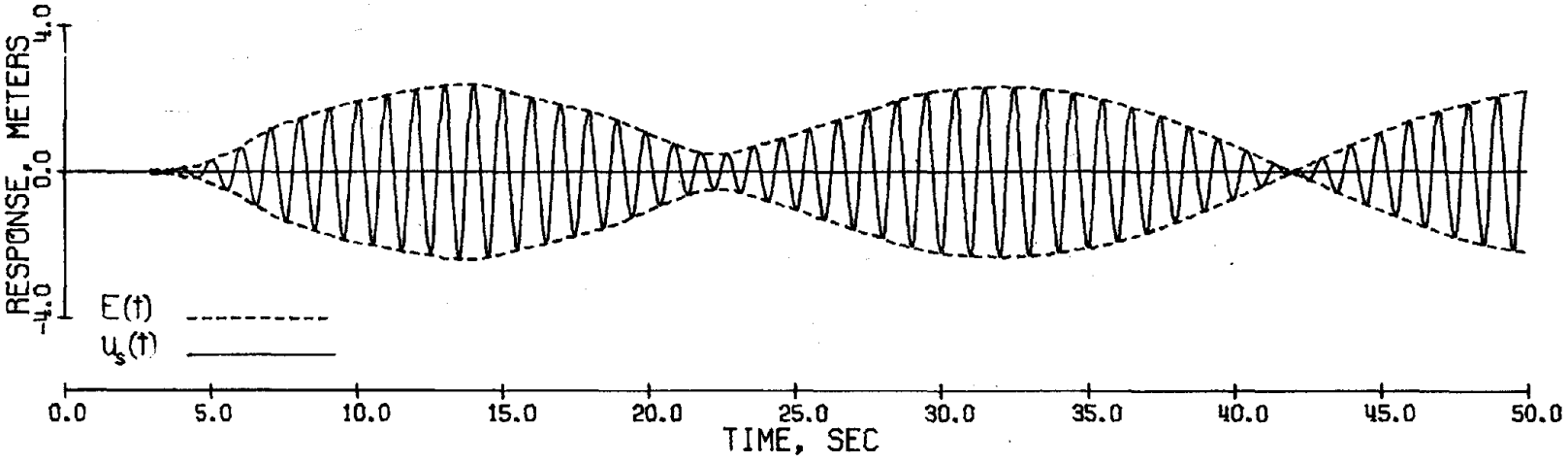

Figure 4b. Exact Response of Undamped Tuned Secondary System to El Centro Earthquake, $\omega = 2\pi$RPS, T = 1 sec, $\varepsilon = .0025$

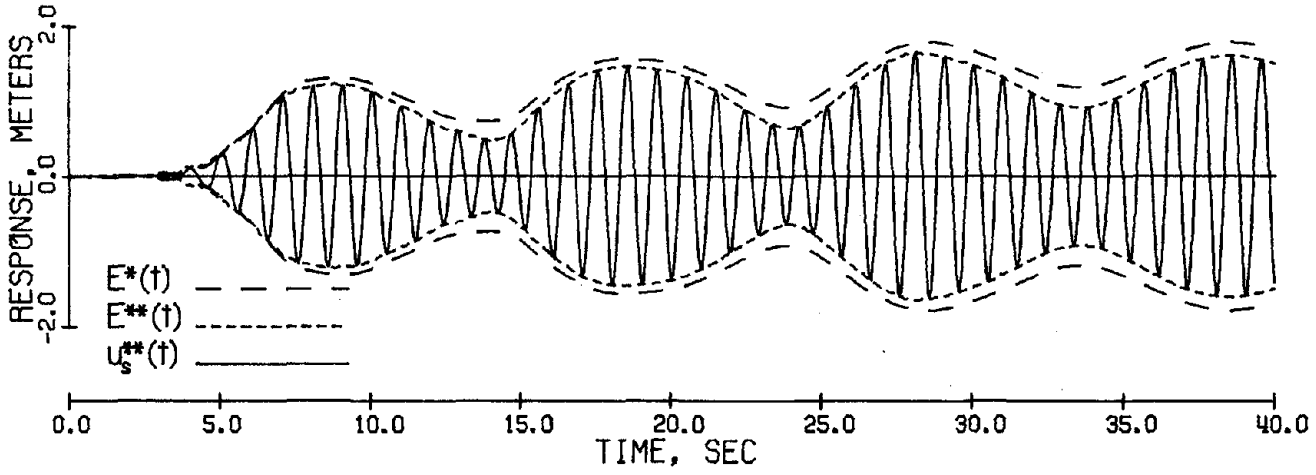

Figure 4c. Approximate Response of Undamped Tuned Secondary System to El Centro Earthquake, $\omega = 2\pi$RPS, T = 1 sec, $\varepsilon = .01$

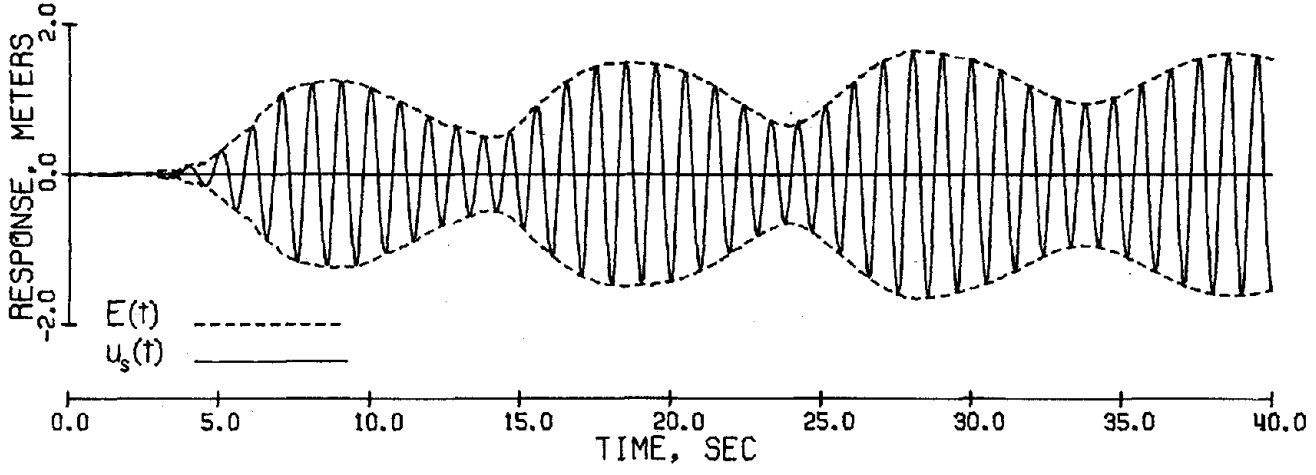

Figure 4d. Exact Response of Undamped Tuned Secondary System to El Centro Earthquake, $\omega = 2\pi$RPS, T = 1 sec, $\varepsilon = .01$

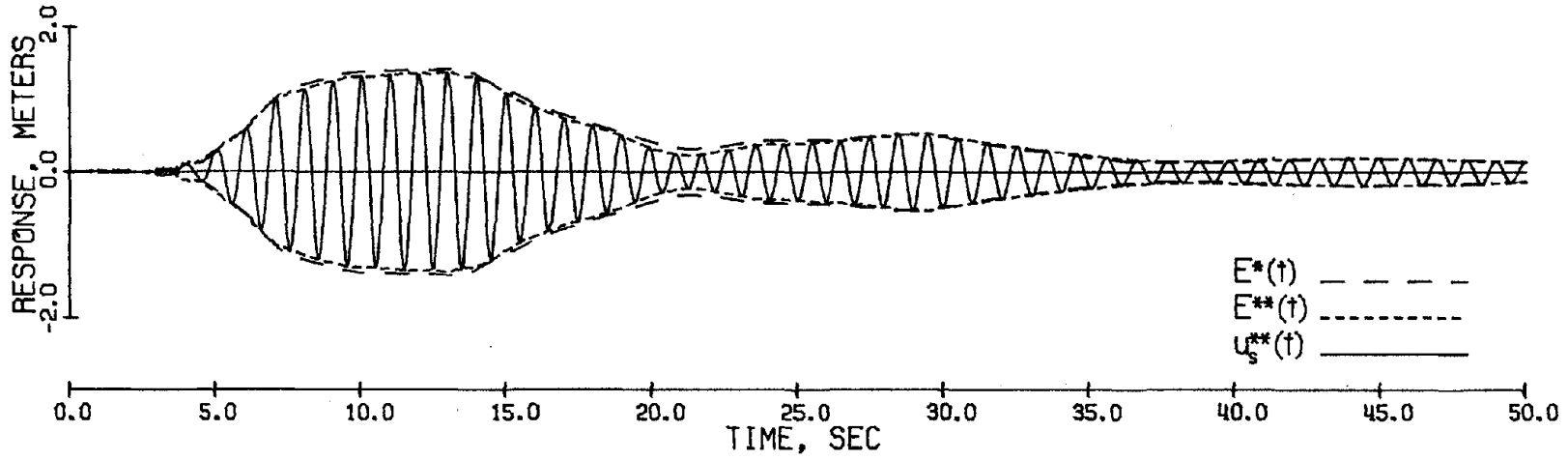

Figure 5a. Approximate Response of Damped Tuned Secondary System to El Centro Earthquake, $\omega = 2\pi$RPS, T = 1 sec, ε = .0025, ξ = .01

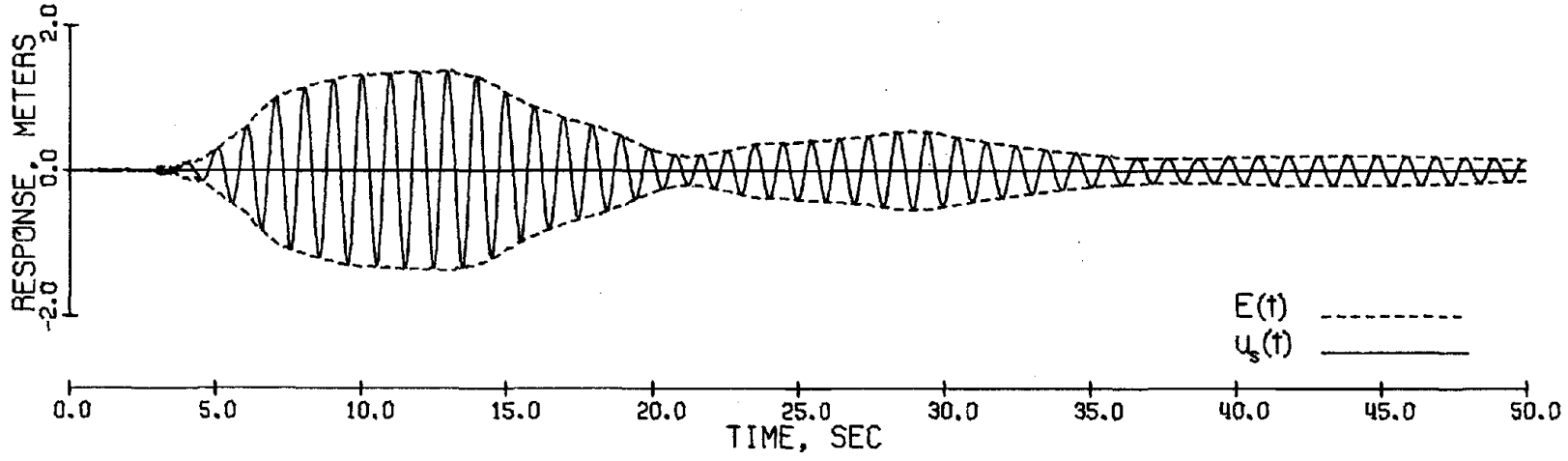

Figure 5b. Exact Response of Damped Tuned Secondary System to El Centro Earthquake, $\omega = 2\pi$RPS, T = 1 sec, ε = .0025, ξ = .01

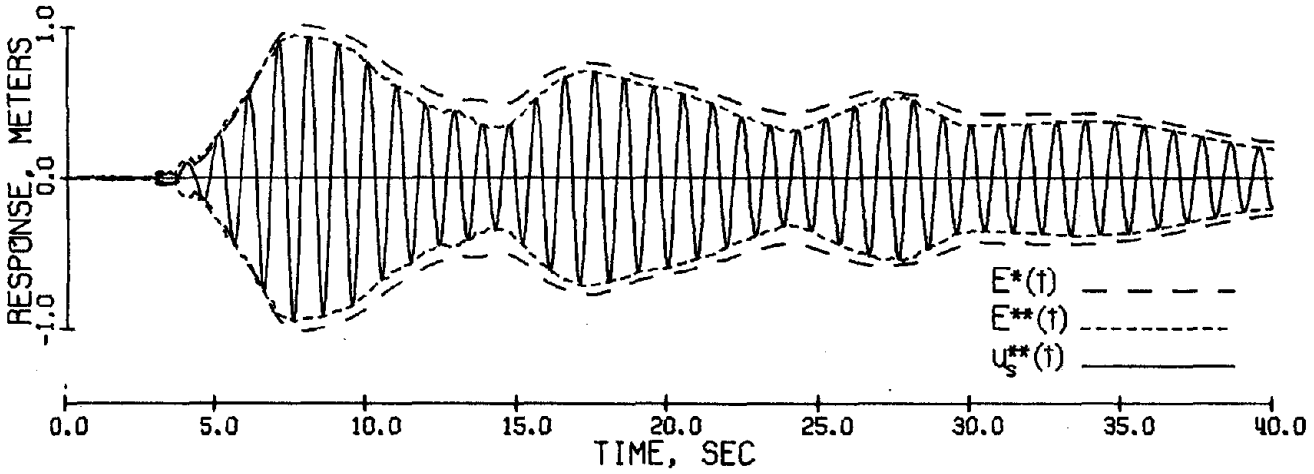

Figure 5c. Approximate Response of Damped Tuned Secondary System to El Centro Earthquake, $\omega = 2\pi$RPS, T = 1 sec, $\varepsilon = .01$, $\xi = .01$

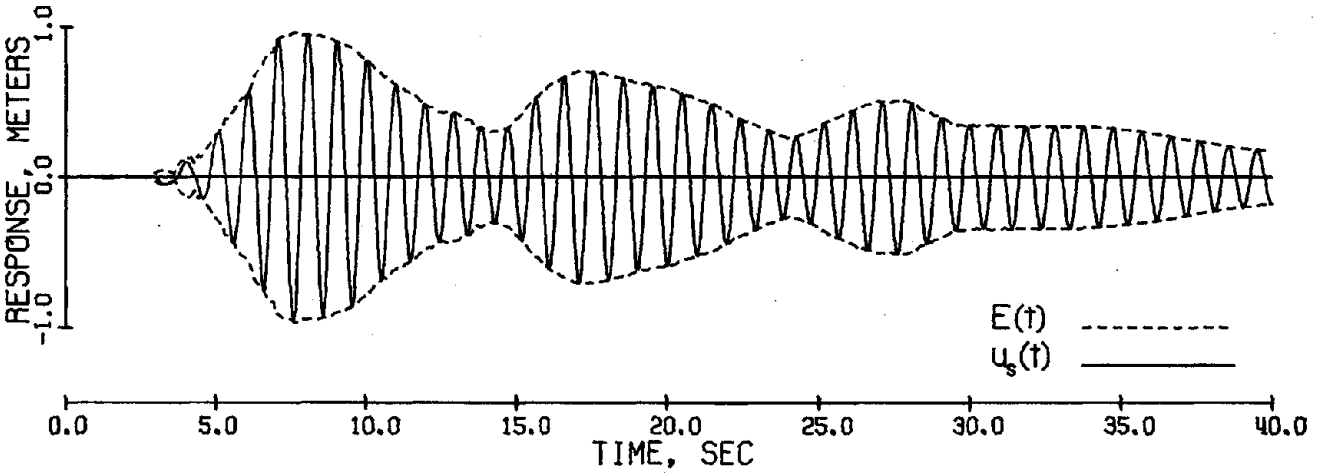

Figure 5d. Exact Response of Damped Tuned Secondary System to El Centro Earthquake, $\omega = 2\pi$RPS, T = 1 sec, $\varepsilon = .01$, $\xi = .01$

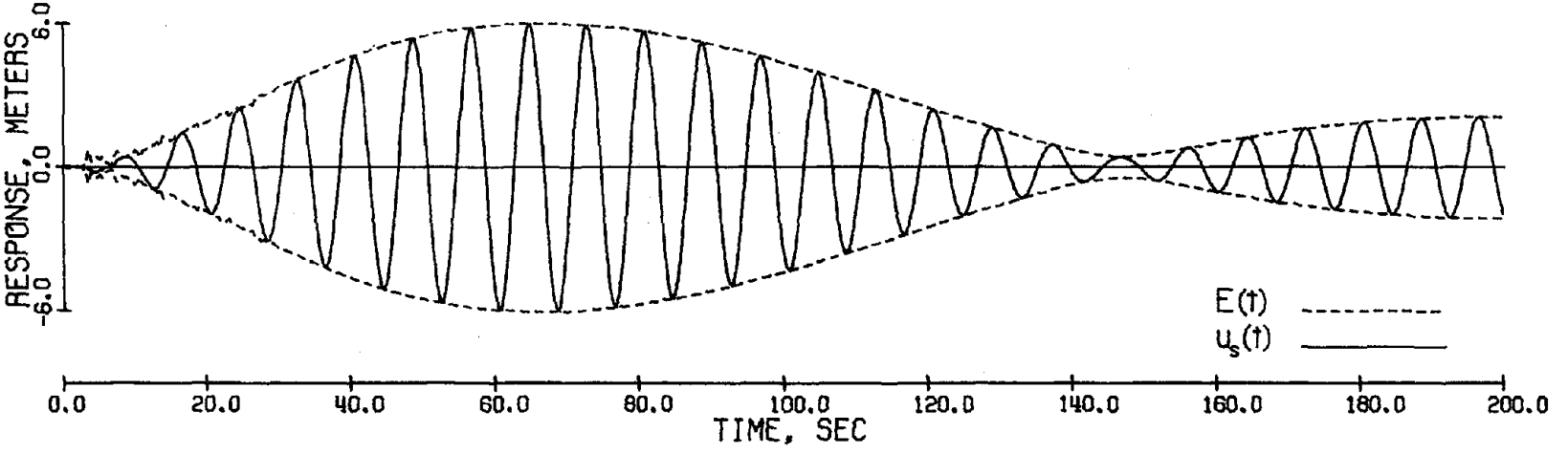

Figure 6a. Response of Damped Tuned Secondary System to El Centro Earthquake, $\omega = .25\pi$RPS, T = 8 sec, $\varepsilon = .0036$, $\xi = .01$

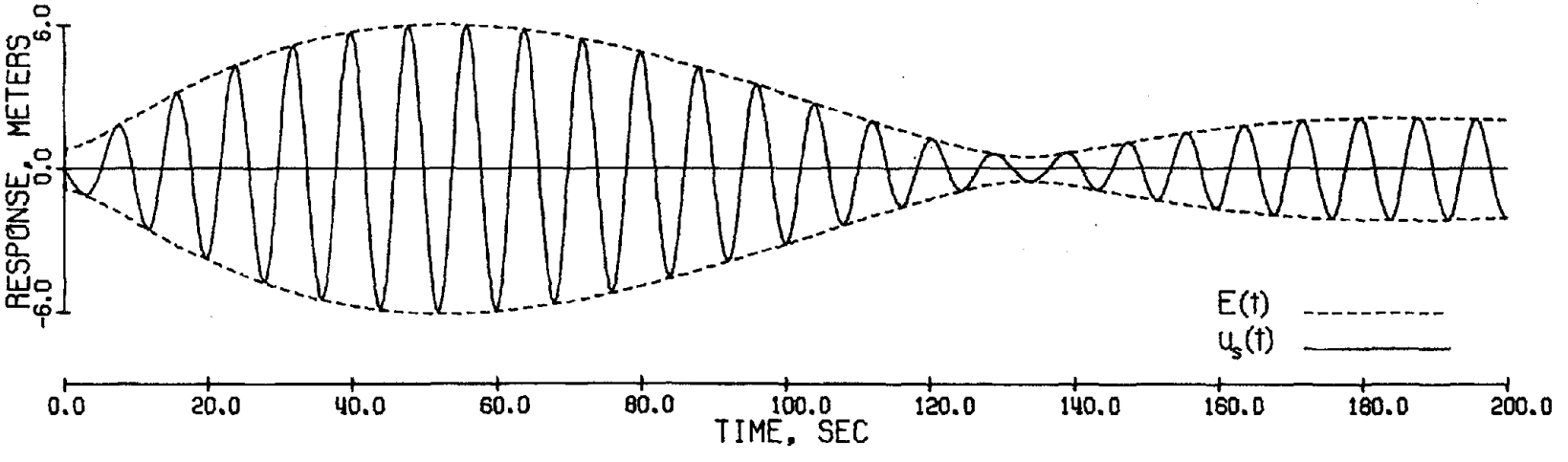

Figure 6b. Response of Damped Tuned Secondary System to Impulse Function, $\omega = .25\pi$RPS, T = 8 sec, $\varepsilon = .0036$, $\xi = .01$

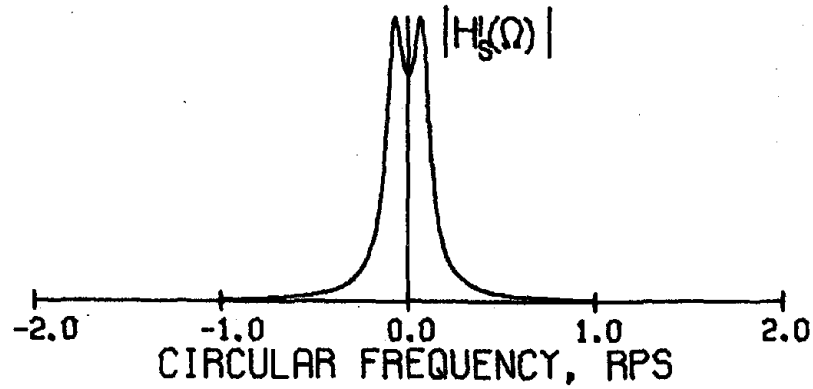

Figure 7a. $|H_s^{\ell}(\Omega)|$ for Tuned Secondary System with $\omega = 1$ RPS, $\varepsilon = .0256$, and $\xi = .04$

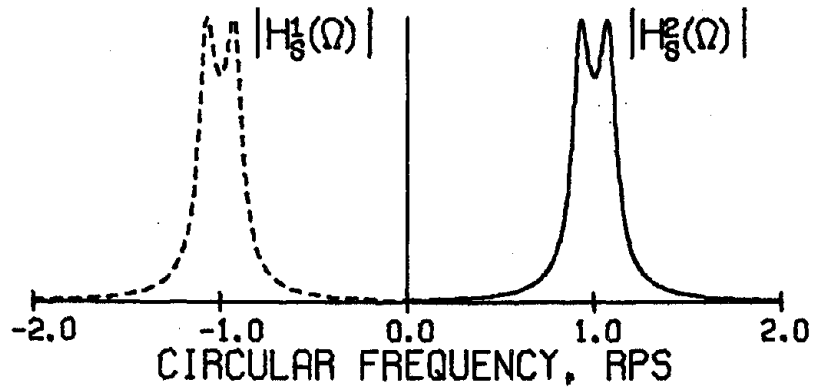

Figure 7b. $|H_s^1(\Omega)|$ and $|H_s^2(\Omega)|$ for Tuned Secondary System with $\omega = 1$ RPS, $\varepsilon = .0256$, and $\xi = .04$

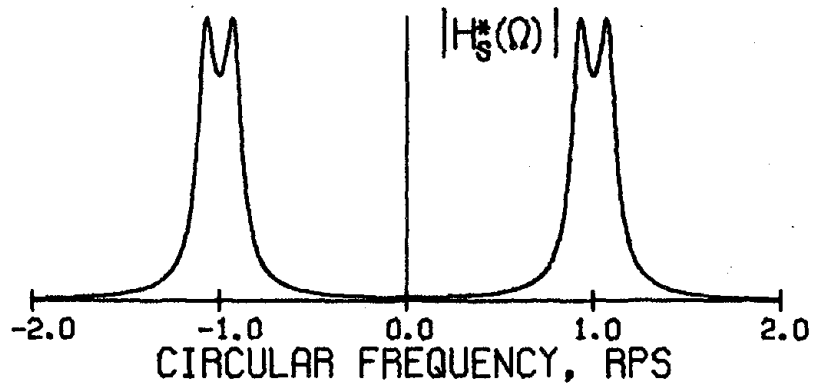

Figure 7c. $|H_s^*(\Omega)|$ for Tuned Secondary System with $\omega = 1$ RPS, $\varepsilon = .0256$, and $\xi = .04$

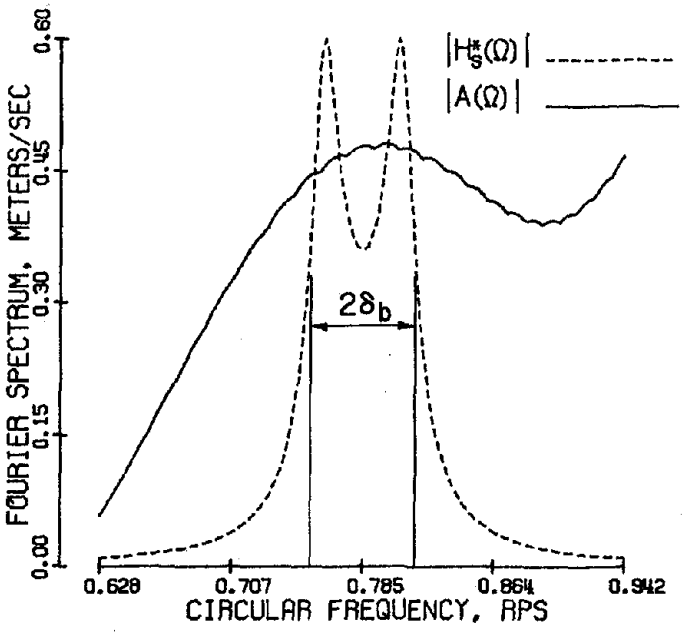

Figure 8a. Frequency Domain Data for Response of Tuned Secondary System to El Centro Earthquake, $\omega = .25\pi$ RPS, $\varepsilon = .0036$, and $\xi = .01$

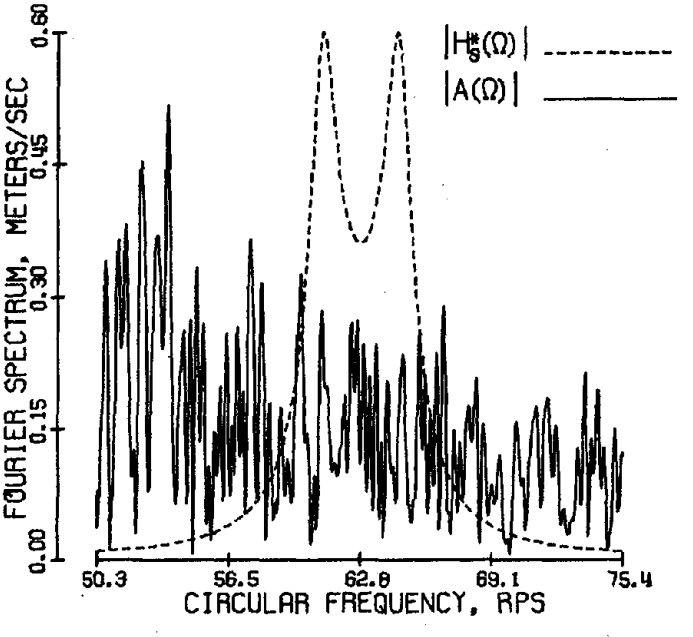

Figure 8b. Frequency Domain Data for Response of Tuned Secondary System to El Centro Earthquake, $\omega = 20\pi$ RPS, $\varepsilon = .0036$, and $\xi = .01$

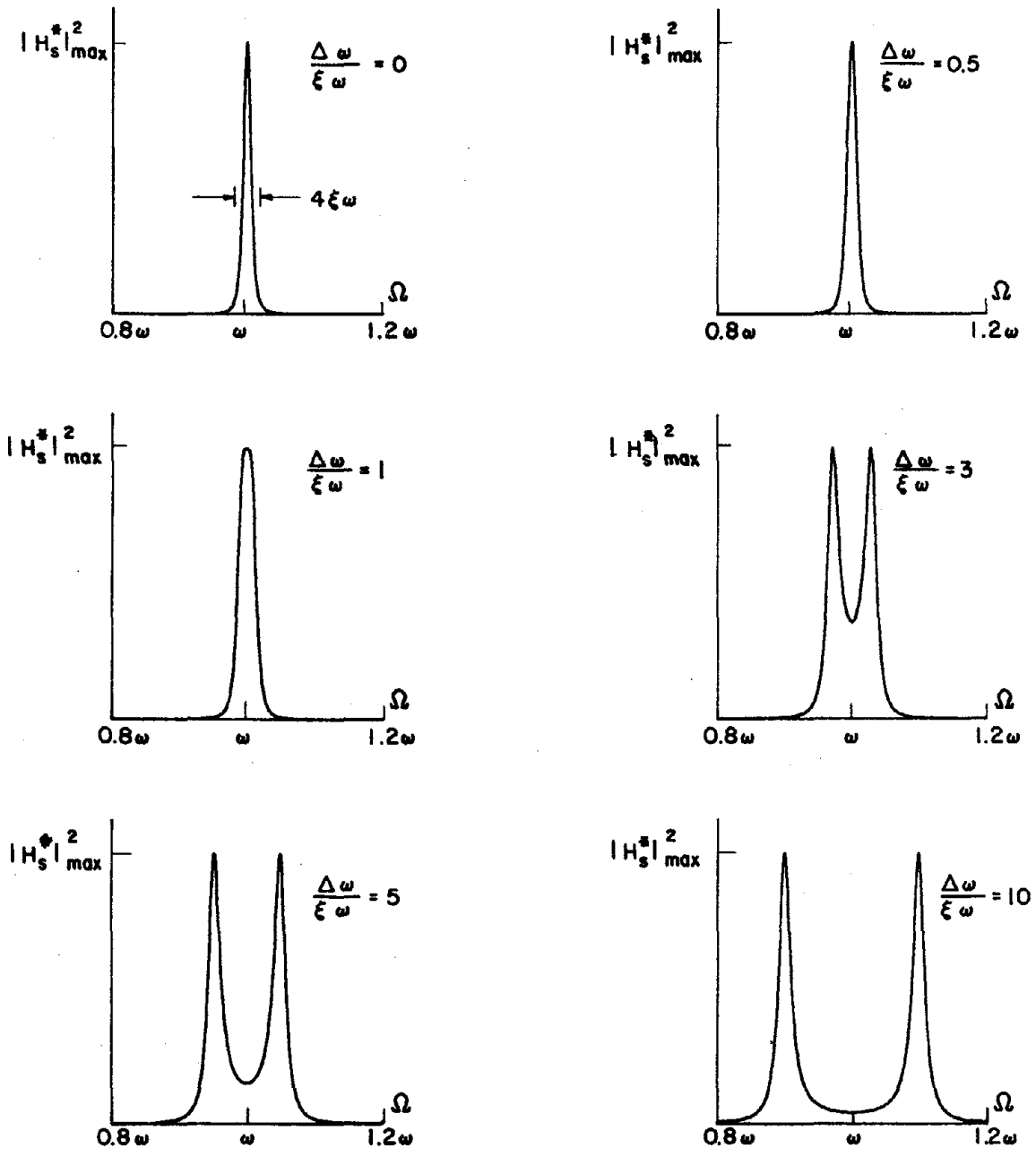

Figure 9. Plots of $|H_s^*(\Omega)|^2$

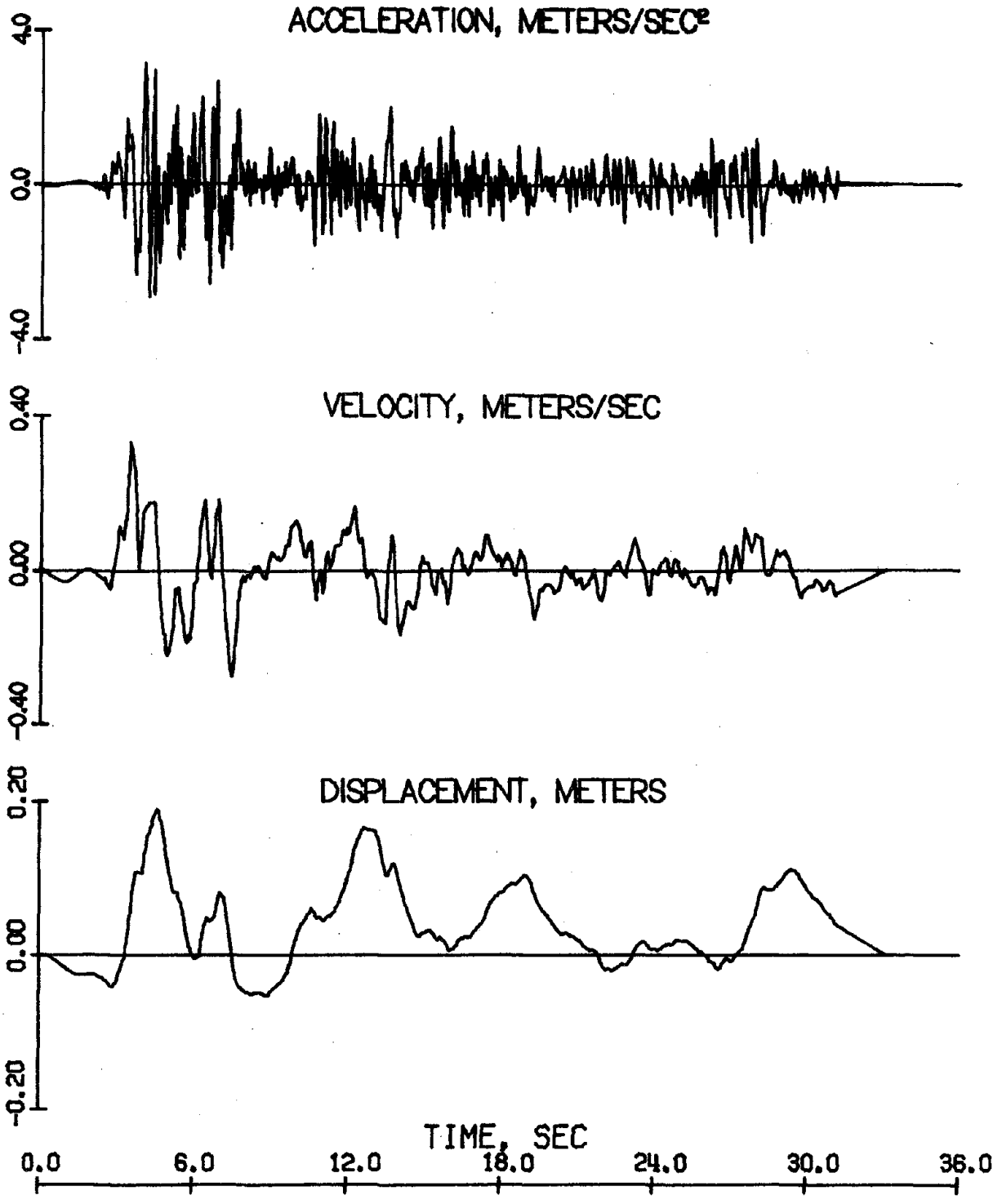

Figure 10. Time History Data for El Centro 1940-NS Earthquake Record

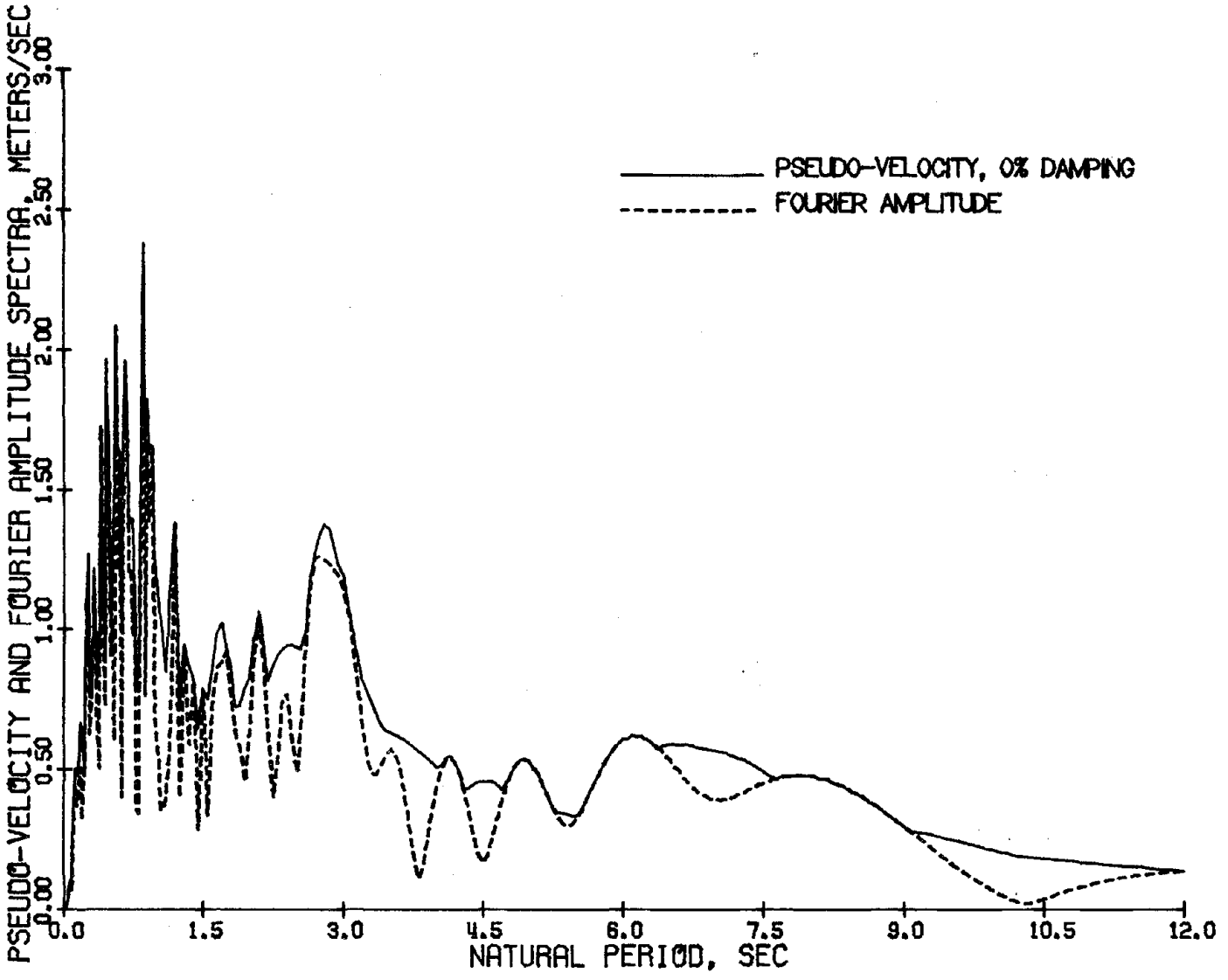

Figure 11. Frequency Domain Data for El Centro 1940-NS Earthquake

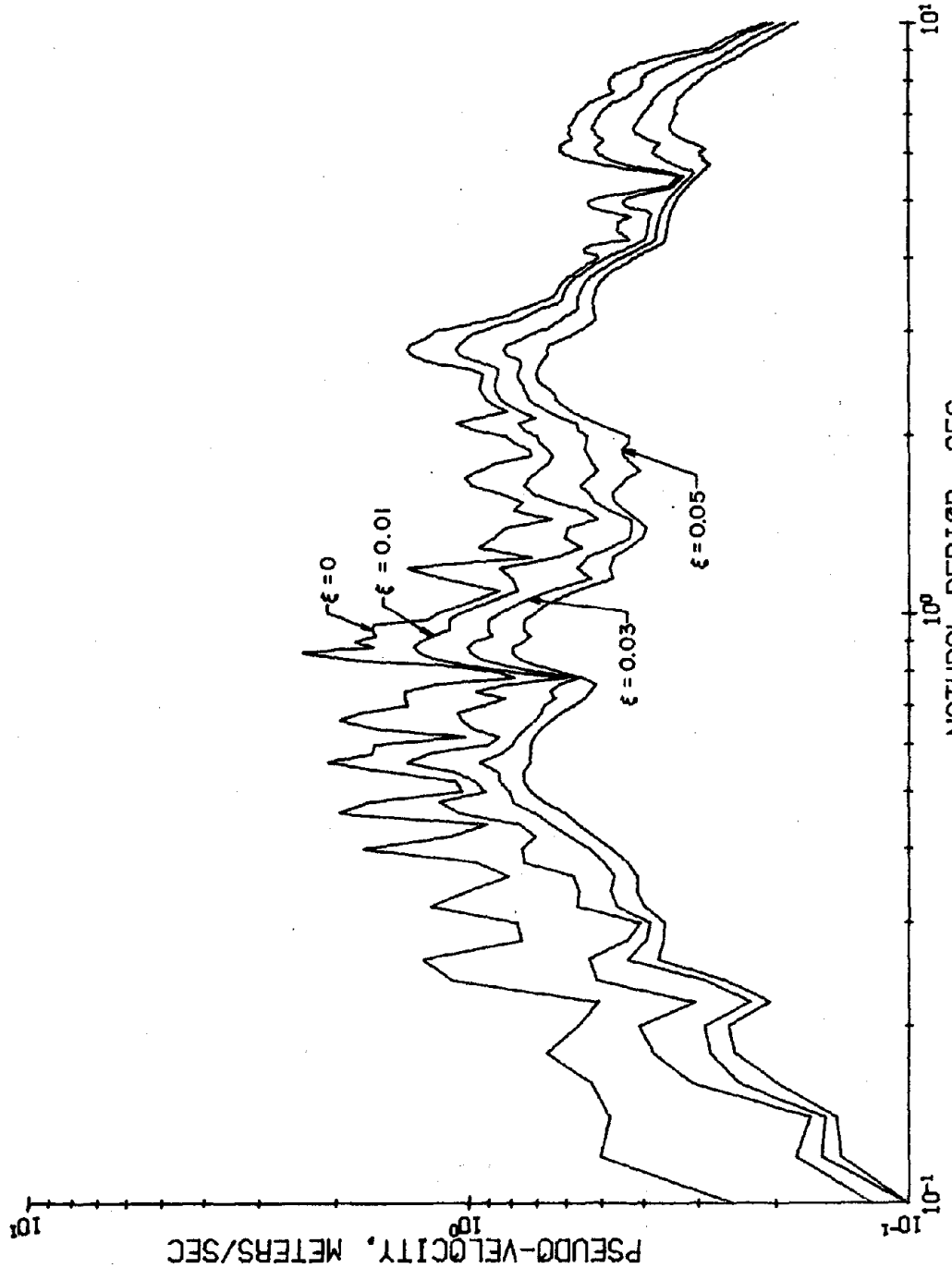

Figure 11 (continued)

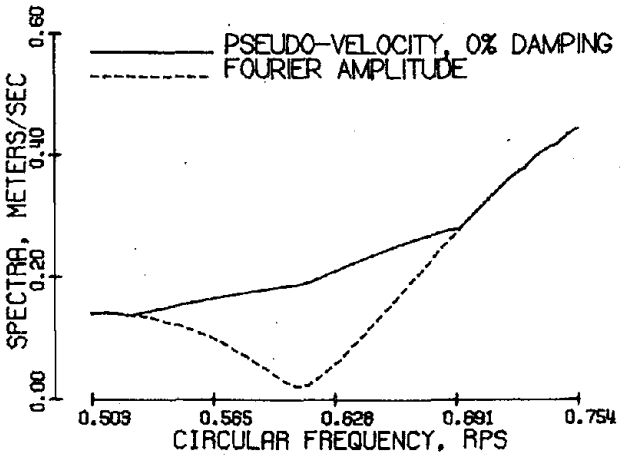

Figure 12a. Frequency Domain Data for El Centro Earthquake in Vicinity of ω = .628 RPS (T = 10 sec)

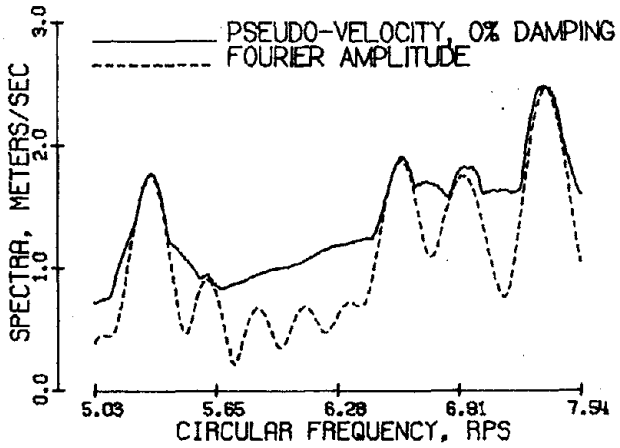

Figure 12b. Frequency Domain Data for El Centro Earthquake in Vicinity of ω = 6.28 RPS (T = 1 sec)

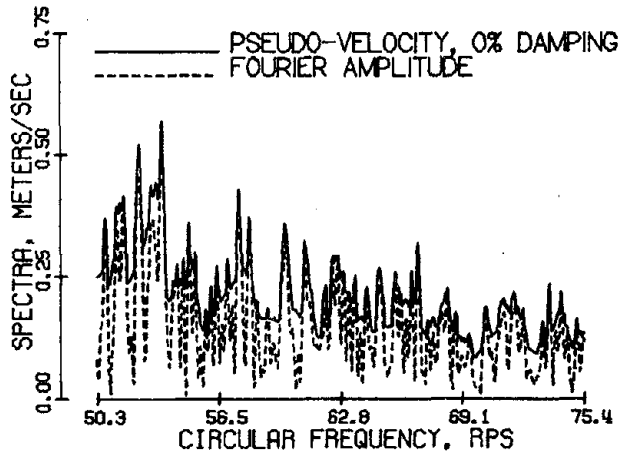

Figure 12c. Frequency Domain Data for El Centro Earthquake in Vicinity of ω = 62.8 RPS (T = .1 sec)

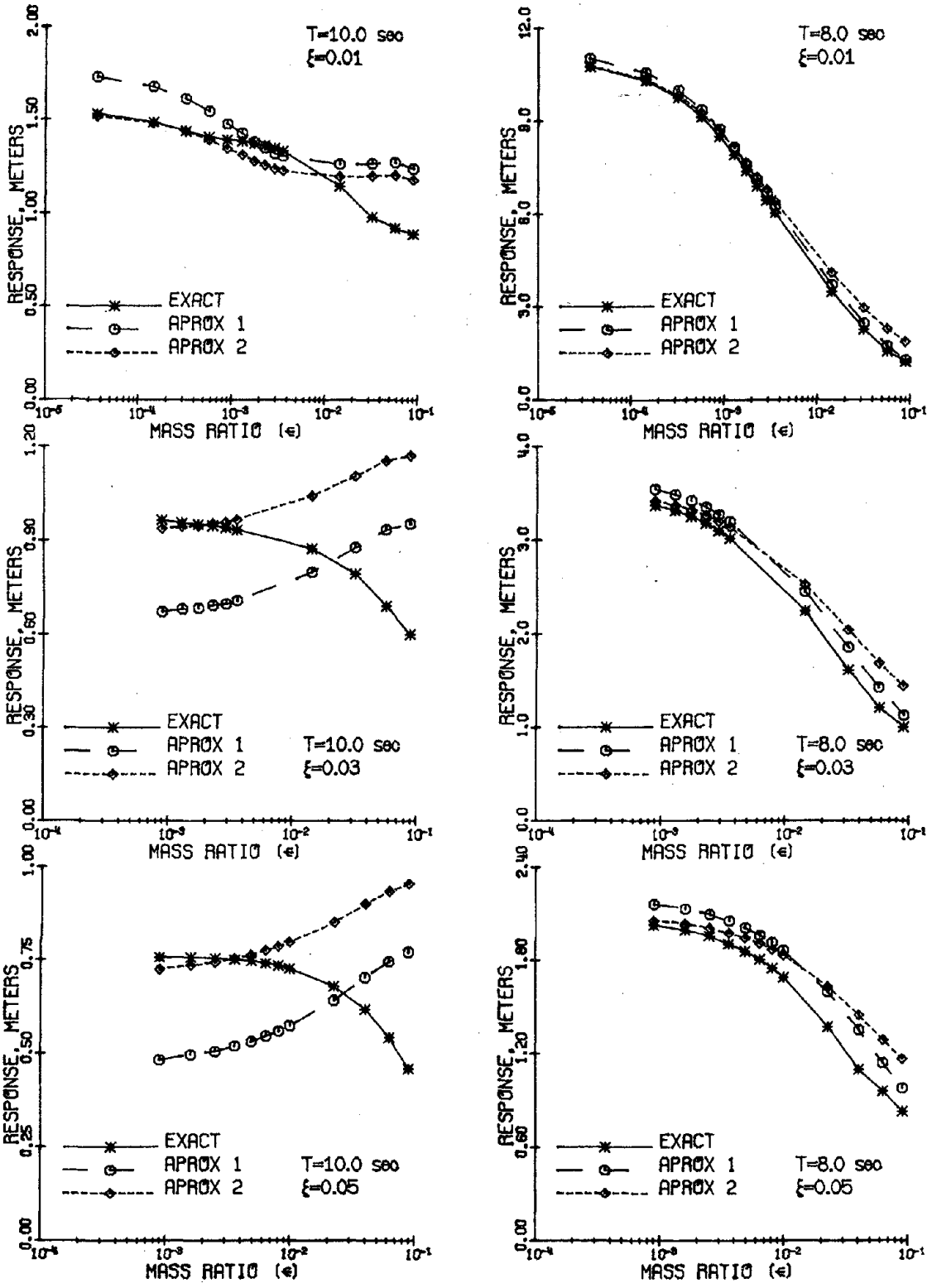

Figure 13. Exact and Approximate Responses of Tuned Secondary System to El Centro Earthquake, T = 10 sec and T = 8 sec

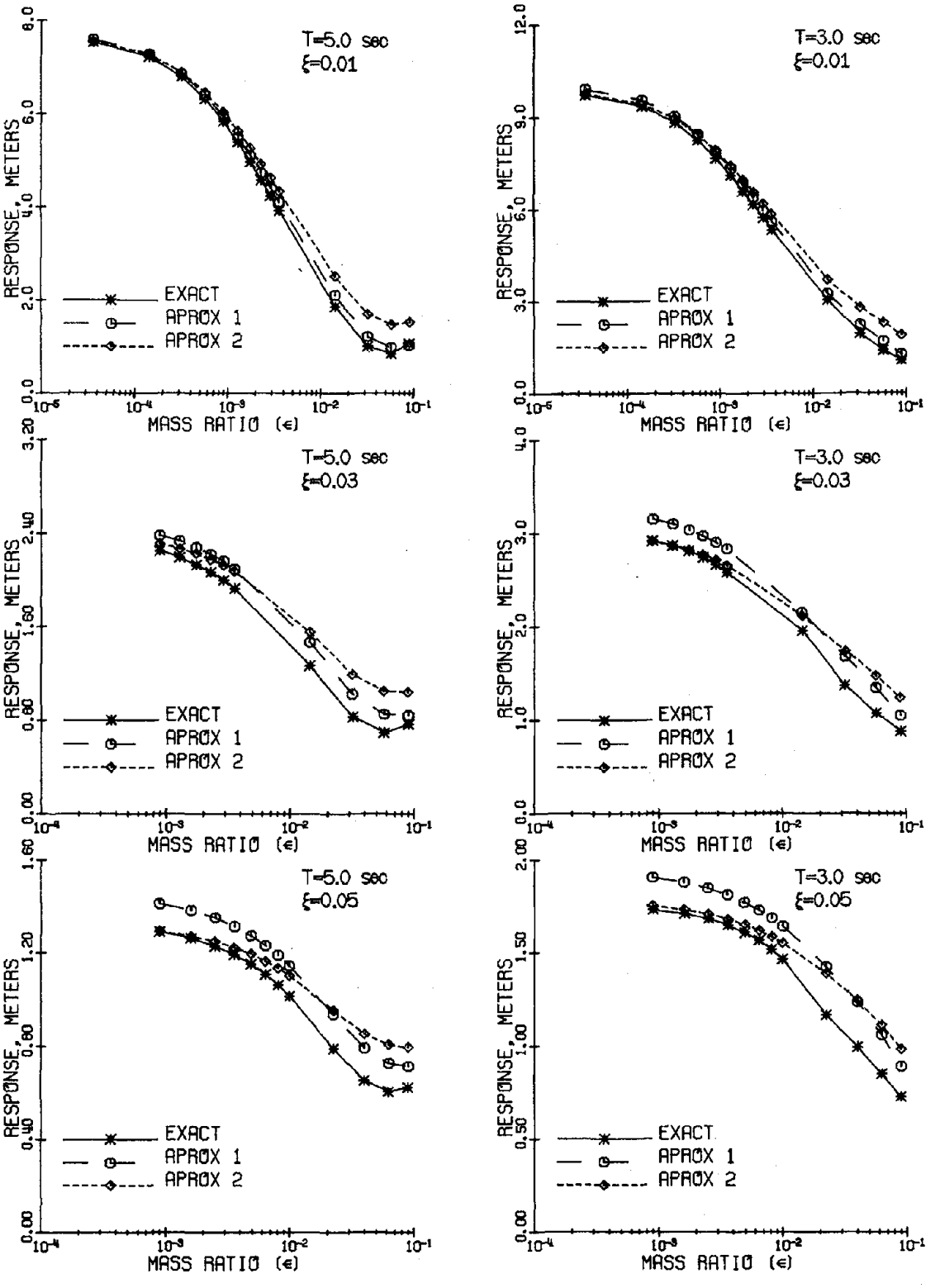

Figure 14. Exact and Approximate Responses of Tuned Secondary System to El Centro Earthquake, T = 5 sec and T = 3 sec

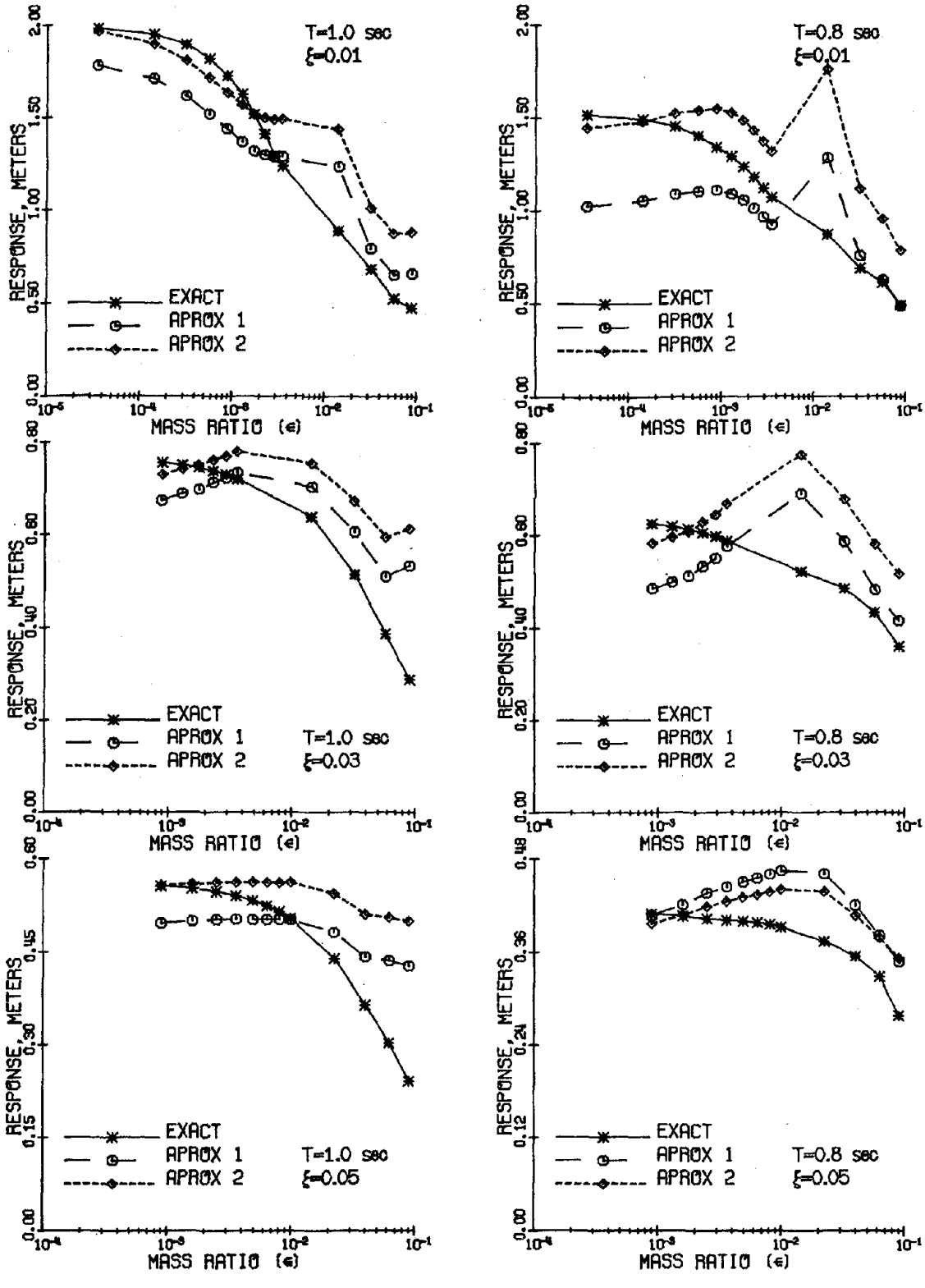

Figure 15. Exact and Approximate Responses of Tuned Secondary System to El Centro Earthquake, T = 1 sec and T = .8 sec

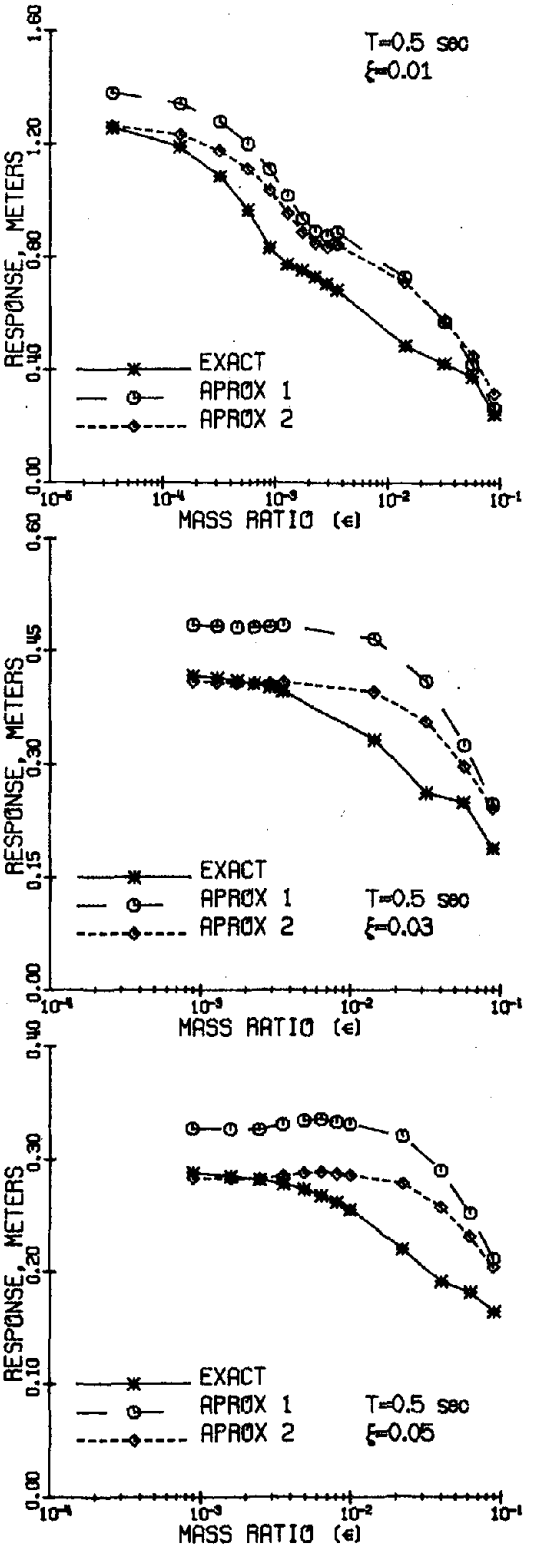

Figure 16. Exact and Approximate Responses of Tuned Secondary System to El Centro Earthquake, T = .5 sec

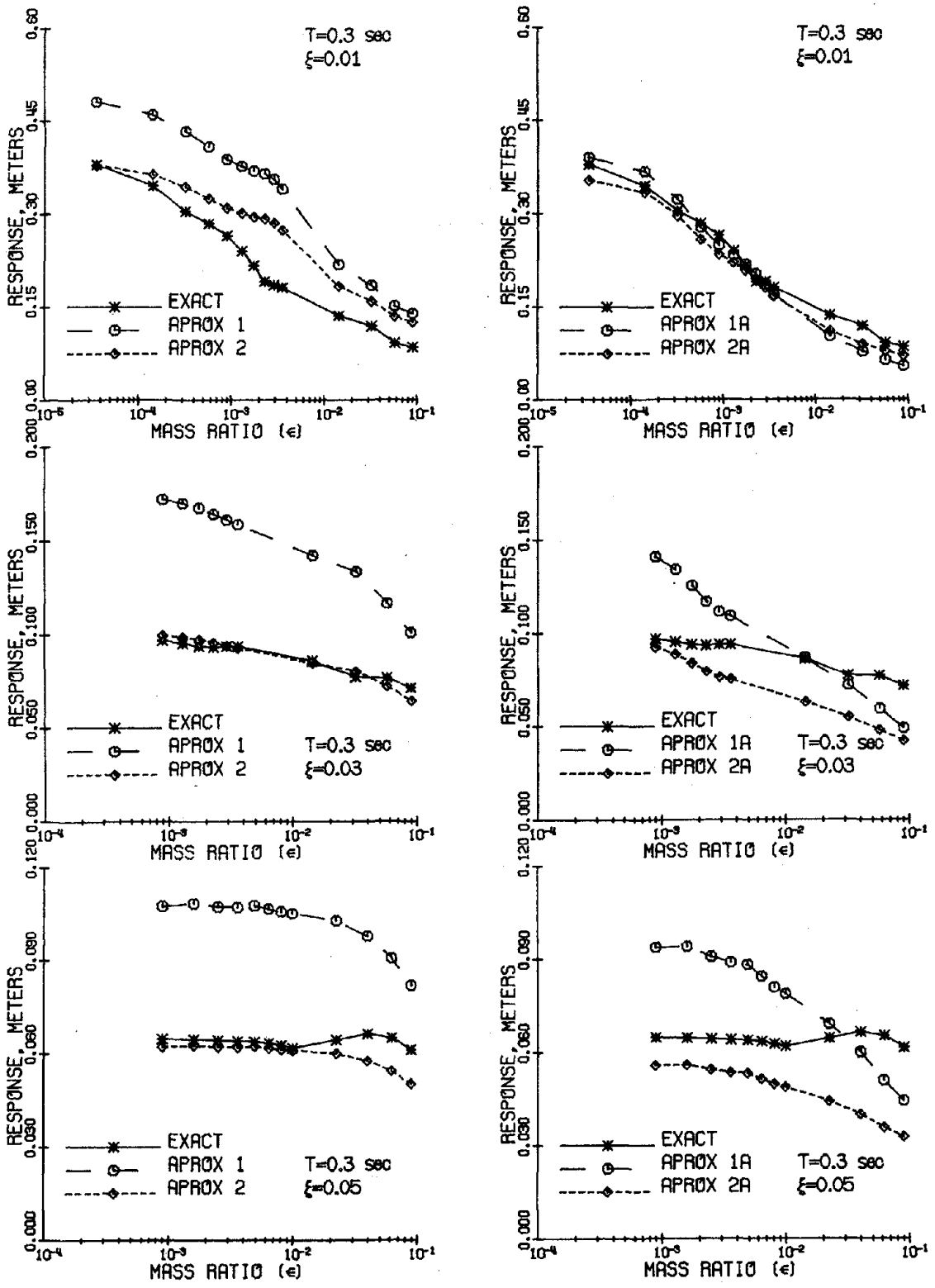

Figure 17. Exact and Approximate Secondary System Responses of Tuned Secondary System to El Centro Earthquake, T = .3 sec

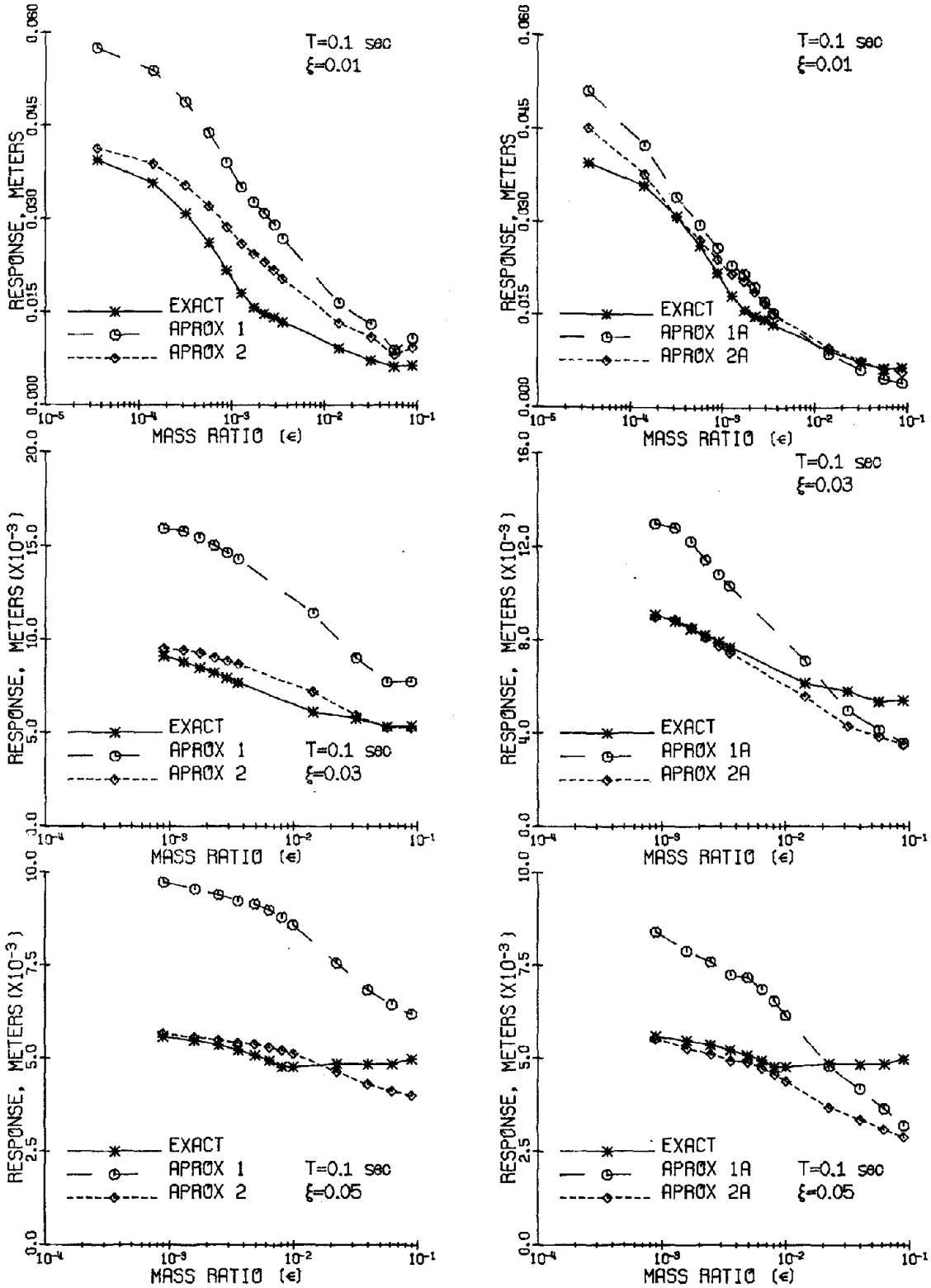

Figure 18. Exact and Approximate Responses of Tuned Secondary System to El Centro Earthquake, T = .1 sec

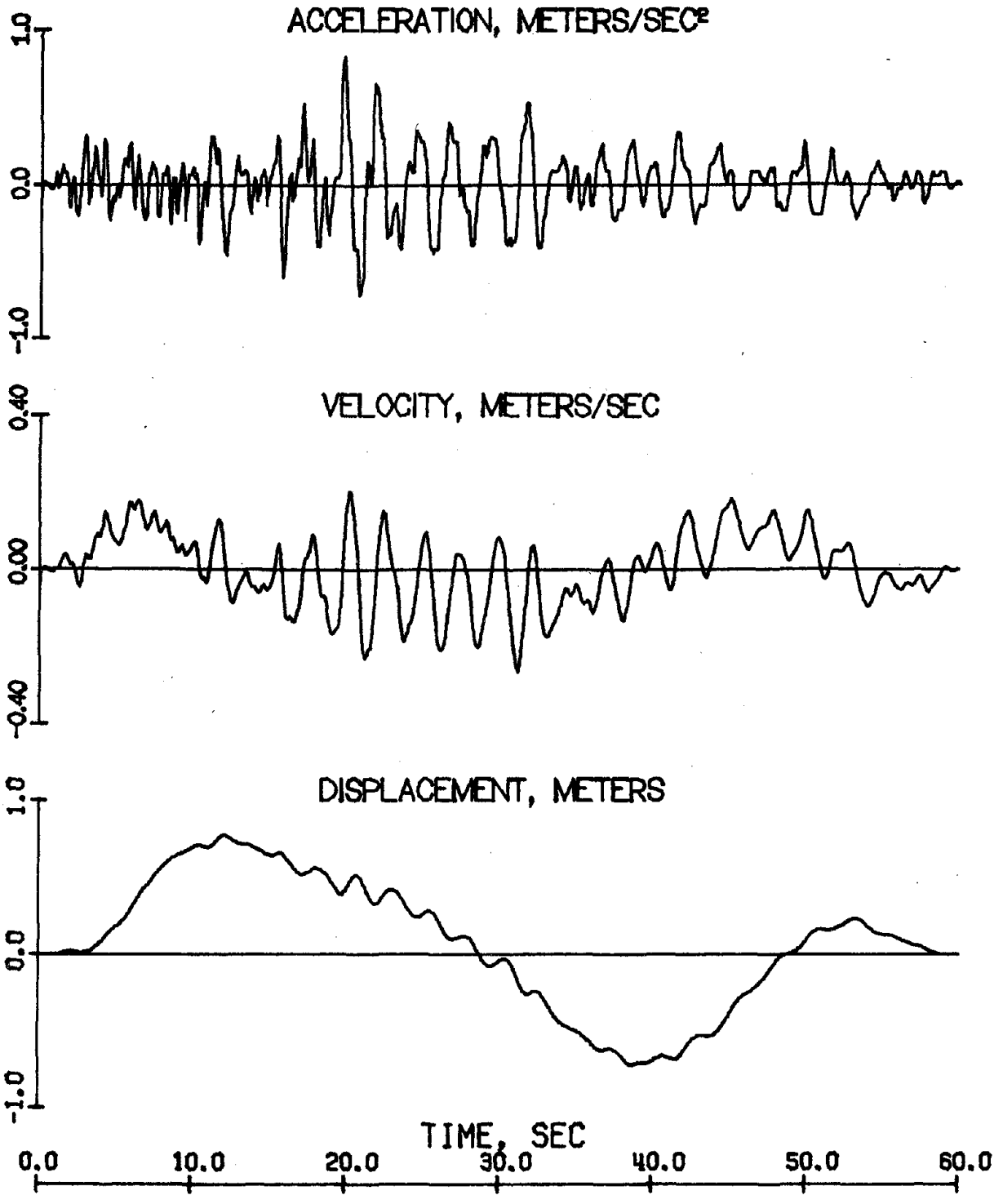

Figure 19. Time History Data for May 11, 1962
Mexico City Earthquake Record

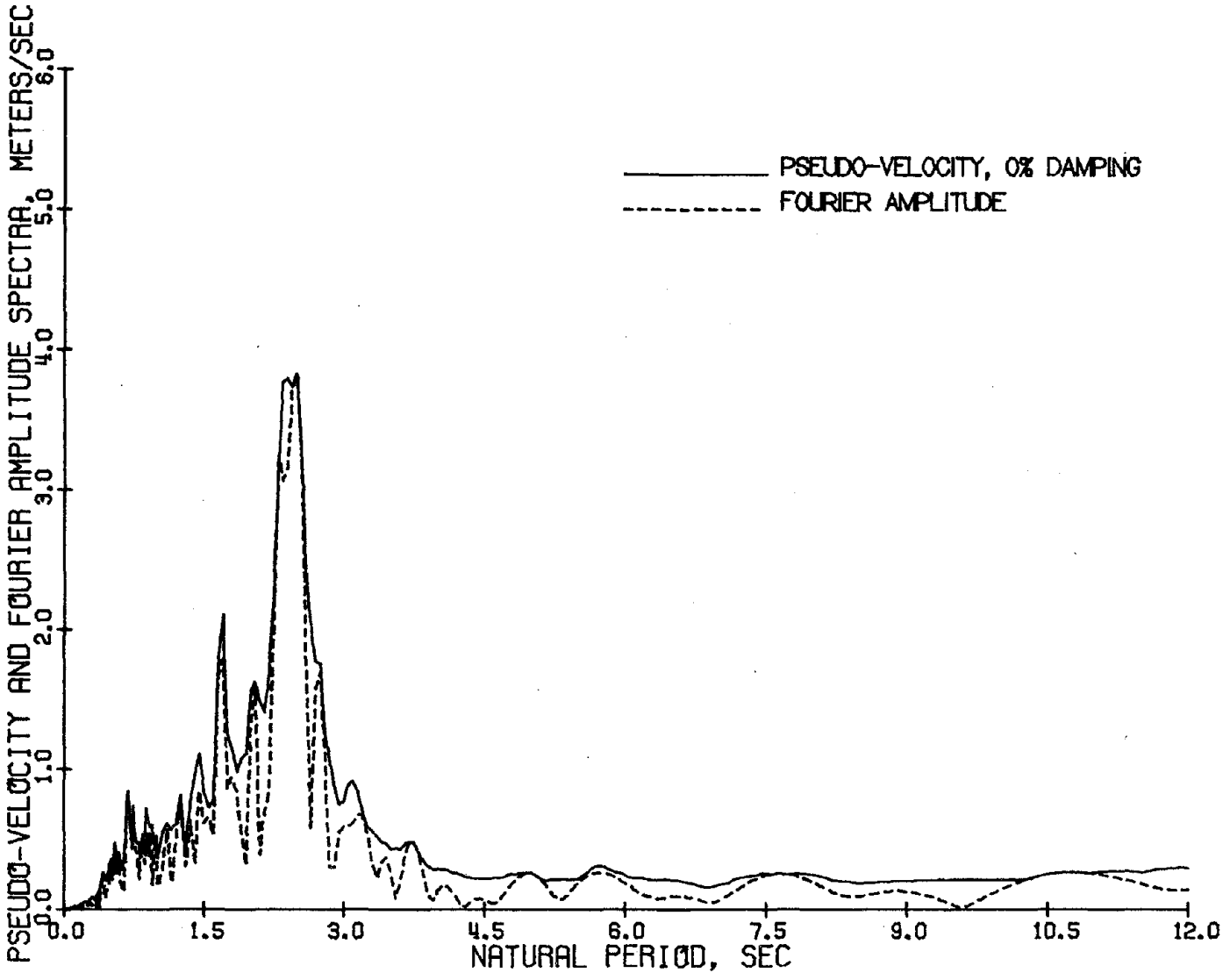

Figure 20. Frequency Domain Data for May 11, 1962 Mexico City Earthquake Record

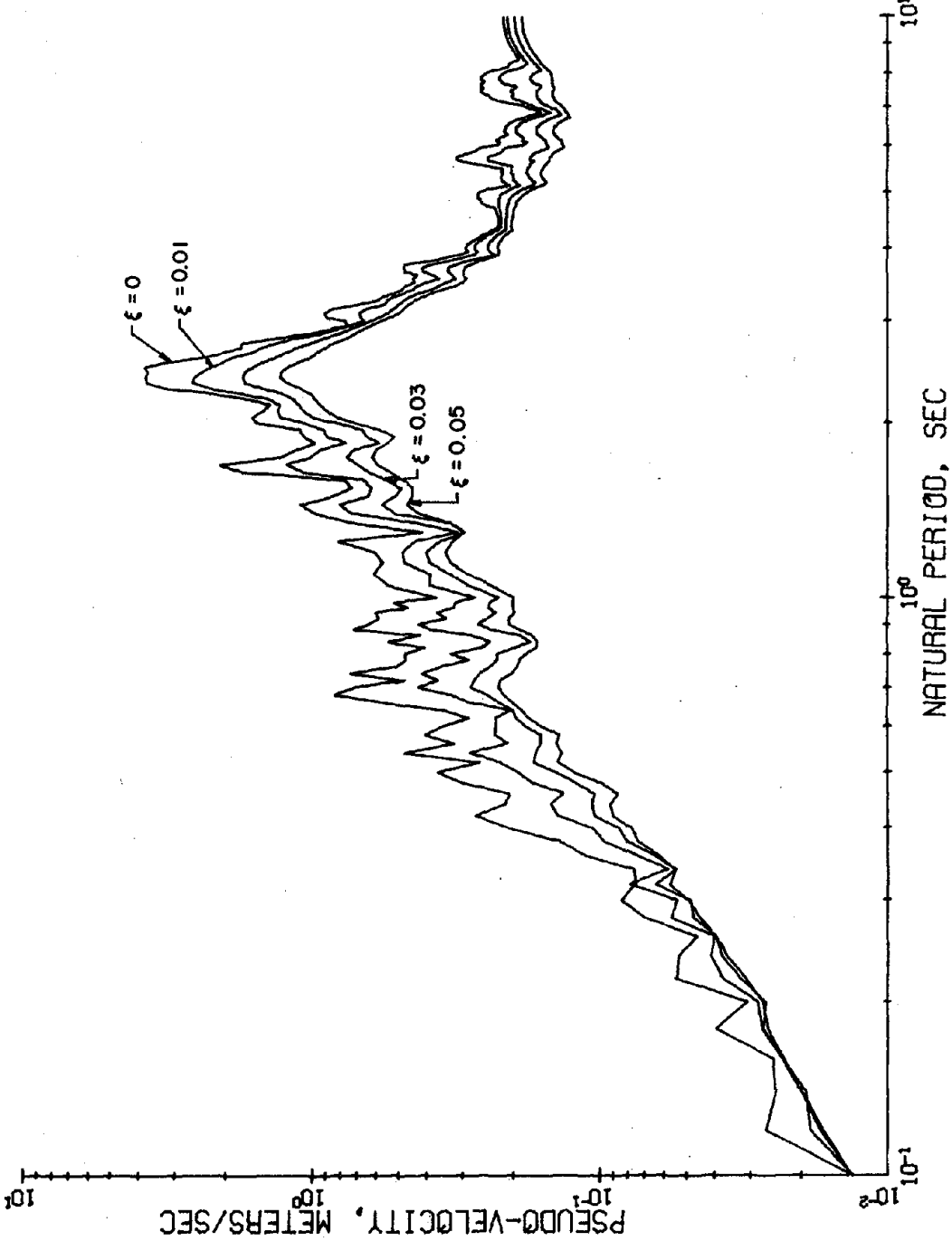

Figure 20 (continued)

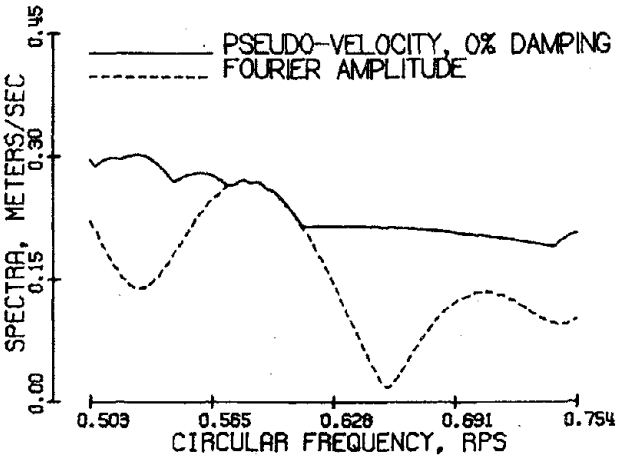

Figure 21a. Frequency Domain Data for Mexico City Earthquake Record in Vicinity of ω = .628 RPS (T = 10 sec)

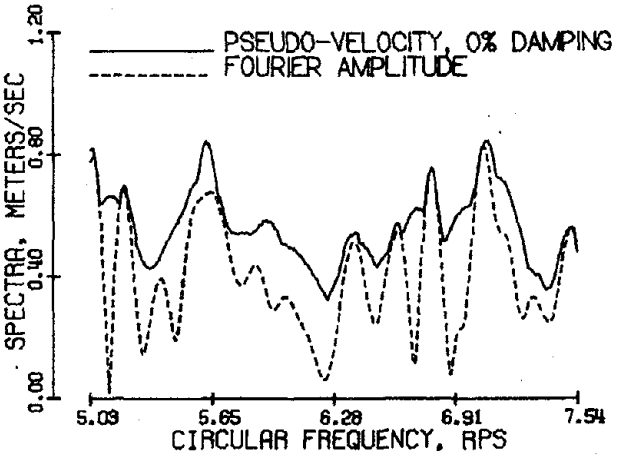

Figure 21b. Frequency Domain Data for Mexico City Earthquake Record in Vicinity of ω = 6.28 RPS (T = 1 sec)

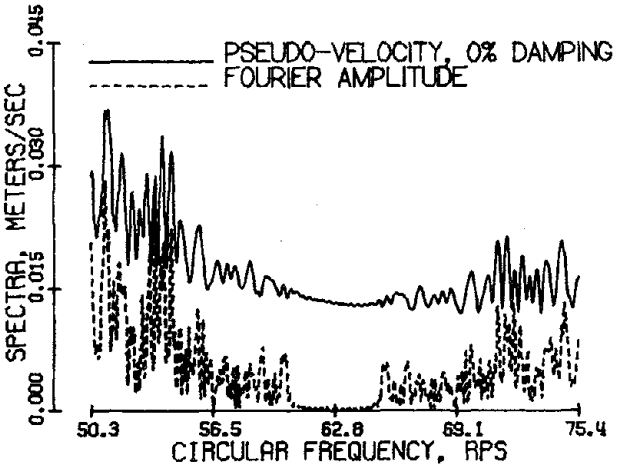

Figure 21c. Frequency Domain Data for Mexico City Earthquake Record in Vicinity of ω = 62.8 RPS (T = .1 sec)

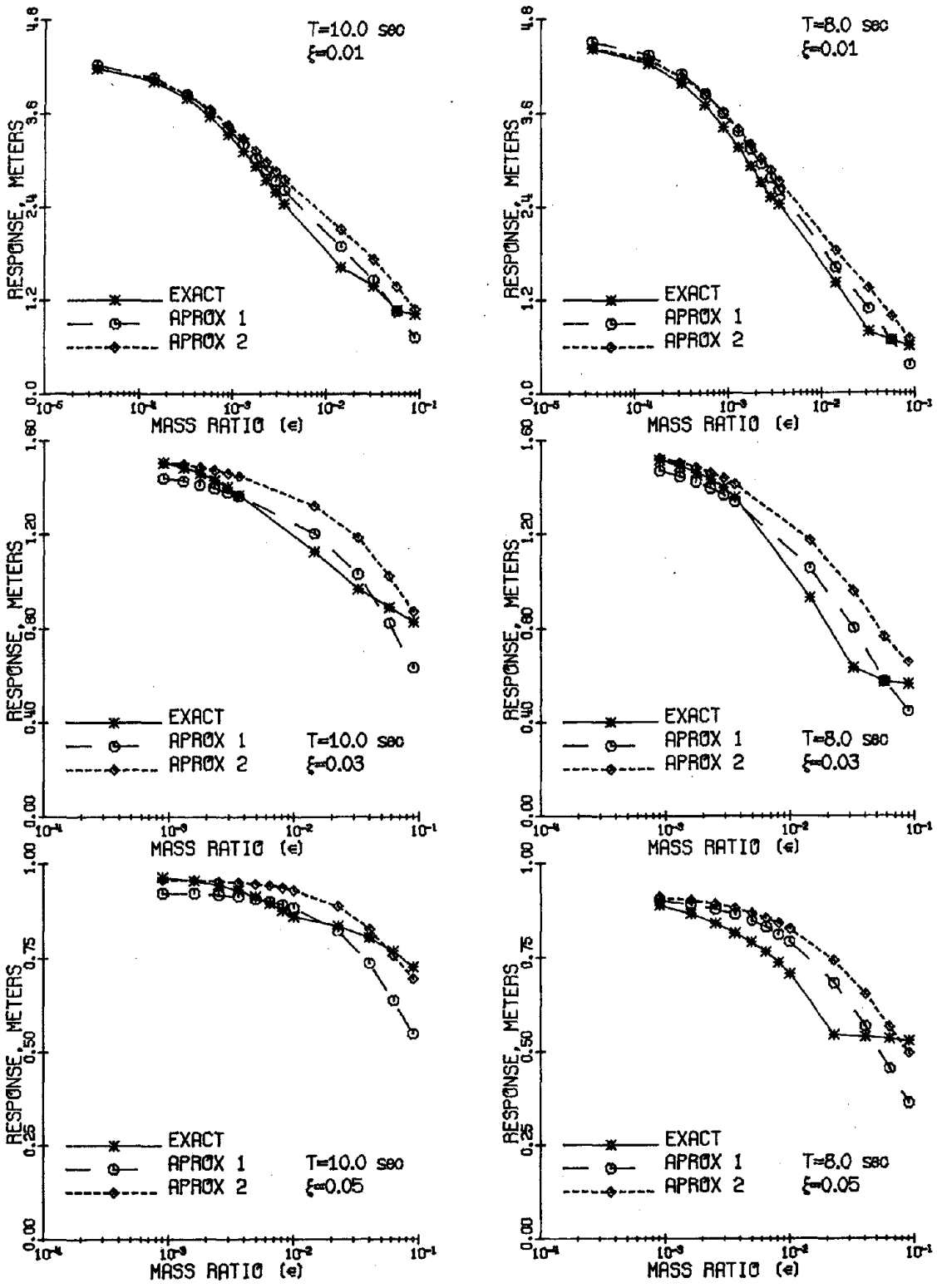

Figure 22. Exact and Approximate Responses of Tuned Secondary System to Mexico City Earthquake, T = 10 sec and T = 8 sec

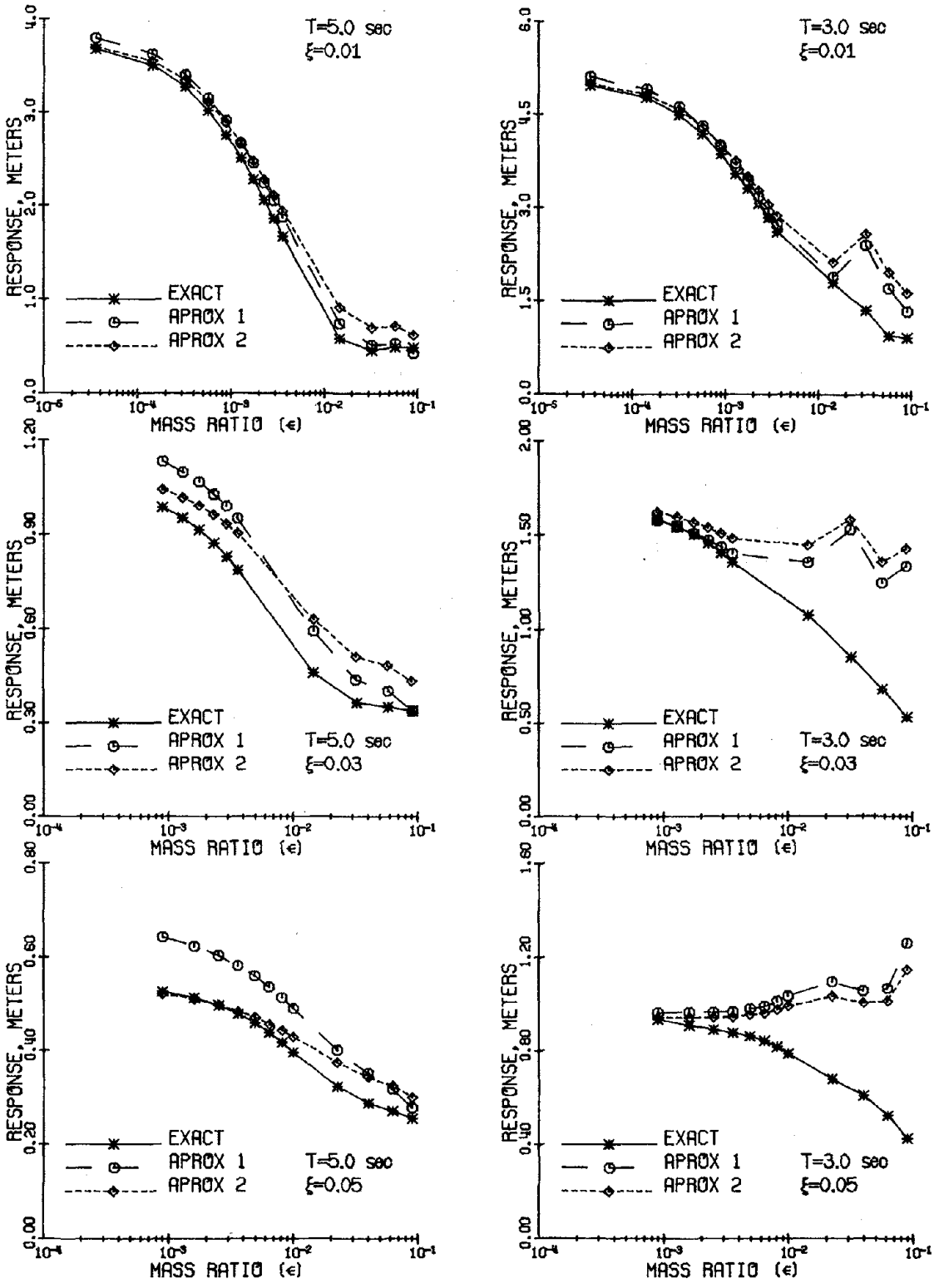

Figure 23. Exact and Approximate Responses of Tuned Secondary System to Mexico City Earthquake, T = 5 sec and T = 3 sec

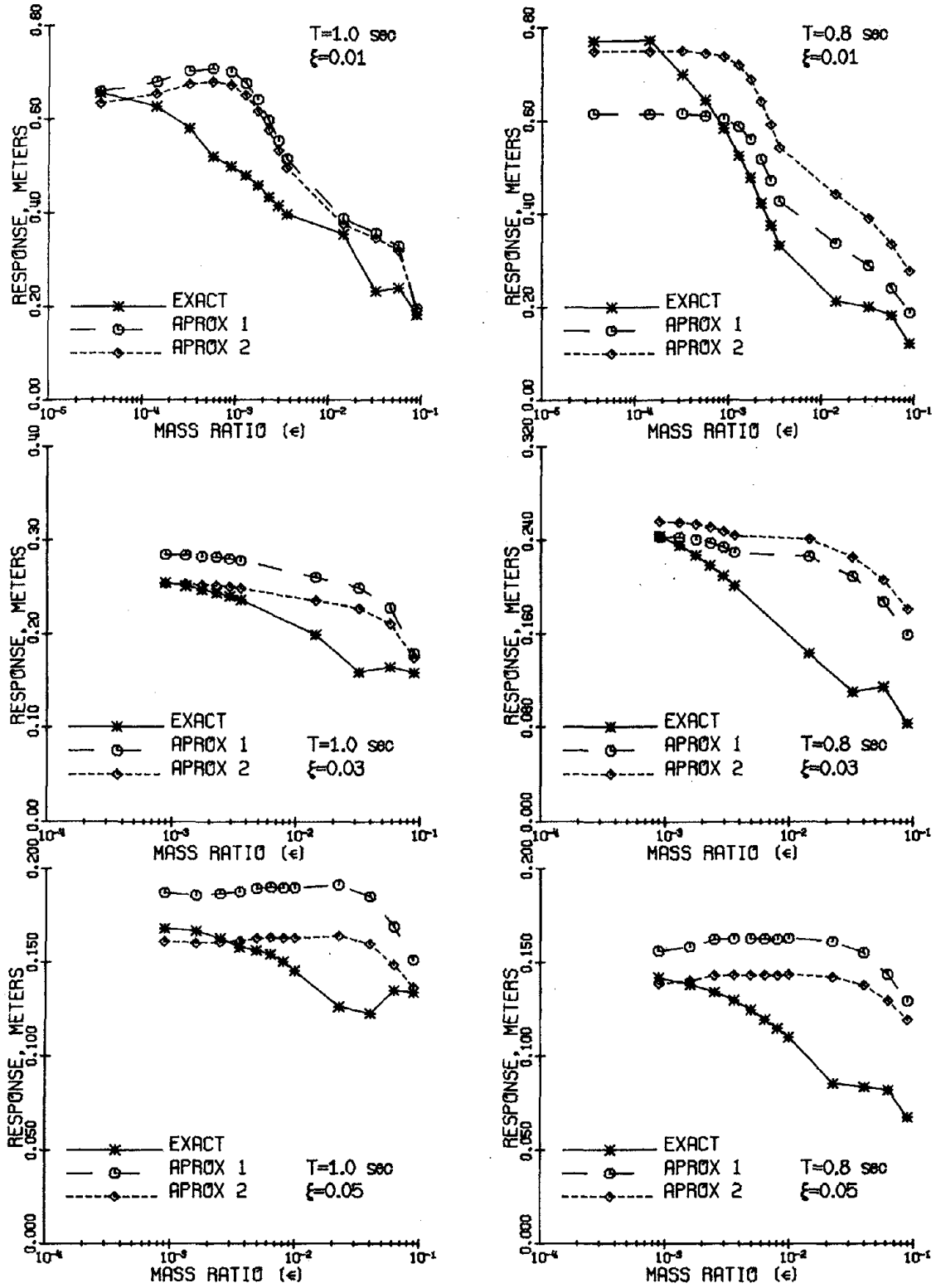

Figure 24. Exact and Approximate Responses of Tuned Secondary System to Mexico City Earthquake, T = 1 sec and T = .8 sec

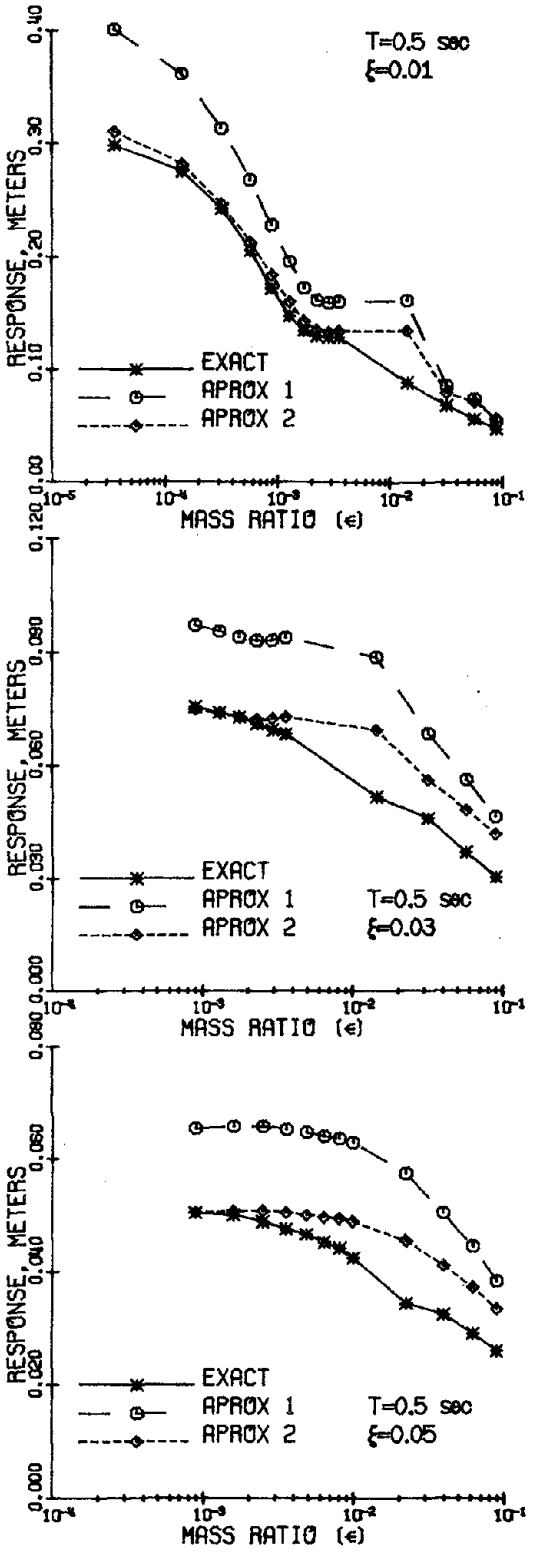

Figure 25. Exact and Approximate Response of Tuned Secondary System to Mexico City Earthquake, T = .5 sec

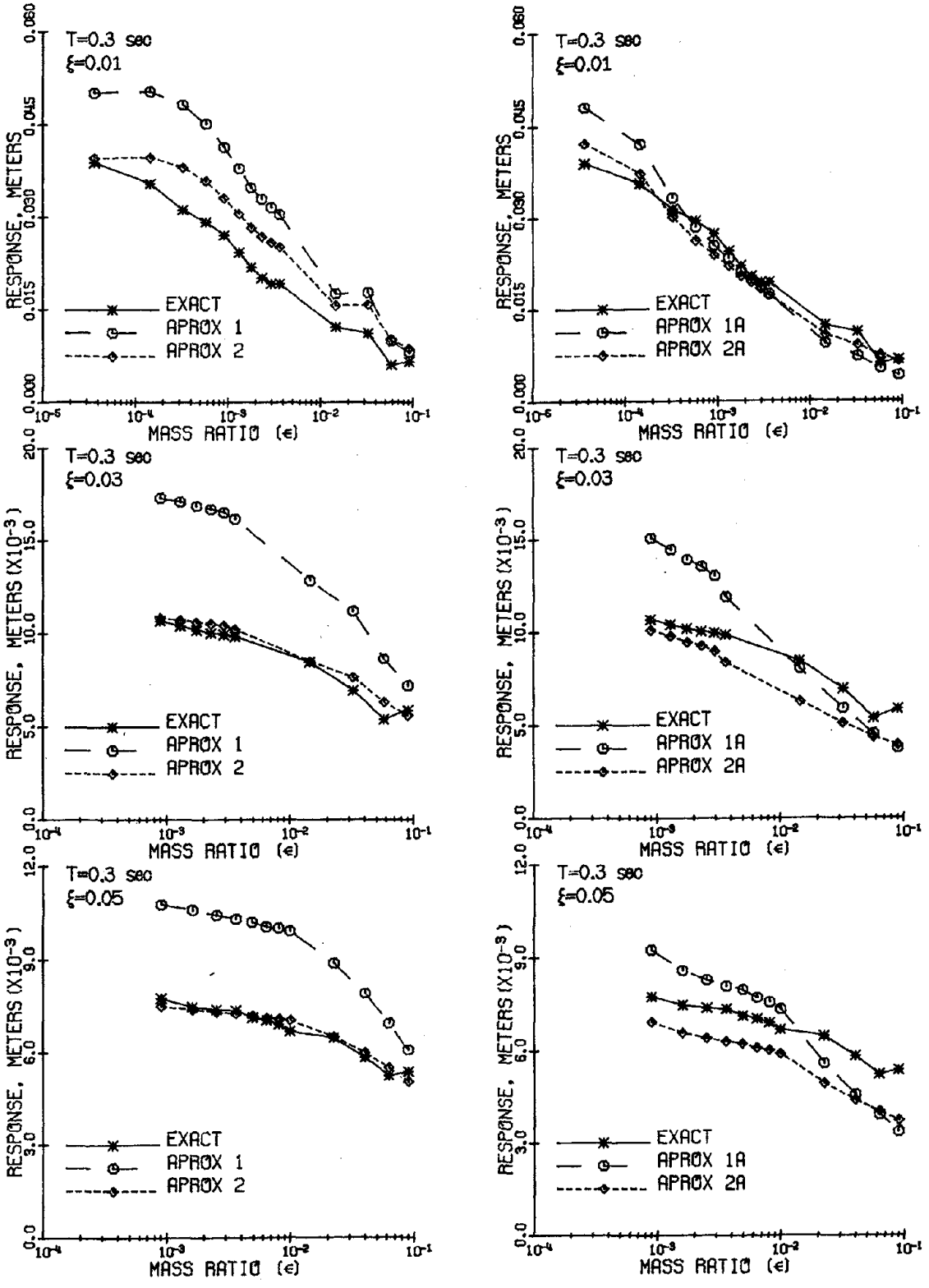

Figure 26. Exact and Approximate Responses of Tuned Secondary System to Mexico City Earthquake, T = .3 sec

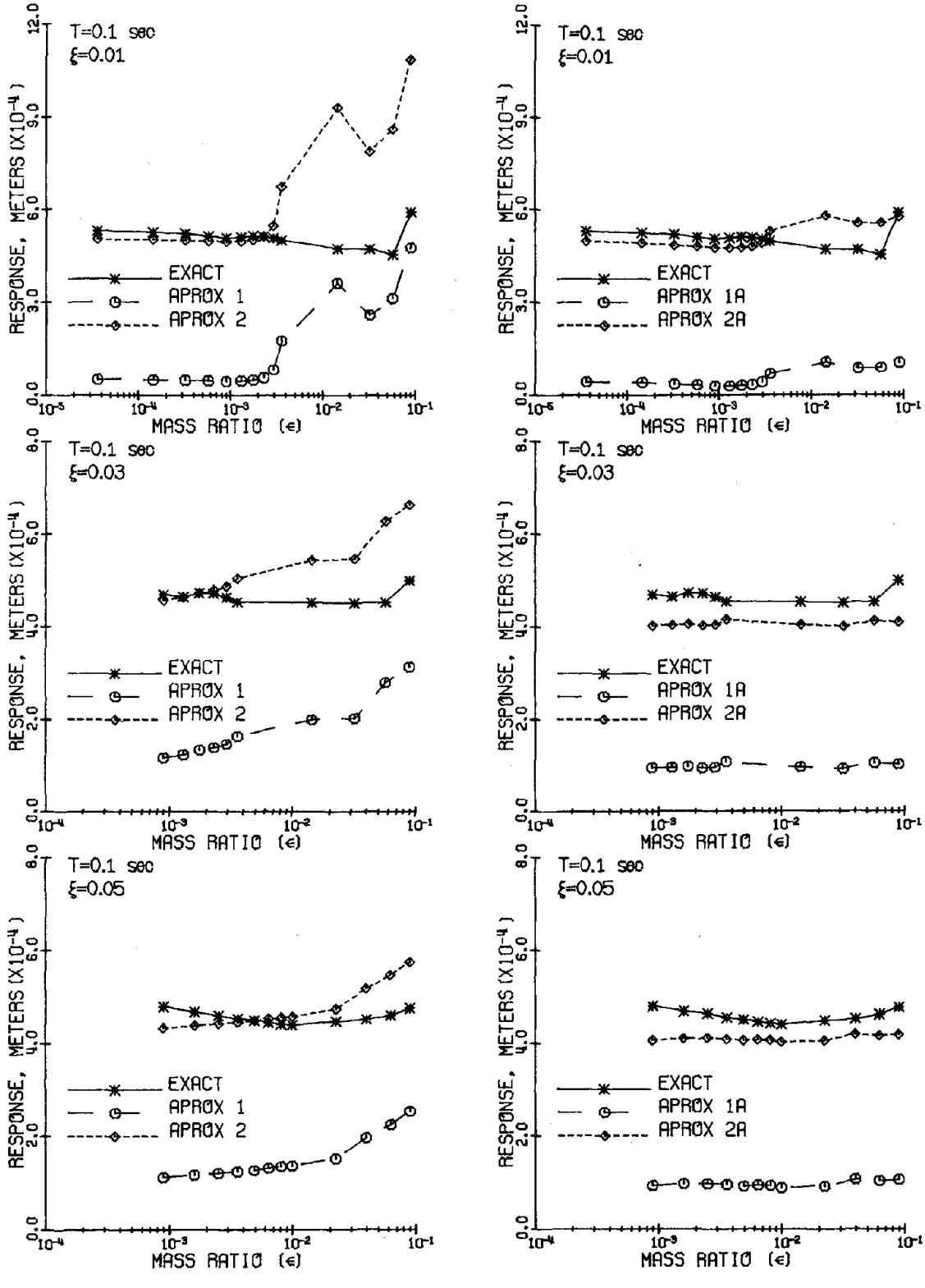

Figure 27. Exact and Approximate Responses of Tuned Secondary System to Mexico City Earthquake, T = .1 sec

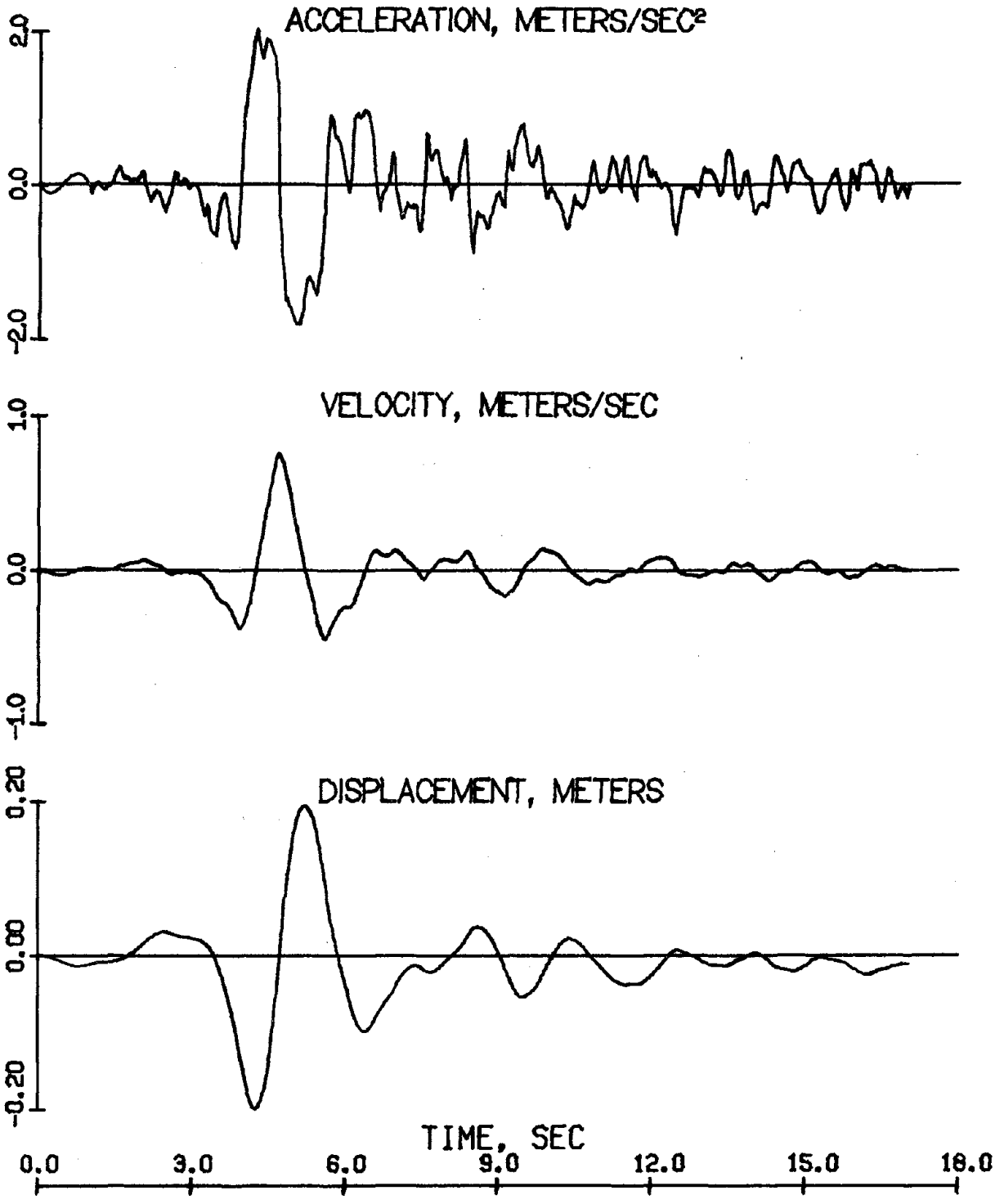

Figure 28. Time History Data for March 4, 1977 Vrancea Earthquake Record

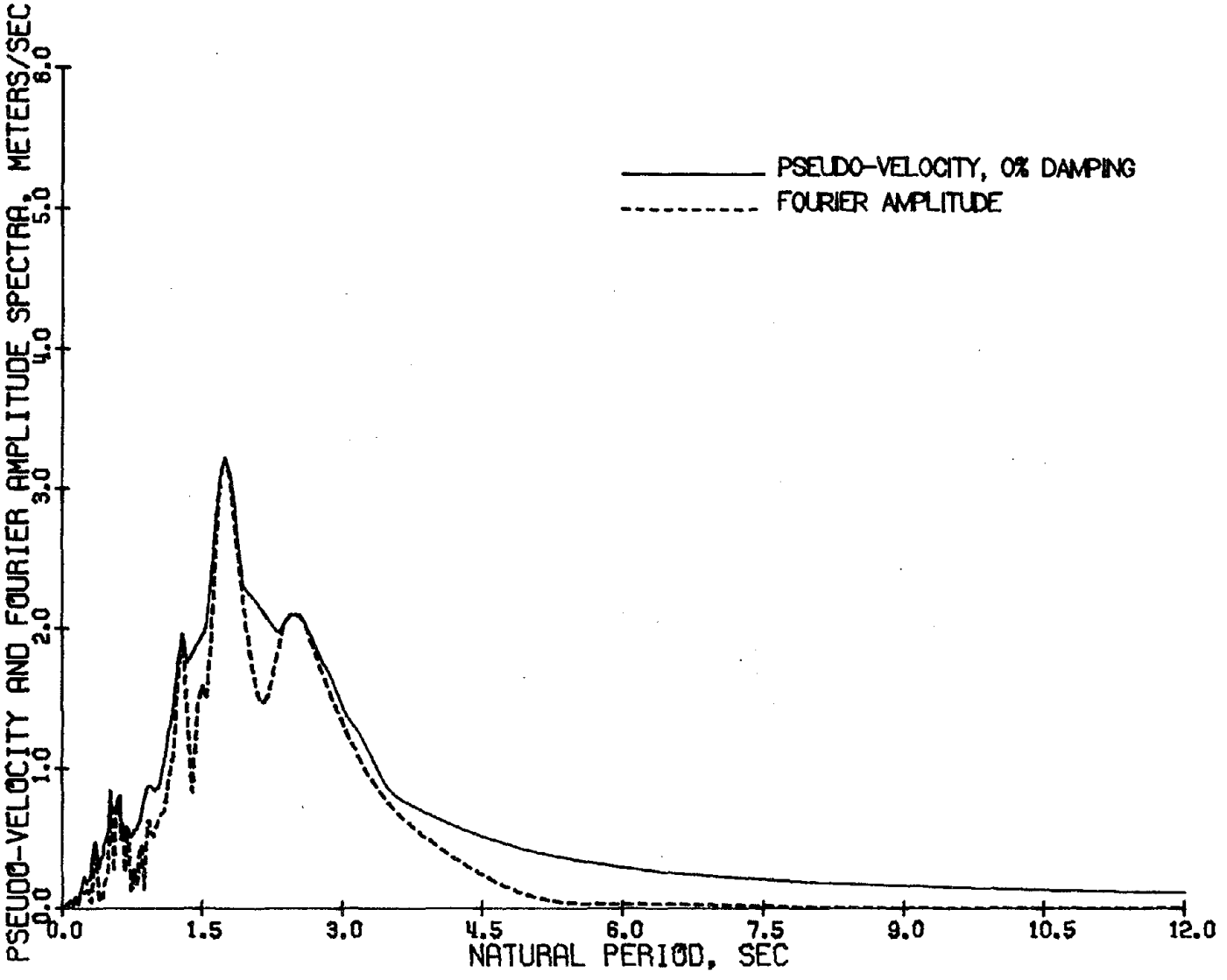

Figure 29. Frequency Domain Data for March 4, 1977 Vrancea Earthquake Record

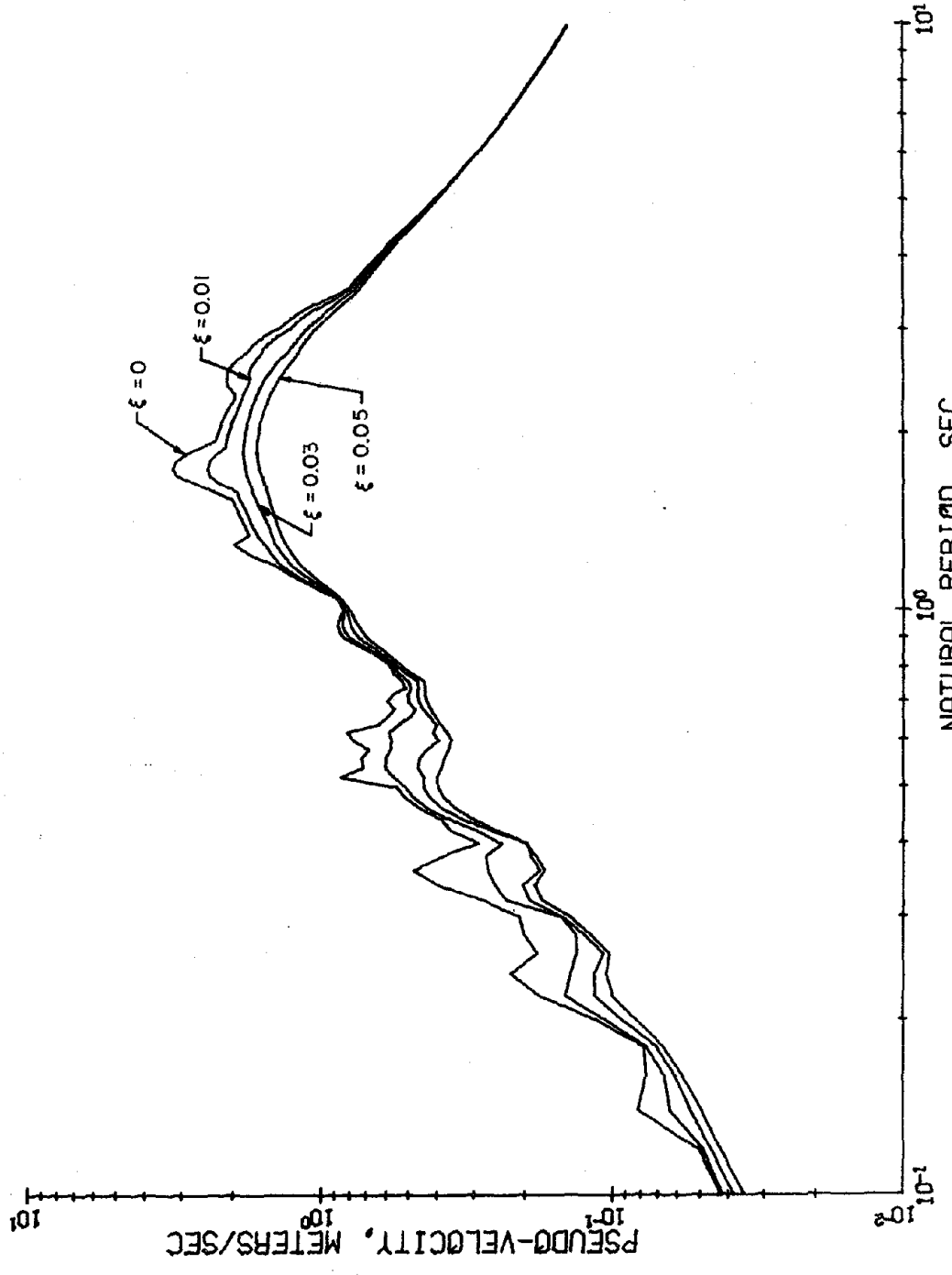

Figure 29 (continued)

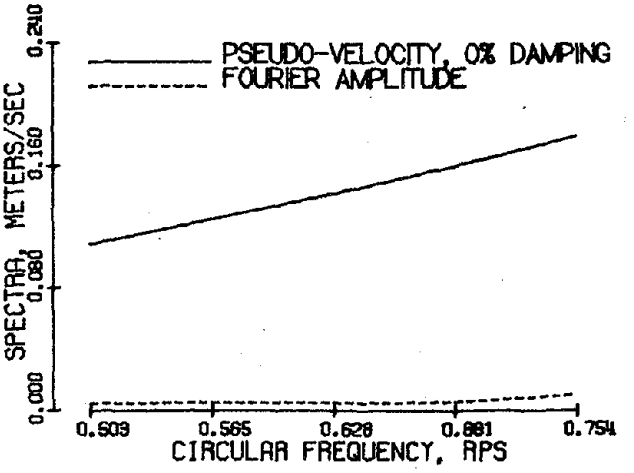

Figure 30a. Frequency Domain Data for Vrancea Earthquake in Vicinity of ω = .628 RPS (T = 10 sec)

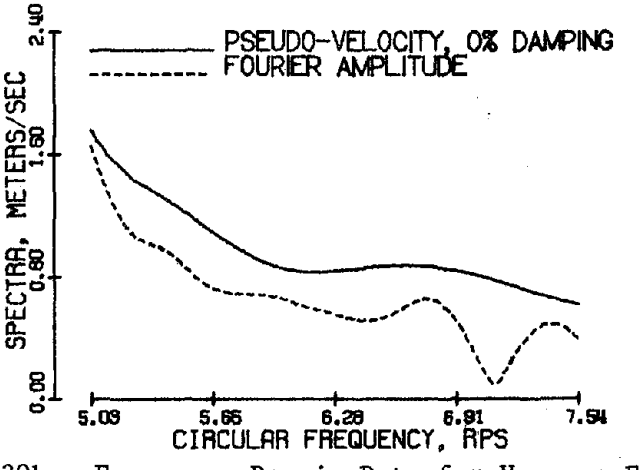

Figure 30b. Frequency Domain Data for Vrancea Earthquake in Vicinity of ω = 6.28 RPS (T = 1 sec)

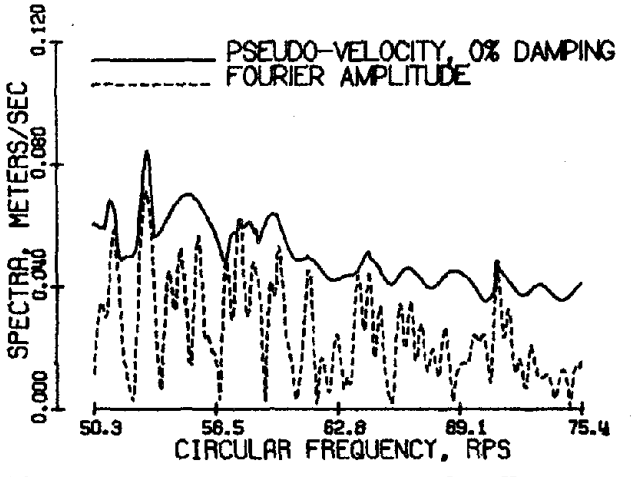

Figure 30c. Frequency Domain Data for Vrancea Earthquake in Vicinity of ω = 62.8 RPS (T = .1 sec)

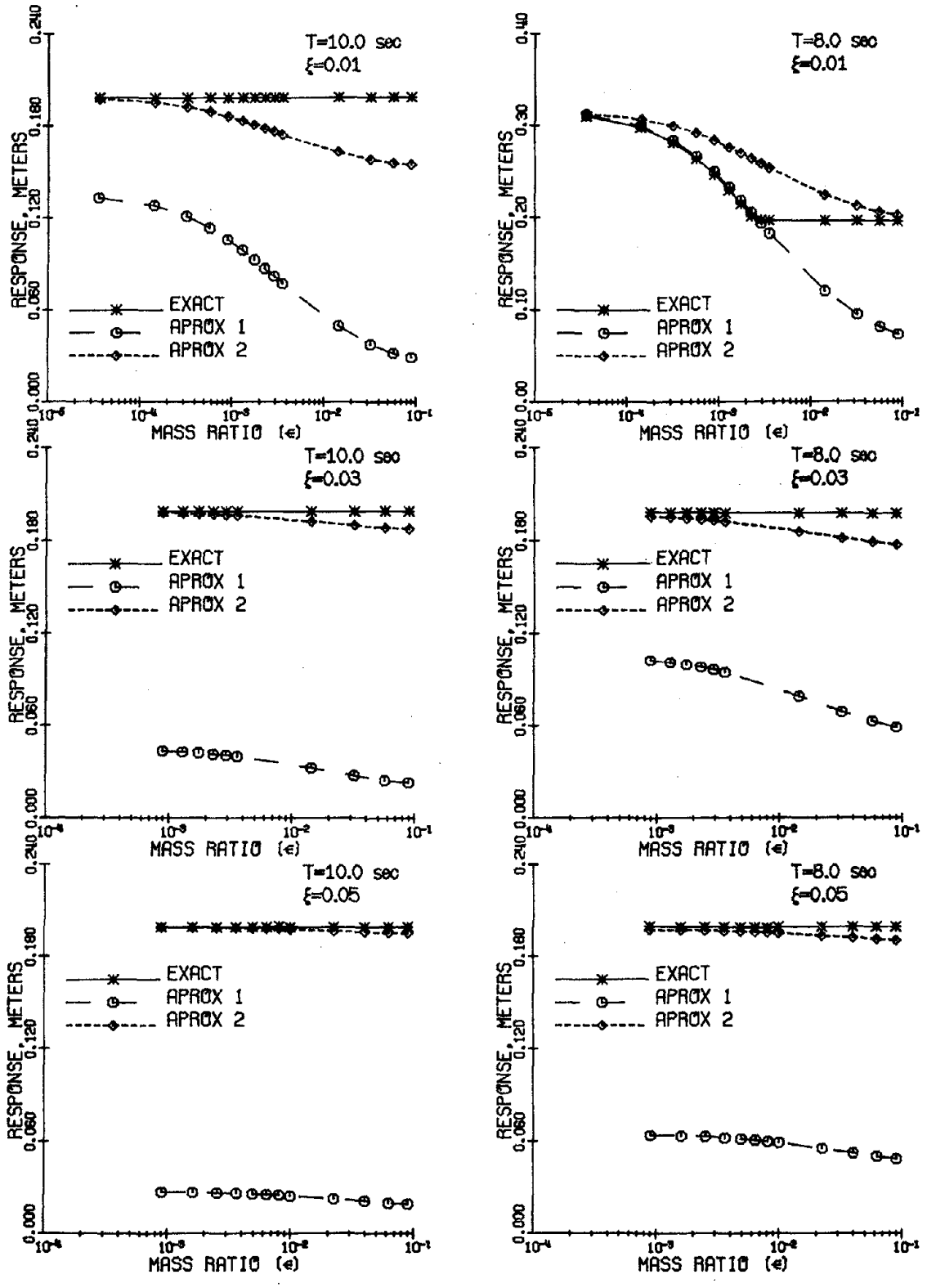

Figure 31. Exact and Approximate Responses of Tuned Secondary System to Vrancea Earthquake, T = 10 sec and T = 8 sec

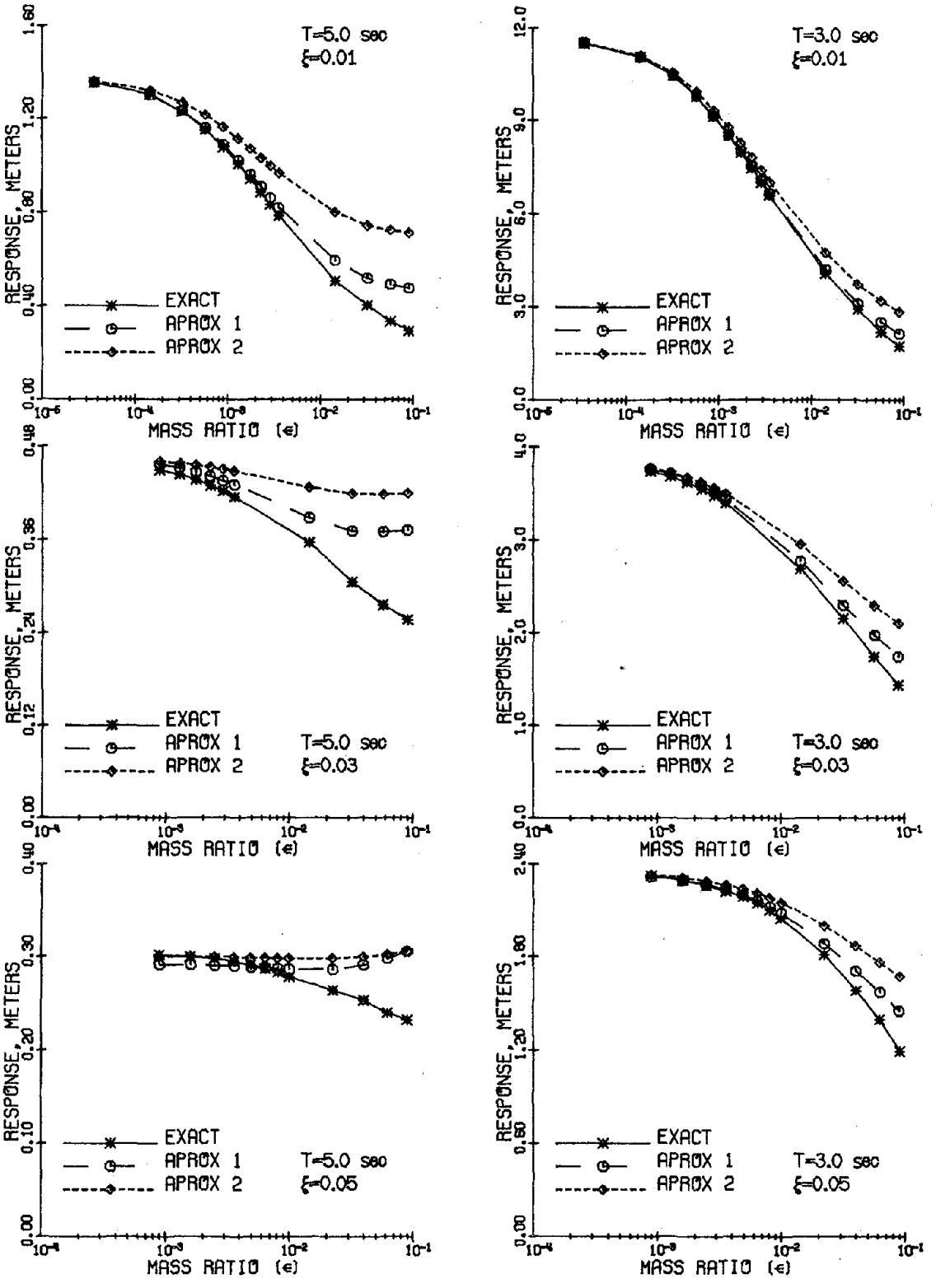

Figure 32. Exact and Approximate Responses of Tuned Secondary System to Vrancea Earthquake, T = 5 sec and T = 3 sec

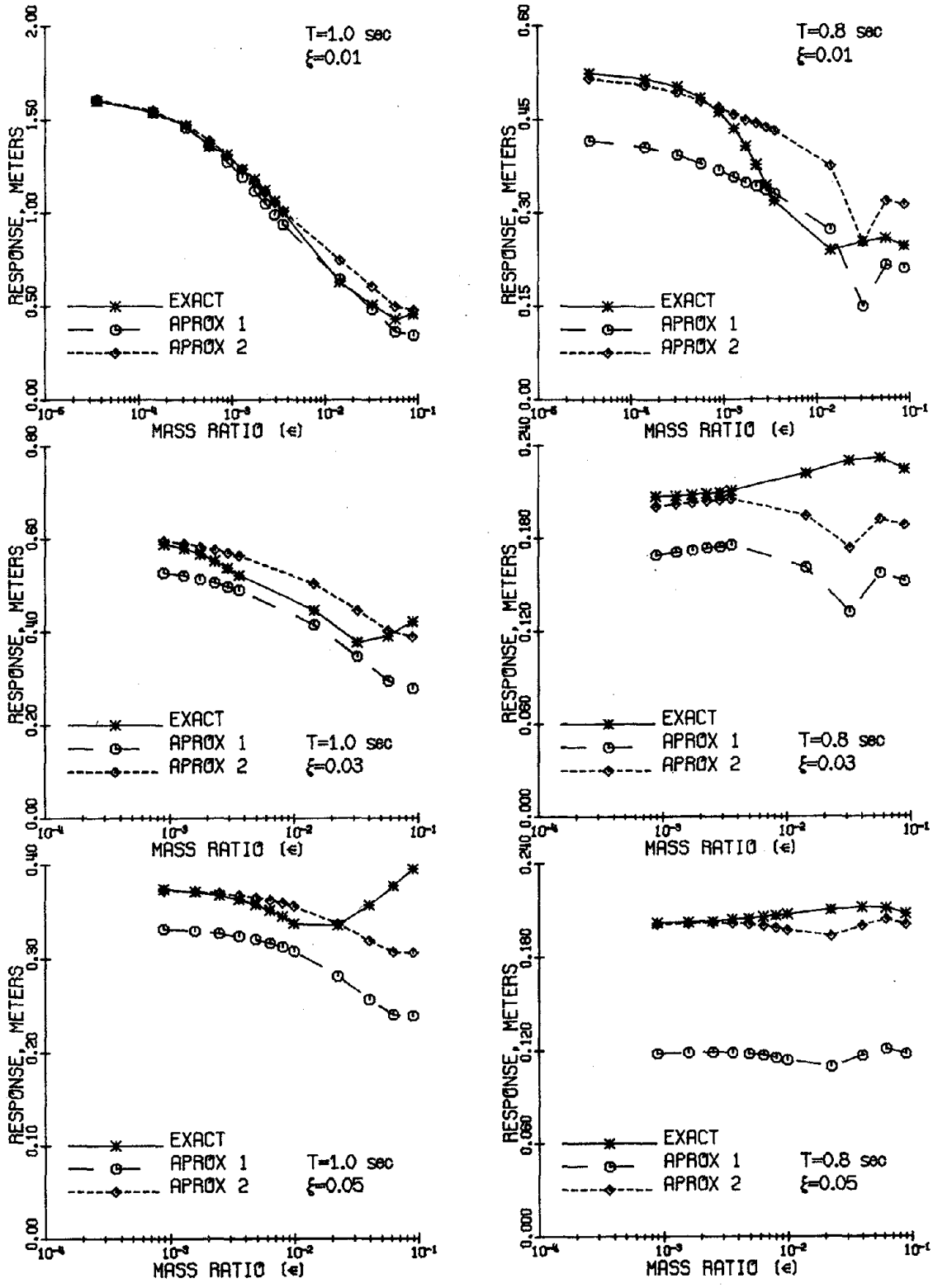

Figure 33. Exact and Approximate Responses of Tuned Secondary System to Vrancea Earthquake, T = 1 sec and T = .8 sec

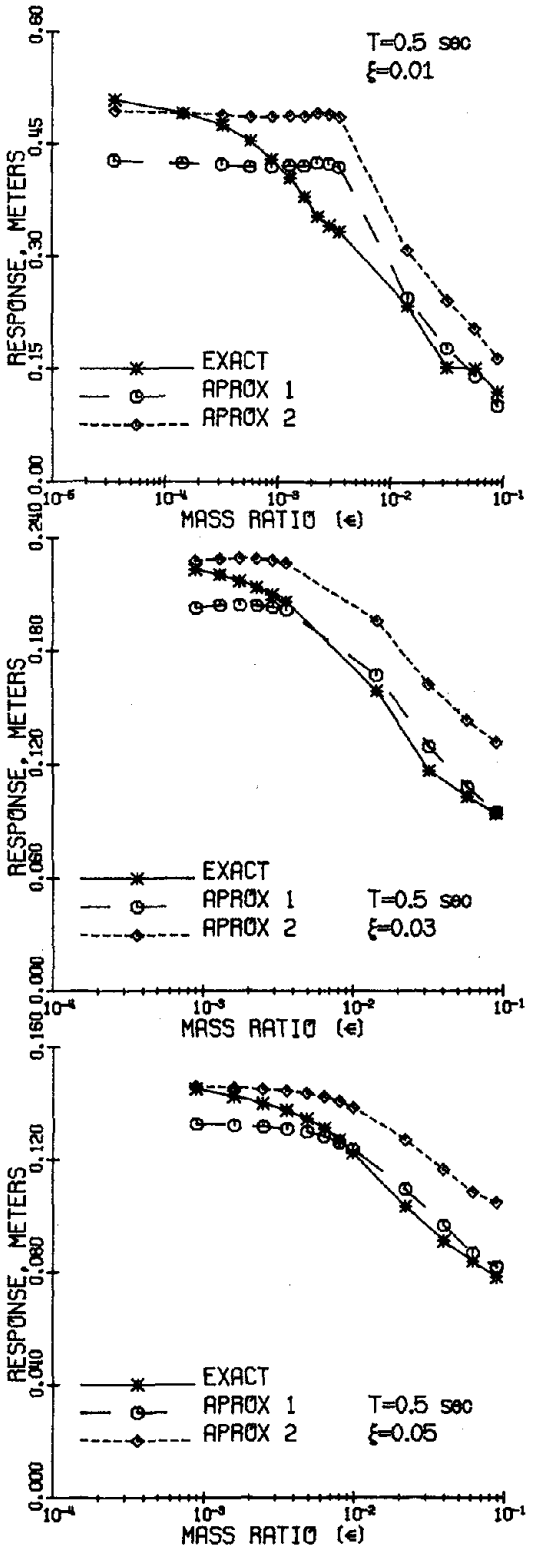

Figure 34. Exact and Approximate Responses of Tuned Secondary System to Vrancea Earthquake, T = .5 sec

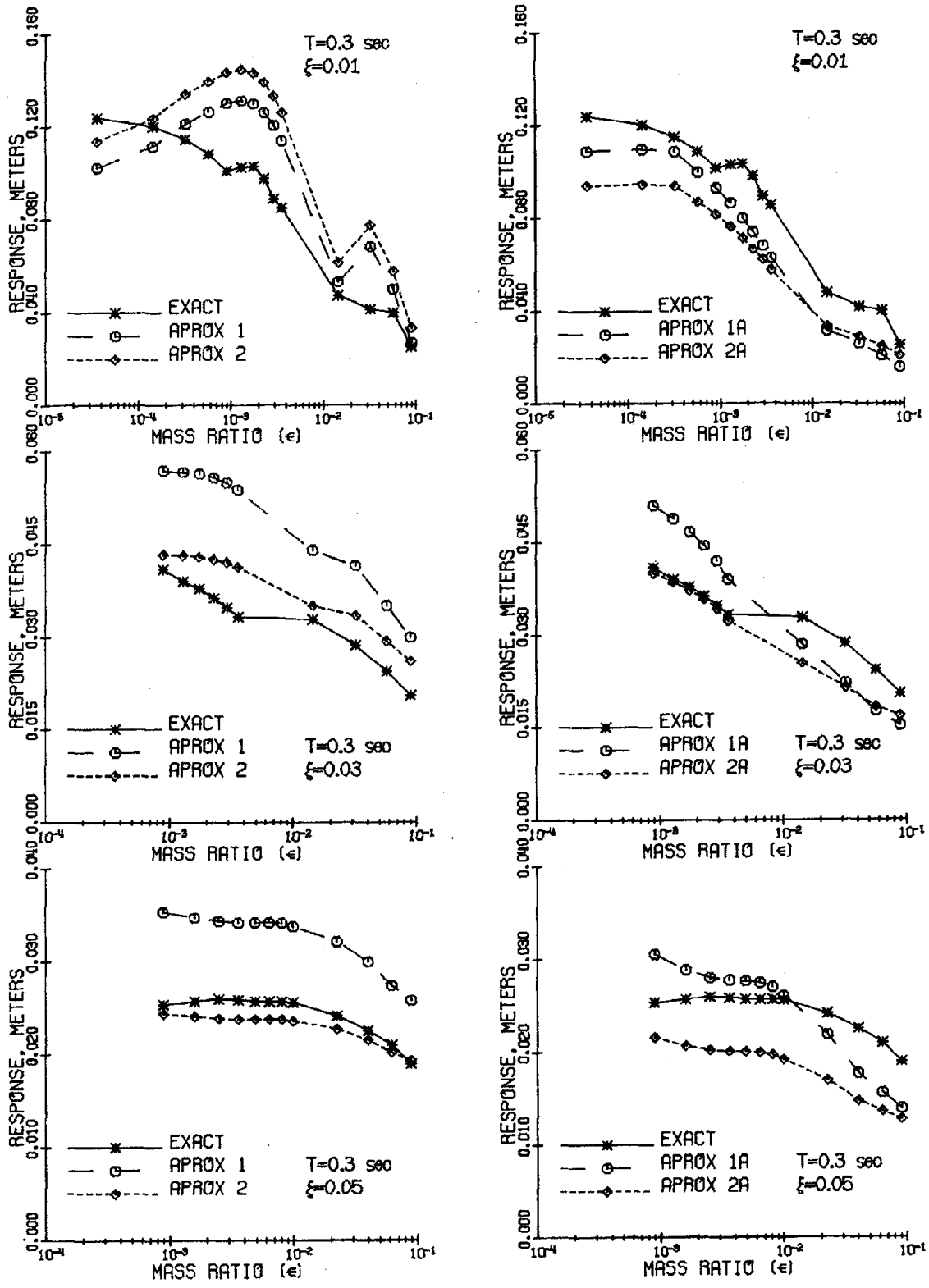

Figure 35. Exact and Approximate Responses of Tuned Secondary System to Vrancea Earthquake, T = .3 sec

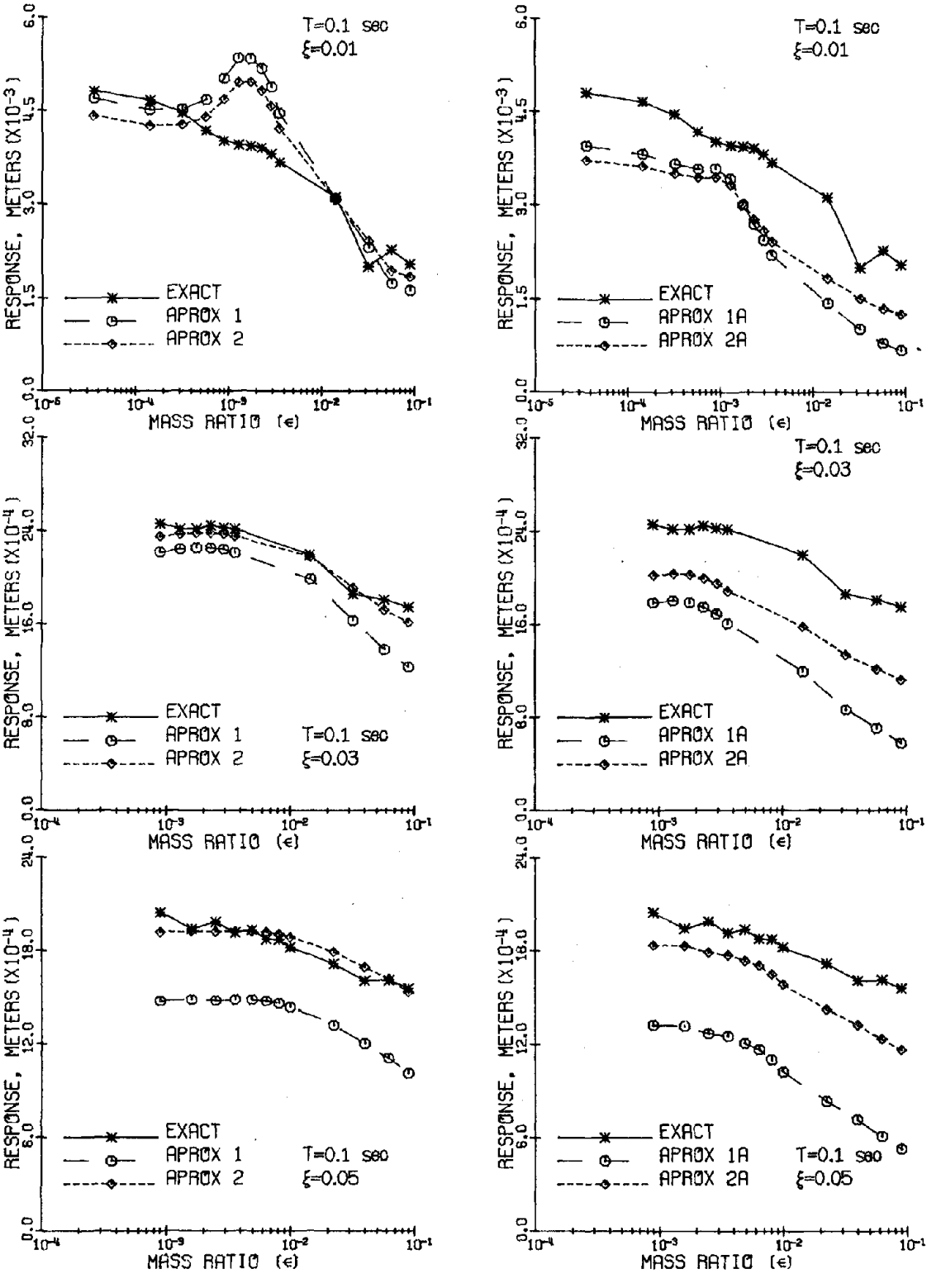

Figure 36. Exact and Approximate Responses of Tuned Secondary System to Vrancea Earthquake, T = .1 sec

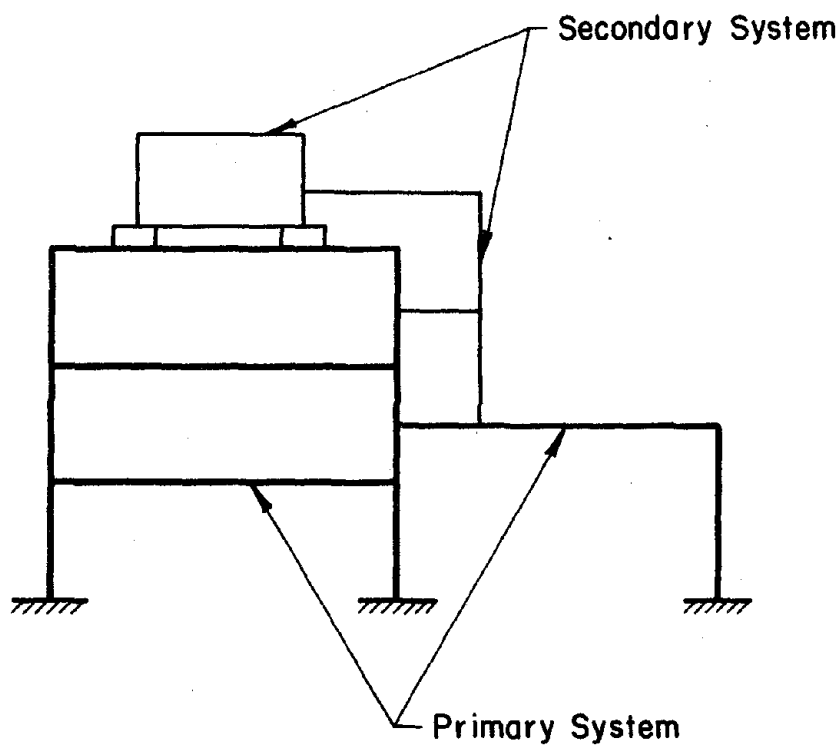

Figure 37. Schematic Diagram of Multi-Degree-of-Freedom Secondary System Attached to Multi-Degree-of-Freedom Primary System